Structural and functional studies on bacterial 6S RNA and characterization of the 6S RNA-RNA polymerase interaction

Inaugural-Dissertation

zur Erlangung des Doktorgrades
der Mathematisch-Naturwissenschaftlichen Fakultät
der Heinrich-Heine-Universität Düsseldorf

vorgelegt von

Benedikt Steuten
aus Meerbusch

Düsseldorf, Oktober 2013

aus dem Institut für Molekularbiologie der Bakterien
der Heinrich-Heine Universität Düsseldorf

Gedruckt mit der Genehmigung der
Mathematisch-Naturwissenschaftlichen Fakultät der
Heinrich-Heine-Universität Düsseldorf

Referent: Prof. Dr. Rolf Wagner
Korreferent: Prof. Dr. Joachim Ernst

Tag der mündlichen Prüfung: 13.12.2013

Results described in this dissertation have been presented in the following publications:

Geißen, R., **Steuten, B.**, Polen, T. and Wagner, R. **(2010)** *E. coli* 6S RNA: a universal transcriptional regulator within the centre of growth adaptation. *RNA Biol* **7**: 564-568.

Rediger, A., Geissen, R., **Steuten, B.**, Heilmann, B., Wagner, R. and Axmann, I. M. **(2012)** 6S RNA - an old issue became blue-green. *Microbiology* **158**: 2480-2491.

Steuten, B. and Wagner, R. **(2012)** A conformational switch is responsible for the reversal of the 6S RNA-dependent RNA polymerase inhibition in *Escherichia coli*. *Biol Chem* **393**: 1513-1522.

Steuten, B., Setny, P., Zacharias, M. and Wagner, R. **(2013)** Mapping the spatial neighborhood of the regulatory 6S RNA bound to *Escherichia coli* RNA polymerase holoenzyme. *J Mol Biol* **425**: 3649-3661.

Steuten, B., Schneider, S. and Wagner, R. **(2013)** 6S RNA: recent answers - future questions. Invited review, *submitted to Mol Microbiol.*

Author contributions:

***E. coli* 6S RNA: a universal transcriptional regulator within the centre of growth adaptation.**
Discussion and evaluation: 25%
Manuscript writing: 25%

6S RNA - an old issue became blue-green.
Research design: 20%
Experimental work: 30%
Data analysis and evaluation: 30%
Manuscript writing: 20%

A conformational switch is responsible for the reversal of the 6S RNA-dependent RNA polymerase inhibition in *Escherichia coli*.
Research design: 80%
Experimental work: 100%
Data analysis and evaluation: 60%
Manuscript writing: 50%

Mapping the spatial neighborhood of the regulatory 6S RNA bound to *Escherichia coli* RNA polymerase holoenzyme.
Research design: 80%
Experimental work: 90%
Data analysis and evaluation: 60%
Manuscript writing: 40%

6S RNA: recent answers – future questions.
Investigation: 50%
Manuscript writing: 50%
Discussion: 50%

Abbreviations

A	adenine
bp	base pair
B. subtilis	*Bacillus subtilis*
C	cytosine
DMS	dimethylsulfate
E. coli	*Escherichia coli*
$E\sigma^{70}$	RNA polymerase holoenzyme containing σ^{70}
FeBABE	p-bromoacetamidobenzyl-EDTA, iron (III) chelate
Fig.	figure
FIS	factor for inversion stimulation
G	guanine
H-NS	histone-like nucleoid structuring protein
ILP	in line probing
LRP	leucine-responsive regulatory protein
ncRNA	non-coding RNA
nt	nucleotide
NTP	nucleoside triphosphate
pdb	protein data bank
ppGpp	effector nucleotide; guanosine-3',5'-bis(diphosphate)
rRNA	ribosomal RNA
RNAP	RNA polymerase
RNase	ribonucleic acid nuclease (ribonuclease)
sRNA	small RNA
StpA	suppression of td phenotype
T	thymine
T. aquaticus	*Thermus aquaticus*
TSS	transcription start site
T. thermophilus	*Thermus thermophilus*
U	uracil
5' UTR	5' untranslated region

Content

1 Summary 1
2 Introduction 2
2.1 The bacterial 6S RNA 2
2.1.1 Biogenesis and physiological implications of 6S RNA 2
2.1.2 6S RNA structure-dependent interaction with RNAP 4
2.1.3 6S RNA-templated pRNA transcription 8
2.1.4 Specialized 6S RNA regulation in other organisms 10
2.2 The bacterial RNA polymerase: Structural insights 12
2.3 Aims of this work 15
3 Results 16
3.1 Heterologous investigation of cyanobacterial 6S RNA function 16
3.1.1 Supplemental material: Rediger *et al.* 2012 29
3.2 The pRNA-mediated structural rearrangement of 6S RNA 38
3.2.1 Supplemental material: Steuten and Wagner 2012 49
3.3 A spatial assignment of 6S RNA to the three-dimensional structure of the RNAP holoenzyme 50
3.3.1 Supplemental material: Steuten *et al.* 2013 64
4 Discussion 66
4.1 Conclusions from heterologous studies 66
4.2 The mechanism of pRNA-mediated structural and functional change of 6S RNA 70
4.3 Comparison of RNAP interaction with 6S RNA and promoter DNA 72
4.3.1 The binding mode 73
4.3.2 The transcription mode 75
5 References 80
6 Appendix 85
6.1 Review: 6S RNA: recent answers – future questions 85
6.2 Point-of-View article (Geißen *et al*. 2010) 97

Zusammenfassung
Erklärung
Danksagung

1 Summary

Transcription of genes is a fundamental process in all biological systems. In prokaryotic cells the transcription is catalysed by a single RNA polymerase (RNAP), which is thus subject to a complex regulatory network. The activity of RNA polymerase is controlled by a variety of molecules including proteins, low-molecular compounds and nucleic acids. Although RNA is the actual product of transcription the bacterial 6S RNA is a prime example for the regulation of transcription via a small, non-coding RNA. In this PhD thesis structural and functional implications of the 6S RNA-RNAP interaction were investigated.

In addition to the well-studied 6S RNA from *E. coli* the secondary structures of several 6S RNAs from the phylogenetically distant cyanobacteria were analysed in detail. Due to the structural similarity those RNAs were used for heterologous *in vitro* studies with *E. coli* RNAP. Despite the lack of major sequence conservation the 6S RNAs from *E. coli* and the cyanobacterial species exhibit the same characteristics, comprising RNAP binding and pRNA-mediated release from RNAP. The common 6S RNA structure allows the positioning in the RNAP active site resulting in an unusual RNA-templated transcription of short product RNAs (pRNA). A structural probing of the 6S-pRNA hybrid revealed that 6S RNA undergoes a conformational rearrangement, which facilitates the release from RNAP and probably induces the intracellular degradation of 6S RNA. The significance of this structural transition of 6S RNA *in vivo* was underscored by a chemical footprint technique.

Additionally, the 6S RNA-RNAP interaction sites were further scrutinized in this work. Therefore the spatial neighborhood between functional domains of the RNAP σ^{70} subunit and 6S RNA was mapped by applying the chemical nuclease FeBABE. The spatial assignment of the generated 6S RNA cleavage sites and tertiary structure predictions of 6S RNA fragments allowed the modelling of a three-dimensional 6S RNA structure relative to the high resolution crystal structure of RNAP. This model nicely reflects the helical topology of the RNA and proposes a reliable path of 6S RNA across the RNAP. Moreover, extension of the studies with 6S RNA mutants emphasize the importance of asymmetric bulge loops within the 6S RNA internal stem as potential interaction sites for RNAP.

2 Introduction

Regulating gene expression at the transcriptional and post-transcriptional level with non-coding RNAs (ncRNAs) is a common feature in all kingdoms of life. As a representative for the branch of prokaryotes, the gram-negative bacterium *Escherichia coli* encodes about 100 small RNAs (sRNA) that are non-translated, short (~50-300 nucleotides) RNA regulators (Raghavan *et al.* 2011; Storz *et al.* 2011). In general, bacterial sRNAs can be divided into three classes depending on their mode of action. The major group acts by base pairing with target mRNAs affecting mRNA stability or translation (Waters and Storz 2009). Another group of small RNAs is transcribed as part of the 5'-UTR of mRNAs that they regulate. These riboswitches can bind ligands and influence steps of transcription termination or translation initiation (Nudler and Mironov 2004). The third group consists of those sRNAs, which act by modifying protein-activity or sequestration of proteins. The 6S RNA as a member of the last group of small, regulatory RNAs has a somewhat special position due to its direct effect on transcription. 6S RNA is the riboregulator that this work focusses on.

2.1 The bacterial 6S RNA

Although the *E. coli* 6S RNA was discovered early and sequenced as the first sRNA its function remained elusive for three decades (Hindley 1967; Brownlee 1971). It was known that 6S RNA is part of a large ribonucleoprotein complex, the protein binding partner was first identified as the multi-subunit RNA polymerase (RNAP) in 2000, however (Lee *et al.* 1978; Wassarman and Storz 2000). Further analysis revealed that 6S RNA is a highly abundant RNA species, which accumulates during the bacterial growth cycle. By comparison of *in vivo* and *in vitro* transcripts its intracellular concentration was estimated to change from 1,000 to 10,000 copies per cell in stationary phase (Wassarman and Storz 2000). Due to this expression profile and the stable association with RNAP 6S RNA was established as important riboregulator for growth phase-dependent adaptation of transcription.

2.1.1 Biogenesis and physiological implications of 6S RNA

In *E. coli* 6S RNA is encoded by the *ssrS* gene, which is part of the highly conserved bacterial operon *ssrS-ygfA*. The downstream located and co-transcribed open

reading frame *ygfA* encodes the metabolic enzyme 5-formyltetrahydrofolate cycloligase, which is involved in C_1-metabolism (Jeanguenin *et al.* 2010). The transcription of the di-cistronic RNA is driven by two tandem promoters, the proximal P1 promoter with a transcription start site (TSS) at -9, relative to the mature 6S RNA and the P2 promoter located more upstream with a TSS at -224. Both promoters are used differentially by the RNA polymerase holoenzyme that contains a variable σ subunit for promoter recognition and transcription initiation. Transcription from the P1 promoter is σ^{70}-dependent and P2 transcription is both σ^{70}- and σ^{38}-dependent (Kim and Lee 2004). Additionally, the P1 and P2 promoter are subjected to differential feedback regulation by 6S RNA. Overexpression of 6S RNA leads to increased P1 transcription and decreased P2 transcription (Lee *et al.* 2013). Moreover, the involvement of several growth phase and stress regulators in 6S RNA expression was documented. The global regulators H-NS, LRP and StpA show a direct negative regulation, FIS, however, shows a dual functional role on *ssrS* regulation (Neußer *et al.* 2008). Transcription of at least the 6S RNA sequence is terminated by a Rho-dependent transcription termination site 90 base pairs downstream of the 3' end of mature 6S RNA (Chae *et al.* 2011). Besides this differential expression of the *ssrS* gene contributing to growth phase-dependent accumulation of 6S RNA there is also a differential processing of the primary transcripts modulating cellular 6S RNA levels as well. The longer P2 transcript is exclusively processed by the endoribonucleolytic RNase E at the 5' end, whereas the short P1 precursor is processed by both RNase E and RNase G at the 5' end. Details of the 3' processing mechanism are not yet solved, although exoribonucleolytic trimming was hypothesized (Kim and Lee 2004).

The search for a physiological function of 6S RNA was originally impeded by the lack of a detectable phenotype for either 6S RNA deletion or overexpressing *E. coli* strains (Hsu *et al.* 1985; Lee *et al.* 1985). Nevertheless, a more recent study showed that conditions of late stationary growth (2 days) provoke a competitive disadvantage of a 6S RNA-deficient strain compared to the wild type. Moreover, these mutant cells exhibit a decreased viability after long-term stationary phase (3 weeks) (Trotochaud and Wassarman 2004). Another growth phenotype related to the loss of 6S RNA was discovered under conditions of high pH, at which cells without 6S RNA are able to survive better than wild-type cells. Thereby a direct gene target of 6S RNA, *pspF*, a transcriptional activator of bacterial stress response, could be identified. Transcription

of *pspF* is normally down-regulated by 6S RNA, hence contributing to efficient allocation of nutrients and growth conditions (Trotochaud and Wassarman 2006).

A more recent study revealed another challenging connection between 6S RNA and the growth phase-specific effector molecule ppGpp. It was shown that the basal ppGpp level was significantly increased in a 6S RNA deletion strain during early stationary growth (Neußer *et al.* 2010). The regulation of ribosomal RNA transcription and most of the translational components is to a great extent mediated by ppGpp during a range of growth conditions. Additionally ppGpp plays a major role in the rapid decrease of rRNA synthesis when cells enter stationary phase (Baracchini and Bremer 1988; Hernandez and Bremer 1990; Aviv *et al.* 1996). As a consequence the loss of 6S RNA and the accompanied elevation of basal ppGpp lead to a reduction in the expression of rRNAs and other ribosomal components during early stationary phase, although this has no detectable effect on the growth rate between Δ*ssrS* mutant and wild type (Neußer *et al.* 2010). In *E. coli* the ppGpp concentration is adjusted by two different enzymes, the ribosome-associated RelA responsible for the rapid synthesis to high concentrations triggered by binding of uncharged tRNAs to the A-site of the ribosome and the bi-functional SpoT, regulating the basal ppGpp concentration by a balanced synthesis and hydrolysis activity. Results from the above study were obtained with both *relA*$^-$ and *relA*$^+$ strains indicating that the lack of 6S RNA is compensated by an altered basal ppGpp level in response to the SpoT activity. In reverse it is unlikely that 6S RNA has a direct effect on SpoT activity although it has been reported that uncharged tRNAs inhibit the hydrolytic activity (Richter 1980). Considering the finding that 6S RNA seems to influence several enzymes of the purine metabolism, an altered purine pool was proposed as cellular signal for SpoT activity (Neußer *et al.* 2010). However, in an independent study the expression of RelA was shown to be directly inhibited by 6S RNA, thus leading to elevated ppGpp levels in the 6S RNA deletion strain (Cavanagh *et al.* 2010). Additional experiments are necessary to unravel this ambiguity and to elucidate the link between 6S RNA and ppGpp.

2.1.2 6S RNA structure-dependent interaction with RNAP

The striking feature of 6S RNA, experimentally and computationally verified in about 100 bacterial species so far, is its characteristic and conserved secondary structure. In general the structure of 6S RNA (Fig. 2.1) can be reduced into three conserved

domains, which are separated by variable stem and bulge structures (Barrick *et al.* 2005). The first domain is called the closing stem composed of the ≥15 nt mainly double-stranded portions of the 5' and 3' sequence ends. Several base pairs and bulged nucleotides are highly conserved in this region. Secondly, the large single-stranded region in the centre of the molecule is termed central bubble. The 5' side of this bulge loop has an average length of 15 nt and is usually longer than the opposite 3' side. Whereas the 5' side has a very low guanosine content and no potential for base pairing interactions the 3' side contains four conserved bases that can form a short hairpin loop with remaining bases. Mutations that close the central bubble or shorten one of its sides abolish the capability to bind RNAP or to inhibit transcription (Trotochaud and Wassarman 2005). The third domain is the terminal loop, which shows lineage-specific variations in overall length and numbers of bulge loops.

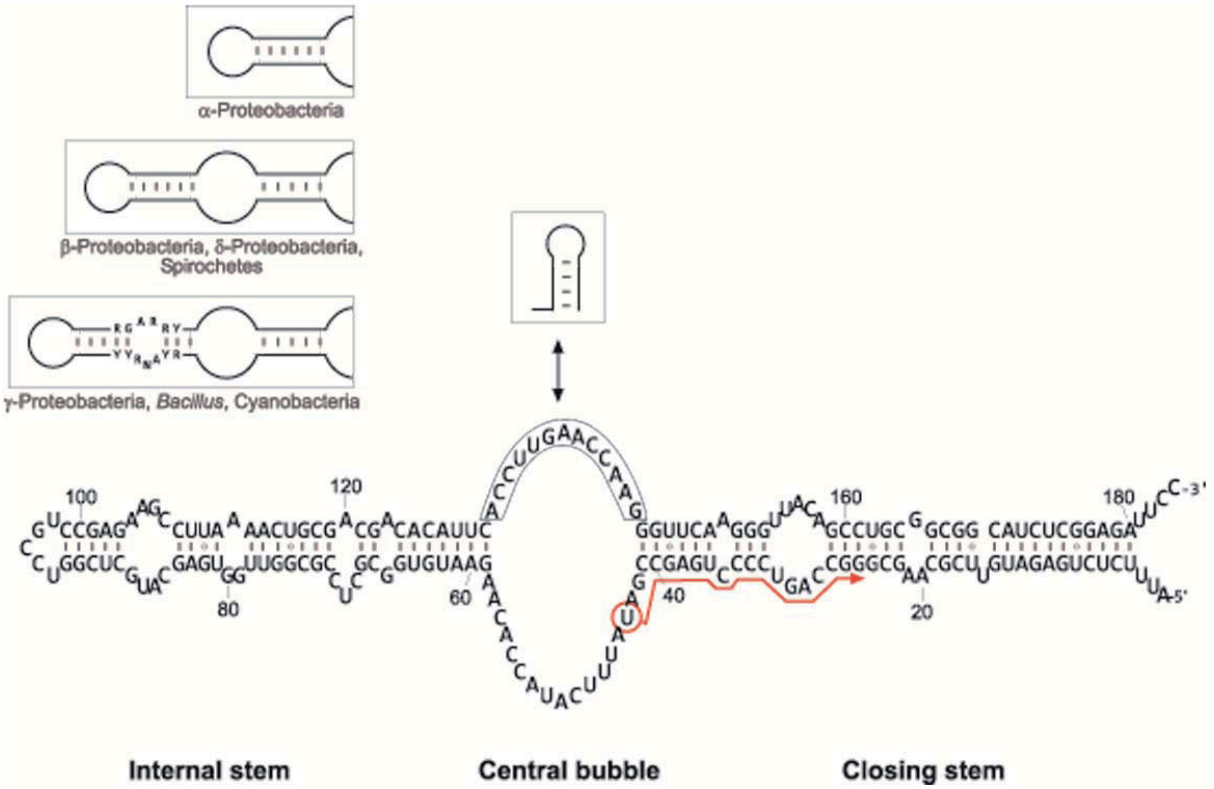

Figure 2.1: *E. coli* 6S RNA secondary structure and lineage-specific variations of the internal stem (boxes on the left; based on (Barrick *et al.* 2005)). The 3' part of the central bubble is in equilibrium of either single-stranded or 4 bp hairpin conformation (box in the middle). The three conserved domains are given below. The pRNA TSS is encircled; the pRNA template region is marked by an arrow.

The characteristics of the 6S RNA secondary structure support the hypothesis that it mimics open promoter DNA. Although there is no similarity with any core promoter sequences within 6S RNA a stable complex formation between 6S RNA and RNAP can be observed. *In vitro* assays demonstrated a preferential binding to the σ^{70}-containing holoenzyme of RNAP ($E\sigma^{70}$). Only modest interaction with 6S RNA was shown for other forms of RNAP ($E\sigma^{38}$, $E\sigma^{32}$ or core RNAP) in the presence of competitor indicating that these complexes are rather non-specific or at least of less specificity than the 6S-$E\sigma^{70}$ complex. No association could be observed between 6S RNA and sigma factor alone. Structural details of the interaction between 6S RNA and $E\sigma^{70}$ from previous studies are rather crude. Several nucleotides of the 3' side of the central bubble and the surrounding stem regions are in close contacts to RNAP subunits β, β' and σ^{70} (Wassarman and Storz 2000; Trotochaud and Wassarman 2005; Gildehaus *et al.* 2007). Moreover, residues around position U44 in the central bubble 5' side of *E. coli* 6S RNA were mapped to be close to the active centre of RNAP (Wassarman and Saecker 2006). The association of 6S RNA and RNAP highly depends on the σ^{70} region 4.2, known to be responsible for the recognition of the -35 promoter DNA element. A mutational analysis of this region showed that positively charged amino acid residues are important for 6S RNA binding. These residues overlap but are also distinct from residues that recognize promoter DNA (Cavanagh *et al.* 2008; Klocko and Wassarman 2009).

Probably due to the low *in vitro* affinity of 6S RNA for RNAP holoenzymes associated with alternative sigma factors, such as σ^{38}, stable endogenous complexes were only detected for RNAP containing the highly abundant, housekeeping sigma factor of *E. coli*, σ^{70} (Wassarman and Storz 2000). σ^{38} is an important regulator for stationary phase transition and maintenance in response to environmental stresses. Although in stationary phase σ^{38} levels are roughly three times lower than for σ^{70}, and, moreover, the affinity for core RNAP is markedly lower in the case of σ^{38}, there is an efficient utilization of σ^{38} in stationary phase (Jishage and Ishihama 1995; Kusano *et al.* 1996). Considering the *in vivo* situation with 1,000 to 3,000 copies of core enzyme per cell and about 700 copies of σ^{70} per cell the vast majority of $E\sigma^{70}$ is complexed by excess 6S RNA thus contributing to preferential σ^{38}-directed transcription initiation in stationary phase (Jishage and Ishihama 1995; Wassarman and Storz 2000). As a consequence a global inhibition of σ^{70}-dependent promoters and an indirect

activation of σ^{38}-dependent promoters would be expected, though several studies indicate a more complicated mechanism of 6S RNA regulation. *In vitro* transcription assays with purified components revealed that 6S RNA interferes with transcription initiation but both σ^{70}- and σ^{38}-dependent promoters as well as their respective holoenzymes are inhibited in the presence of 6S RNA (Gildehaus *et al.* 2007). In contrast, *in vivo* experiments denoted a selective inhibition of some, but not all σ^{70}-dependent promoters in late stationary phase indicating that some kind of promoter specificity must exists for 6S RNA regulation. Moreover, no general activation of stationary phase specific transcription could be observed in these studies (Trotochaud and Wassarman 2004; Cavanagh *et al.* 2008). Comparative and mutational analysis of several promoters in late stationary phase has led to propose two core promoter characteristics that determine sensitivity towards 6S RNA regulation. Whilst the -10 promoter element (consensus sequence TATAAT), which is recognized by σ^{70} region 2, is of less importance for 6S RNA interference the -35 element (consensus TTGACA) interacting with σ^{70} region 4 seems to be critical for this regulation. It was shown that promoters with a weak -35 element (i.e. three or fewer matches to consensus) are inhibited by 6S RNA while those with a perfect consensus are not. Moreover, the presence of an extended -10 element characterized by a 'TG' motif two base pairs upstream of the -10 element (consensus TGnTATAAT) also favours 6S RNA inhibition. Considering these two promoter features hundreds of mapped *E. coli* promoters were predicted to be down-regulated by 6S RNA. A further microarray analysis of a late stationary transcriptome reinforced the 6S RNA-dependent inhibition of 68% of the predicted genes (Cavanagh *et al.* 2008). By reason of the remarkable high cellular concentrations of 6S RNA, even during exponential growth, an independent microarray analysis was performed with cells grown to mid-exponential and early stationary phase. About 500 genes were differentially expressed in a 6S RNA-dependent manner in this study and the corresponding promoters could neither be correlated to specific promoter classes, such as σ^{70}- or σ^{38}-specific, nor could the promoter features mentioned above be applied entirely (Neußer *et al.* 2010). The inconsistent results between these studies may be explained by the different growth conditions, nevertheless the question of promoter specificity for 6S RNA-mediated regulation is not completely answered.

2.1.3 6S RNA-templated pRNA transcription

The special importance of 6S RNA as a non-coding, regulatory RNA is further highlighted by an unique interaction in which the intrinsically DNA-dependent RNAP engages 6S RNA as a template in the active centre and gives rise to the *de novo* synthesis of small product RNAs (pRNAs) (Wassarman and Saecker 2006; Gildehaus *et al.* 2007). For *E. coli* 6S RNA the position U44 in the 5' side of the central bubble was identified as the start site of pRNA transcription directing the RNAP to read the 6S template towards the 5' end (see Fig. 2.1). However, the 5' end is not fully transcribed and *in vitro* transcription experiments yielded pRNAs with 14 to 20 nt in length. Moreover, these *in vitro* assays revealed that efficient pRNA transcription is activated by generally higher substrate NTP concentrations than required for DNA-dependent transcription. As a consequence of this reaction the stable 6S RNA-RNAP complex becomes disintegrated which is accompanied by a detachment of the 6S-pRNA hybrid from RNAP (Wassarman and Saecker 2006; Gildehaus *et al.* 2007; Wurm *et al.* 2010). These findings were also experimentally verified for the *in vivo* situation. Although there is no detection of endogenous pRNA in stationary phase, when 6S RNA levels are highest, pRNA synthesis was shown to emerge under conditions of outgrowth from stationary phase. Outgrowth is connected to a rapid increase in NTP pools likely triggering pRNA transcription by the predominant 6S-RNAP complexes (Murray *et al.* 2003; Wassarman and Saecker 2006). This mechanism allows the release of the inhibitory 6S RNA from RNAP, which can resume transcription when cells enter exponential growth again (Fig. 2.2). Efficient pRNA synthesis is an intrinsic property of genuine 6S RNAs. Expression of a mutant *E. coli* 6S RNA, which was modified in the 5' side of the central bubble and showed likewise neither pRNA transcription nor release from $E\sigma^{70}$ resulted in significant delay of outgrowth. In addition overexpression of this mutant in stationary grown cells led to a decreased viability further demonstrating the importance of de-repression of 6S RNA inhibition by pRNA-mediated release (Cavanagh *et al.* 2011).

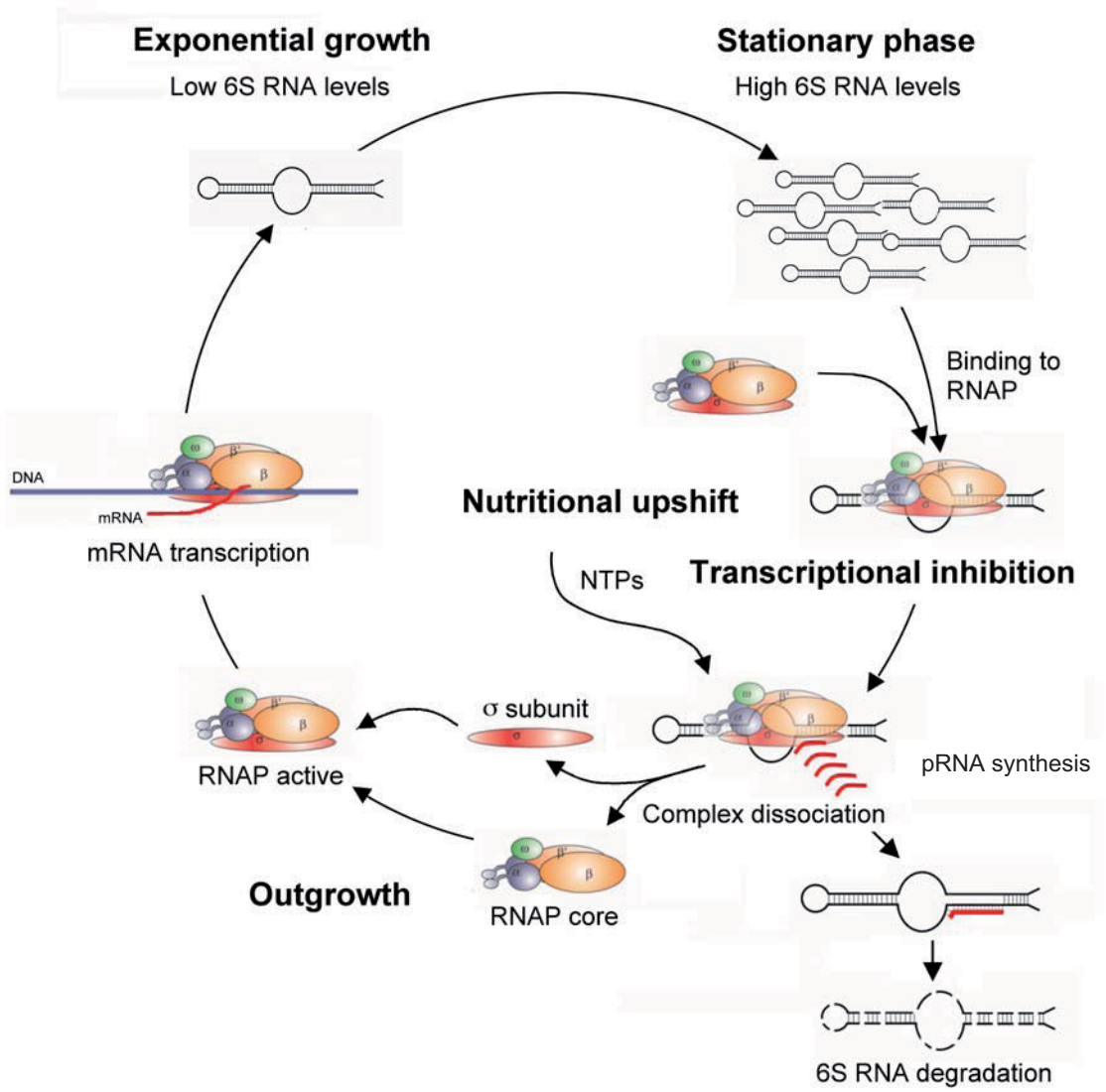

Figure 2.2: Schematic cycle of growth phase-dependent transcription regulation through 6S RNA (taken from (Wurm *et al.* 2010)).

The pRNAs synthesized *in vivo* accumulate immediately (in a range of seconds) after nutritional upshift and exhibit time-dependent length heterogeneity. There is an initial burst of smaller transcripts (10-13 nt), which are subsequently replaced by longer ones (16-20 nt). The latter are stably hybridized to the 6S RNA template. These results indicate that pRNAs are generated by multiple round transcription thus resembling abortive transcripts, which are a common feature of all RNA polymerases initiating at DNA promoters (Carpousis and Gralla 1980; Wurm *et al.* 2010). The synthesis of pRNAs ceases after approximately 10 minutes and the short half-life of free pRNAs was estimated to be less than 30 seconds. Moreover, even 6S RNA itself

is destabilized upon pRNA transcription. An apparent half-life of less than 30 minutes was calculated probably due to the complex decay with RNAP and intramolecular structural alterations of 6S RNA (see 3.2). The fact that pRNA synthesis yields transcripts with a length of about 20 nt, which stay annealed to the 6S template, is unusual and different to DNA-dependent transcription. The ordinary RNA-DNA heteroduplex reaches a length of about 10 bp before it is destabilized and the growing RNA chain leaves the RNA polymerase via the exit channel. The heteroduplex is thermodynamically disfavoured relative to the corresponding DNA double strand, which, involving the conserved lid structure of the RNAP β' subunit, leads to the release of the nascent RNA chain (Naryshkina *et al.* 2006). In case of the 6S-pRNA duplex, which shows perfect complementarity compared to the original secondary structure in the pRNA template region reannealing of 6S RNA structure is impeded and synthesis of longer RNA chains is enabled. It is likely that this property has structural consequences finally contributing to the disintegration of the 6S-pRNA-RNAP complex (Wurm *et al.* 2010).

2.1.4 Specialized 6S RNA regulation in other organisms

Although first discovered and characterized intensively in *E. coli*, 6S RNA is distributed widely among eubacteria. It is not only found among the large class of γ-proteobacteria, to which *E. coli* belongs to, but also far distant bacilli species (phylum firmicutes) harbour 6S RNA homologues. A well-studied representative of this group is *Bacillus subtilis*. Interestingly, *B. subtilis* has two differentially expressed 6S RNAs, 6S-1 and 6S-2, which are not conserved in their primary sequence. While 6S-1 RNA has a similar expression profile as *E. coli* 6S RNA with maximal concentrations in stationary phase, the 6S-2 RNA level exhibits a peak in mid-logarithmic phase and declines afterwards (Barrick *et al.* 2005; Beckmann *et al.* 2011). Both 6S-1 and 6S-2 RNA bind the housekeeping form of RNAP ($E\sigma^A$ in *B. subtilis*) but only 6S-1 RNA was shown to serve as a template for efficient pRNA synthesis and release from RNAP (Beckmann *et al.* 2011; Cavanagh *et al.* 2011). Intriguingly, cells expressing 6S-2 RNA in the absence of 6S-1 RNA display a delayed outgrowth from stationary phase indicating that there is a different biological function of each 6S RNA (Cavanagh *et al.* 2011). The reason for unequal pRNA transcription and deregulation of $E\sigma^A$ by 6S-2 RNA was recently shown to reside in the sequence of the central bubble region. Particularly the identity of the starting nucleotide (iNTP), which is GTP

for 6S-1 and ATP for 6S-2 RNA, contributes to efficient pRNA transcription initiation by *B. subtilis* RNAP but not *E. coli* RNAP (Cabrera-Ostertag *et al.* 2013). Quite recently an additional phenotype for a 6S-1 RNA deletion strain was discovered. Cells lacking 6S-1 RNA were shown to initiate the formation of endospores at earlier times than wild-type cells indicating that 6S-1 RNA is important for regulation of drastic developmental processes upon starvation or nutrient limitation. In this context a faster reduction of the nutrient content of the environment was observed for the 6S-1 RNA deletion strain compared to either wild-type or 6S-2 RNA deletion strains (Cavanagh and Wassarman 2013).

In addition to *E. coli* and *B. subtilis* several studies have led to the identification of 6S RNA homologous in pathogenic bacterial species. In *Legionella pneumophila* (class γ-proteobacteria) for instance 6S RNA was found based on secondary structure predictions, expression analysis and coimmunoprecipitation with RNAP. As a deletion of 6S RNA significantly reduced the intracellular multiplication in protist and mammalian host cells, 6S RNA is considered to optimize gene expression for such pathogenic developmental stages in *L. pneumophila* (Faucher *et al.* 2010). Other 6S RNA-containing pathogens are *Staphylococcus aureus* (class bacilli) and *Helicobacter pylori* (class ε-proteobacteria) (Bohn *et al.* 2010; Sharma *et al.* 2010). Next to these even the distantly related photoautotrophic phylum of cyanobacteria was shown to harbour 6S RNAs (Watanabe *et al.* 1997). Several 6S RNA molecules of this group are further characterized in this work (3.1).

Surprisingly, functional homologues of bacterial 6S RNA can actually also be found in eukaryotic systems. Mouse B2 RNA and human Alu RNA bind highly specific to RNA polymerase II thereby repressing transcription at promoters related to heat shock. In contrast to 6S RNA the eukaryotic RNA regulators co-occupy RNA polymerase II bound to DNA, thus preventing proper DNA-RNAP interactions during closed complex formation. The altered conformation of such a ternary complex remains transcriptionally inactive on the DNA (Espinoza *et al.* 2004; Yakovchuk *et al.* 2009). Moreover, B2 RNA was mapped to the DNA cleft and the active site region of RNAP II (Ponicsan *et al.* 2013). As a consequence B2 RNA can serve as a template for a 18 nt extension on its 3’ end by RNAP II. This reaction destabilizes the RNA-RNAP interaction and facilitates the removal of B2 RNA from RNAP II catalysed by an additional factor present in nuclear extracts (Wagner *et al.* 2013).

2.2 The bacterial RNA polymerase: Structural insights

RNA polymerase is the central enzyme of gene expression and exists as multisubunit protein complex in two major forms. The catalytic core RNAP in bacteria consists of five subunits ($\alpha_I\alpha_{II}\beta\beta'\omega$), which are conserved in structure and function among all cellular organisms. Whereas six to ten additional proteins are required in eukaryotes and archaea, only a single polypeptide termed σ subunit is necessary to constitute the bacterial holo form of RNAP, which is necessary for promoter recognition and transcription initiation (Werner and Grohmann 2011). The *E. coli* σ^{70} subunit (or σ^{A} in other bacteria) belongs to a primary σ factor family with conserved domains, which are described in more detail in 3.3. Therefore the important functional domains within the rest of the holo RNAP shall be presented here in short.

The overall structure of the *E. coli* RNAP σ^{70} holoenzyme, as determined recently by X-ray, is similar to the crystal structures of RNAPs from the *Thermus* genus resembling a crab-claw-like shape (Murakami *et al.* 2002; Vassylyev *et al.* 2002; Murakami 2013). This structure consists of two pincers, which constitute the DNA-binding cleft and the active site of the enzyme (Fig. 2.3). The pincers are formed by the two largest subunits β and β'. While the remaining core subunits α_2 and ω assemble on the opposite of the claw structure, the σ^{70} subunit stretches along the core on the dorsal side. There are several interaction sites between σ^{70} and the core, the most extensive ones are formed between the u-shaped part of σ^{70} (regions 1.2 to 2.4) and the N-terminal portion of the β' subunit. The σ^{70} regions 3.0 and 3.1 are loosely bound to the core although bridging the two pincers of the claw. Region 3.2 shows a well ordered loop structure that protrudes into the active site cleft establishing several contacts to the rudder and lid structures of the β' subunit. Finally, the C-terminal region 4 of σ^{70} interacts with the flap tip helix of β and the β' zinc finger domain (Vassylyev *et al.* 2002). The active centre of the RNAP is defined by three aspartate residues of the absolutely conserved NADFDGD β' motif, which is responsible for chelating the Mg^{2+} ion (Zaychikov *et al.* 1996). Another important structural motif of the active site is the β' subunit bridge helix separating the deep RNAP cleft into a DNA-binding main channel and a secondary channel, which serves for the entry of substrate NTPs (Zhang *et al.* 1999). The bridge helix plays a crucial role in the nucleotide addition cycle comprising the binding of new NTPs and the translocation of the RNA/DNA hybrid. Several crystallographic studies revealed the

bridge helix in either a straight or bent form indicating alternating conformations, which are important for translocation (Cramer *et al.* 2001; Vassylyev *et al.* 2002). This action is assisted by the β' subunit trigger loop helix.

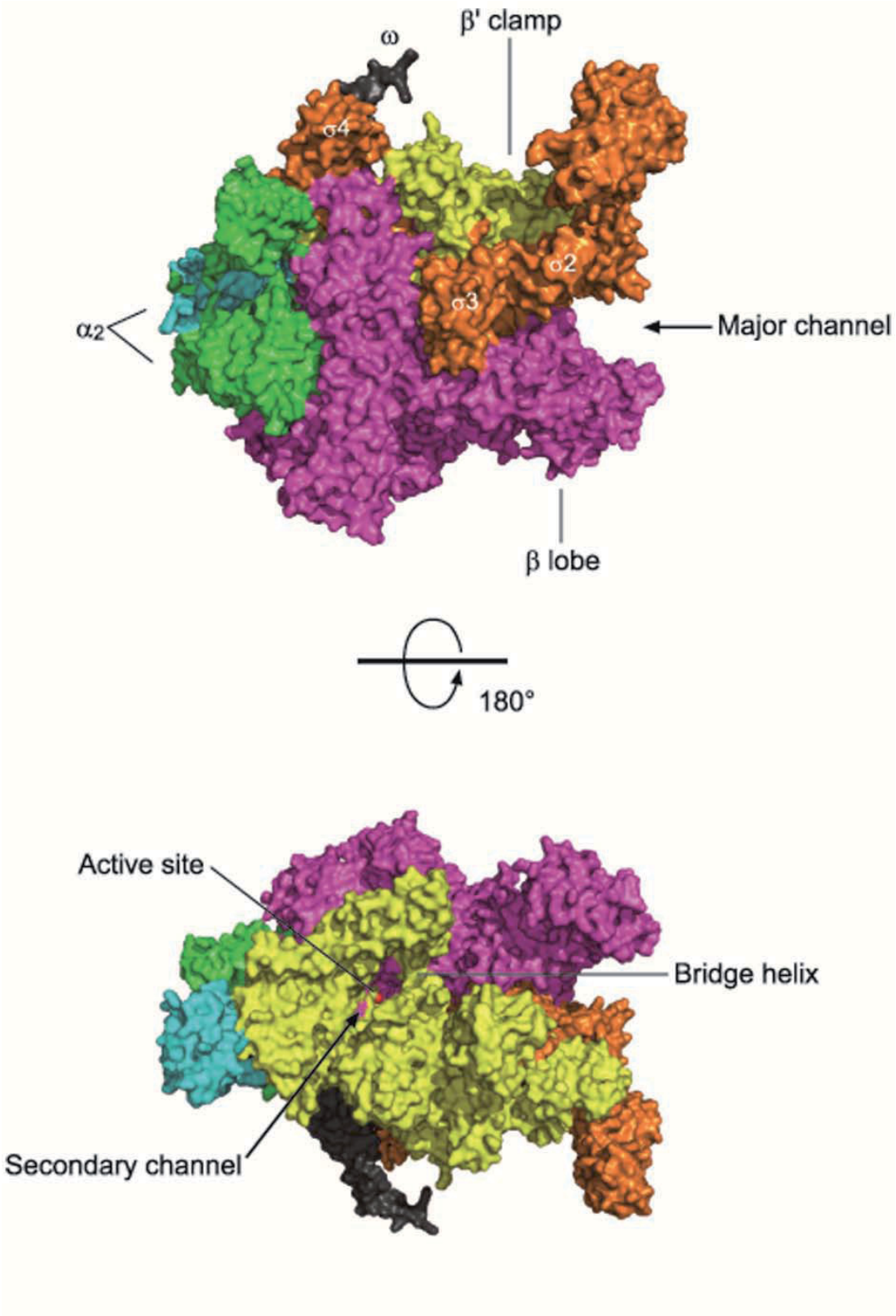

Figure 2.3: Overview and selected details of the *E. coli* RNAP σ^{70} holoenzyme crystal structure (pdb ID: 4IGC). The RNAP is shown in surface representation and the subunits are coloured as follows: α_I, green; α_{II}, cyan; β', yellow; β, magenta; ω, black; σ^{70}, orange. The Mg^{2+} in the active site is shown as red sphere. The β' clamp and the β lobe mainly constitute the two pincers of the crab-claw structure. Distribution of the σ^{70} regions 2-4 is given.

2.3 Aims of this work

The regulatory 6S RNA was shown to stably associate with the major form of RNA polymerase holoenzyme ($E\sigma^{70}$) and to inhibit transcription from many promoters in a growth phase-specific manner. The interaction with RNAP bases on a characteristic 6S RNA secondary structure, which mimics an open DNA promoter. In addition the single-stranded central domain of 6S RNA is placed in the RNAP active site in a way that allows the unusual RNA-templated transcription of small RNA oligomers (pRNAs). The limited structural information about the 6S-RNAP complex is restricted to rough assignments of 6S RNA residues to RNAP subunits. Therefore this work is intended to deepen the structural knowledge and the molecular details of this ribonucleoprotein complex and 6S RNA-dependent pRNA synthesis, respectively.

In a first approach the secondary structures of several putative cyanobacterial 6S RNAs shall be determined. Heterologous binding assays of these 6S RNAs and *E. coli* RNAP should give new information on 6S RNA diversity. A comparison of the RNAs likely allows us to identify 6S RNA regions important for RNAP interaction. Moreover, focussing on *E. coli* 6S RNA structural probing experiments of free 6S RNA and 6S-pRNA hybrids are planned. These should unravel structural alterations of 6S RNA and molecular details of the 6S-RNAP complex decay upon pRNA transcription.

A subsequent analysis of 6S RNA in complex with RNAP shall give a picture of 6S-RNAP interaction sites in a three-dimensional manner due to the lack of a solved 6S RNA or 6S-RNAP crystal structure. Therefore a biochemical approach is scheduled using a chemical nuclease that can be tethered to single cysteine residues distributed along functional domains of the σ^{70} protein. A deduced three-dimensional model based on the gathered cleavage data should yield new insights into the functional and structural properties of 6S RNA in complex with RNA polymerase.

3 Results

The major topic of this PhD thesis was an extended structural and functional analysis of the transcriptional riboregulator 6S RNA from *E. coli*. Thereby both conformational states of 6S RNA, free and in complex with its protein binding partner RNA polymerase were studied. Furthermore 6S RNAs from *E. coli* and distantly related cyanobacteria were analysed for structural transitions upon the transcription of 6S RNA-regulating pRNAs. The results pertinent to this research topic were summarized in three publications, one Point-of-View article and a review article, which has recently been submitted.

3.1 Heterologous investigation of cyanobacterial 6S RNA function

The article “6S RNA – an old issue became blue-green” engages in the characterization of four predicted 6S RNAs from the cyanobacterial species *Synechocystis*, *Synechococcus*, *Prochlorococcus* and *Nostoc*. After the capability of these 6S RNAs to bind *E. coli* RNA polymerase has been ascertained, heterologous studies were initiated including pRNA synthesis and 6S RNA-RNAP complex decay assays. In addition, three of four cyanobacterial 6S RNA secondary structures were determined by enzymatic and chemical probing experiments. Taken together these data established the RNAs studied as bona fide 6S RNAs that inhibit the properties of *E. coli* 6S RNA. Moreover, initial *in vivo* experiments denoted a noticeable growth defect phenotype for a *Synechocystis* 6S RNA deletion mutant. Thus a general role of 6S RNA in providing a better fitness under certain growth conditions could be reinforced.

Microbiology (2012), **158**, 2480–2491 DOI 10.1099/mic.0.058958-0

6S RNA – an old issue became blue-green

Anne Rediger,[1]† René Geißen,[2]† Benedikt Steuten,[2] Beate Heilmann,[1] Rolf Wagner[2] and Ilka M. Axmann[1]

Correspondence
Rolf Wagner
r.wagner@rz.uni-duesseldorf.de

[1]Institute for Theoretical Biology, Charité-Universitätsmedizin, Invalidenstraße 43, D-10115 Berlin, Germany

[2]Molecular Biology of Bacteria, Heinrich-Heine University Düsseldorf, Universitätsstr. 1, D-40225 Düsseldorf, Germany

6S RNA from *Escherichia coli* acts as a versatile transcriptional regulator by binding to the RNA polymerase and changing promoter selectivity. Although homologous 6S RNA structures exist in a wide range of bacteria, including cyanobacteria, our knowledge of 6S RNA function results almost exclusively from studies with *E. coli*. To test for potential structural and functional conservation, we selected four predicted cyanobacterial 6S RNAs (*Synechocystis*, *Synechococcus*, *Prochlorococcus* and *Nostoc*), which we compared with their *E. coli* counterpart. Temperature-gradient gel electrophoresis revealed similar thermodynamic transition profiles for all 6S RNAs, indicating basically similar secondary structures. Subtle differences in melting behaviour of the different RNAs point to minor structural variations possibly linked to differences in optimal growth temperature. Secondary structural analysis of three cyanobacterial 6S RNAs employing limited enzymic hydrolysis and in-line probing supported the predicted high degree of secondary structure conservation. Testing for functional homology we found that all cyanobacterial 6S RNAs were active in binding *E. coli* RNA polymerase and transcriptional inhibition, and had the ability to act as template for transcription of product RNAs (pRNAs). Deletion of the 6S RNA gene in *Synechocystis* did not significantly affect cell growth in liquid media but reduced fitness during growth on solid agar. While our study shows that basic 6S RNA functions are conserved in species as distantly related as *E. coli* and cyanobacteria, we also noted a subtle degree of divergence, which might reflect fundamental differences in transcriptional regulation and lifestyle, thus providing the first evidence for a possible physiological role in cyanobacteria.

Received 29 February 2012
Revised 13 June 2012
Accepted 4 July 2012

INTRODUCTION

6S RNA was initially discovered in *Escherichia coli* in 1967 (Hindley, 1967), and some years later was shown to exist as a ribonucleoprotein complex in the cell (Lee *et al.*, 1978). No function could be assigned until the year 2000, when a major breakthrough was made by the discovery that the protein associated with 6S RNA is RNA polymerase and that this small non-coding RNA apparently regulates transcription (Wassarman & Storz, 2000). This finding initiated broad interest, and since then a plethora of studies has appeared, generating the basis of our present knowledge of this interesting riboregulator. With rapid genome sequencing and bioinformatics tools it became clear that 6S RNA is widespread in bacteria and characterized by a conserved secondary structure rather than by primary sequence. The structure consists of a single-stranded central bulge within a highly double-stranded molecule and is essential because it mimics a DNA template in an open promoter complex (Barrick *et al.*, 2005; Brow & Ellis, 2005). Thus, the 6S structure enables transcription initiation by RNA polymerase holoenzyme on itself (Barrick *et al.*, 2005; Gildehaus *et al.*, 2007; Trotochaud & Wassarman, 2005). Most of the functional studies were confined to the *E. coli* system, and we know that 6S RNA in that organism accumulates in stationary phase, forming stable complexes with RNA polymerase holoenzyme containing the sigma factor σ^{70}, responsible for exponential growth. This leads to the inhibition of transcription for many but not all σ^{70}-dependent promoters, and facilitates the adaptation to stationary phase and environmental stress (Cavanagh *et al.*, 2008; Gildehaus *et al.*, 2007; Trotochaud & Wassarman, 2004, 2006). Additional functions for 6S RNA have been discovered by genome-wide transcriptome studies, indicating that the molecule is important for central steps in the metabolism of the cell, such as growth phase adaptation or carbon and purine metabolism (Geißen *et al.*, 2010; Neußer *et al.*,

†These authors contributed equally to this work.

Abbreviations: pRNA, product RNA; TGGE, temperature-gradient gel electrophoresis.

Nine supplementary figures and a supplementary table are available with the online version of this paper.

2010). Our previous studies also revealed that there is a link between 6S RNA and the global regulator ppGpp, which affects growth rate, ribosome synthesis and the translational capacity of the cell (Cavanagh *et al.*, 2010; Neußer *et al.*, 2010). A particularly striking discovery was the observation that 6S RNA can serve as a template for the *de novo* transcription of small RNAs [de novo RNAs (dnRNAs) or product RNAs (pRNAs)] when stationary cells encounter better nutritional conditions (Gildehaus *et al.*, 2007; Wassarman & Saecker, 2006; Wurm *et al.*, 2010). This finding implies that the small RNA acting as transcriptional regulator templates its own regulatory RNA (Kugel & Goodrich, 2007).

The widespread nature of 6S RNA among eubacteria has raised the question whether 6S RNA is a universal regulator and if there is functional conservation of 6S RNAs from different organisms. With the exception of a partial characterization of 6S RNA from *Legionella pneumophila*, indicating its involvement in virulence (Faucher *et al.*, 2010), and 6S-1 RNA from *Bacillus subtilis* implicated in transcriptional fine-tuning (Beckmann *et al.*, 2011), almost nothing is known about the function of 6S RNAs in other organisms. Here we were especially interested in the molecular functions of 6S RNA within cyanobacteria because they are different in many features from other bacteria.

The phylum cyanobacteria is highly diverse, with at least 10 000 species known to date populating all regions on Earth such as freshwater, oceans and hot springs, or living in symbioses with plants or marine sponges. Fossil and molecular studies suggest that the archetype of cyanobacteria thrived successfully for billions of years (Schopf, 1993). Photosynthesis evolved early in ancient cyanobacteria, enriching our atmosphere in oxygen.

For two freshwater species, *Synechococcus* PCC 6301 and *Synechocystis* PCC 6803, a 6Sa RNA (encoded by the *ssaA* gene) was described for the first time (Watanabe *et al.*, 1997) without recognizing that the cyanobacterial 6Sa RNA is the orthologue of the γ-proteobacterial 6S RNA. Later on, extensive sequence comparisons revealed that the highly stable secondary structure of 6S RNA can be predicted for cyanobacteria as well (Barrick *et al.*, 2005).

Interestingly, earlier analyses of 6S RNA accumulation in cyanobacteria have revealed different results. In contrast to *E. coli*, where 6S RNA accumulation can be observed during entry into stationary phase, in *Synechococcus* PCC 6301 the opposite has been found (Watanabe *et al.*, 1997). In *Prochlorococcus* MED4, two 6S RNA transcripts exist with different lengths. Maximal accumulation is observed either at high cell densities (220 nt transcript) or earlier (332 nt transcript), probably during entry into stationary phase (Axmann *et al.*, 2007). The expression of 6S RNA of *Prochlorococcus* MED4 is not affected by other conditions employed, and the RNA has been shown to be very stable (half-life >1 h) (Axmann *et al.*, 2005). The existence of two differentially expressed 6S RNAs, 6Sa (6S-2 RNA) and 6Sb (6S-1RNA), has already been shown for *B. subtilis*, in which 6Sb is the orthologue of *E. coli* 6S RNA, and 6Sa has diverged functionally (Barrick *et al.*, 2005).

This study was conducted to test the structural and functional conservation of 6S RNA in cyanobacteria and to compare their properties with the characteristic functions of *E. coli* 6S RNA, which had already been analysed in more detail. The study should contribute to understanding cyanobacterial regulation by small RNAs and enable more specific investigations in future.

METHODS

Bacterial strains and growth conditions. The Δ*ssrS E. coli* strain KS-1, an MG1655 derivative, constructed by a one-step homologous recombination (Datsenko & Wanner, 2000), was a friendly gift of K. Shanmugarajah. Liquid cultures of *Synechocystis* PCC 6803 wild-type and the Δ*ssaA* mutant strains were grown at 30 °C in BG11 medium (Rippka *et al.*, 1979) under continuous illumination with white light of 80 μmol photons·m^{-2}·s^{-1} and a continuous stream of air. The medium for the mutant strains was supplemented with 25 μg kanamycin ml^{-1}.

Mutagenesis. The complete *Synechocystis* sequence region *ssaA* encoding the 6S RNA was deleted and replaced by a resistance marker gene, which enables the isolation of generated mutants. For homologous recombination a construct was generated which included a kanamycin-resistance cassette flanked by 700 bp regions upstream and downstream of the *ssaA* gene (Fig. S7). Primers for the two-step overlap extension PCRs are listed in Table S1, available with the online version of this paper. This construct was used to transform *Synechocystis* as described elsewhere (Ermakova *et al.*, 1993).

Complementation of the *E. coli* 6S RNA deletion strain with cyanobacterial homologues. For the complementation of the *E. coli* Δ*ssrS* strain KS-1 we inserted the PCR-generated 6S RNA genes of *Synechocystis*, or *Synechococcus* flanked by *Eco*RI/*Sma*I restriction sites, into the vector pKK223-3 under the control of the tac promoter. PCR primers are listed in Table S1. Cloning resulted in the vectors pKK-6803-6S and pKK-7942-6S. The vector pKK-6S containing the *E. coli* 6S RNA gene was used as a control. Competent *E. coli* KS-1 cells were transformed and positive transformants selected by their resistance to ampicillin.

Preparation of 6S RNAs. The different 6S RNA sequences were isolated as PCR fragments from genomic DNA of the respective cyanobacteria and transcribed by T7 RNA polymerase (AmpliScribe T7-Flash Transcription kit; Epicentre). Primers for the amplification of the cyanobacterial 6S RNA genes are presented in Table S1. *E. coli* 6S RNA was prepared by *in vitro* transcription with purified T7 RNA polymerase and linearized pUC18-T7 derivatives, which contained the respective 6S RNA gene sequence behind the T7 Φ10 promoter (Gildehaus *et al.*, 2007).

Preparation of *E. coli* RNA polymerase. *E. coli* RNA polymerase holoenzyme was purified according to published procedures (Burgess & Jendrisak, 1975; Gonzalez *et al.*, 1977).

Temperature-gradient gel electrophoresis (TGGE). Temperature-dependent structural transitions of *in vitro*-transcribed 6S RNAs were analysed by TGGE, as described by Rosenbaum & Riesner (1987). Prior to electrophoresis RNAs were heated in 50 mM sodium cacodylate, pH 7.2, 100 mM NaCl, 0.5 mM EDTA, 1 mM DTT for 10 min at 70 °C and slowly refolded (1 °C min^{-1}). Each RNA (1–1.5 μg) was

separated on a native 7.5 % polyacrylamide gel stabilized by GelBond films (Gel-Fix, Serva). Optimal temperature gradients (low temperature 15–21 °C, high temperature 50–70 °C) were determined in pilot experiments. RNAs were visualized by silver staining (Beidler *et al.*, 1982).

RNA 3′ end-labelling. Radioactive labelling of 6S RNAs was done by ligase-catalysed addition of [^{32}P]pCp. One microgram of each RNA was incubated with 20 units T4 RNA ligase (NEB) and 20 μCi [5′-^{32}P]pCp in 10 % DMSO overnight at 4 °C. Samples were extracted with phenol and resolved after ethanol precipitation in 10 mM Tris/HCl, pH 8, 1 mM EDTA.

Enzymic and chemical probing. For the enzymic hydrolysis, ~120 nM radiolabelled 6S RNA was incubated with 10 mU RNase V1 (Pharmacia) in 20 mM Tris/HCl, pH 7.2, 200 mM NaCl and 10 mM $MgCl_2$ or 20 mU RNase T1 (Sankyo) in 50 mM Tris/HCl, pH 7.5 and 1 mM EDTA for 10 min at 30 °C. After phenol/chloroform extraction and ethanol precipitation, the cleavage products were separated on 12 % denaturing polyacrylamide gels. The in-line probing reactions contained ~250 nM radiolabelled 6S RNA, 50 mM Tris/HCl, pH 8.5, and 20 mM $MgCl_2$, and were incubated for 42 h at 23 °C (Soukup & Breaker, 1999). After ethanol precipitation the samples were loaded on 12 % denaturing polyacrylamide gels.

RNA sequencing ladders were generated by alkaline hydrolysis with ~250 nM radiolabelled 6S RNA incubated in the presence of 2 μg tRNA as carrier in 50 mM Na_2CO_3/$NaHCO_3$, pH 9.5, for 5 min at 95 °C.

RNA polymerase binding and complex stability assays. 3′ End-labelled 6S RNAs (15 nM each) were incubated with increasing concentrations of RNA polymerase as indicated for 10 min at 30 °C in 80 mM potassium glutamate, 50 mM Tris/acetate, pH 8, 10 mM magnesium acetate, 1 mM DTT, 0.1 mM EDTA and 10 μg acetylated BSA ml^{-1}. Complexes were challenged with 100 ng heparin μl^{-1} for an additional 5 min at 30 °C. For the analysis of complex stability, pre-formed 6S RNA–RNA polymerase complexes were supplemented with varying NTP concentrations (0–500 μM) and incubated for 5 min at 30 °C. Samples were separated on native 5 % polyacrylamide gels and visualized by autoradiography.

Multiple-round *in vitro* transcription. Multiple-round *in vitro* transcription reactions were performed with 15 nM RNA polymerase in 80 mM potassium glutamate, 50 mM Tris/acetate, pH 8, 10 mM magnesium acetate, 1 mM DTT, 0.1 mM EDTA and 10 μg acetylated BSA ml^{-1}. Five nanomolar superhelical plasmid pSH666-2 (P. Schoengraf, unpublished results) harbouring different *E. coli* promoters (*rrnB* P1, P*tac*, *bolA*, RNA 1 and *hisL*) served as template. Reaction mixtures contained increasing concentrations of 6S RNA (0–500 nM) as indicated. After 5 min at 30 °C transcription was started by the addition of an NTP mix containing 65 μM each of ATP, GTP and UTP, 5 μM CTP and 133 nM [α-^{32}P]CTP. Samples were incubated for an additional 8 min at 30 °C and reactions were stopped by addition of a chase solution (2 mM ATP, CTP, GTP, UTP, 2 μg heparin μl^{-1} and 1 mM Tris/HCl, pH 8). After mixing with formamide loading buffer, samples were separated on 10 % denaturing polyacrylamide gels and visualized by autoradiography.

6S RNA-templated *de novo* synthesis of pRNA. The synthesis of 6S RNA-templated *de novo* products was performed as described previously (Wurm *et al.*, 2010). Reaction mixtures contained 300 nM 6S RNA as template, 50 nM RNA polymerase, 300 μM each of ATP, GTP and UTP, 5 μM CTP and 133 nM [α-^{32}P]CTP. Samples were extracted with phenol, precipitated with ethanol and separated on 15 % denaturing polyacrylamide gels.

RESULTS

Given the bioinformatics prediction of 6S RNA genes in almost all sequenced cyanobacteria and the experimental evidence for several different strains that these genes are expressed (Axmann *et al.*, 2005, 2007; Watanabe *et al.*, 1997) (see also Fig. S1) we wished to know whether predicted cyanobacterial 6S RNA molecules exhibit properties and/or functions similar to those demonstrated for the well-characterized *E. coli* 6S RNA (Gildehaus *et al.*, 2007; Wassarman, 2007; Wassarman & Storz, 2000; Wassarman & Saecker, 2006; Wurm *et al.*, 2010). For the analysis we selected four examples [*Synechocystis* sp. PCC 6803, *Synechococcus elongatus* PCC 7942, *Prochlorococcus* MED4 and *Nostoc* sp. PCC 7120 (named below *Synechocystis*, *Synechococcus*, *Prochlorococcus* and *Nostoc*, respectively)], which were distantly related on the phylogenetic map (Fig. S1). Interestingly, the 6S RNA genes are often located downstream of *purK* (encoding phosphoribosylaminoimidazole carboxylase), which is reminiscent of the situation in many entero- and γ-proteobacteria, where the 6S RNA gene is co-transcribed with the *ygfA* gene, also involved in purine metabolism (Barrick *et al.*, 2005; Jeanguenin *et al.*, 2010).

Comparison of the secondary structures and thermodynamic stabilities of 6S RNAs from cyanobacteria

The secondary structure predictions for the selected cyanobacterial 6S RNAs are generally in agreement with the respective *E. coli* 6S RNA secondary structure, which consists of a largely single-stranded central bulge flanked by two non-contiguous helical stem regions (Figs 1b and S3). This structure has been experimentally verified (Barrick *et al.*, 2005; Gildehaus *et al.*, 2007; Trotochaud & Wassarman, 2005). One exception results from a 5′ sequence extension of the *Prochlorococcus* 6S RNA, which can be transcribed from two different promoters, giving rise to a long (332 nt) and a short form (220 nt) in the cell (Axmann *et al.*, 2007). Both RNAs are significantly longer than *E. coli* 6S RNA or the other cyanobacterial 6S RNAs (generally below 200 nt), slightly obscuring structure comparison.

The secondary structure of *E. coli* 6S RNA gives rise to a very characteristic melting behaviour, which can readily be observed by altered mobilities during TGGE (Wagner, 2006). To test the reliability of the predicted cyanobacterial 6S RNA structures and to analyse their thermodynamic stabilities we performed TGGE experiments (Fig. 1). A characteristic, partly irreversible transition to slower gel mobility was visible at 46 °C for the *E. coli* 6S RNA (Fig. 1a), very likely reflecting the cooperative melting of the structure, which initiates at the two helical arms flanking the central bubble and proceeds into the neighbouring stem regions (see scheme in Fig. 1b). The resulting change in mobility can be taken as a specific signature for typical 6S RNA secondary structures. In fact, all four cyanobacterial 6S RNAs analysed exhibited similar electrophoresis

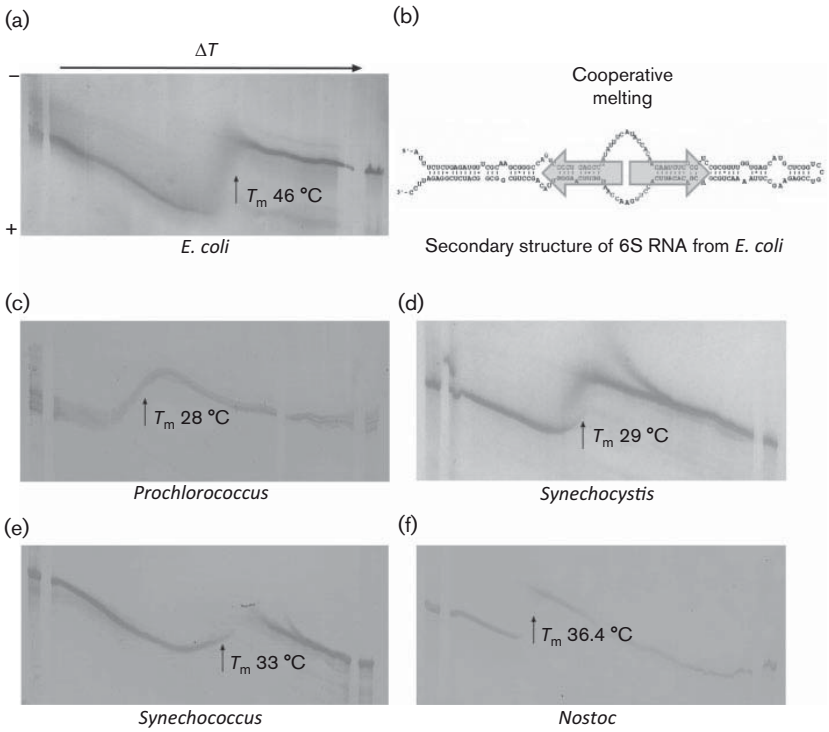

Fig. 1. TGGE analysis of different cyanobacterial 6S RNAs. Representative TGGE analyses are shown for *E. coli* (a), *Prochlorococcus* (c), *Synechocystis* (d), *Synechococcus* (e) and *Nostoc* (f). Temperature gradients are indicated by a horizontal arrow in (a). The electrophoresis direction is from top (−) to bottom (+). The melting temperatures for the main transition are indicated by arrows. The likely direction of cooperative RNA melting is indicated by two open arrows in a secondary structure scheme for *E. coli* 6S RNA presented in (b).

patterns on the TGGE gels (Fig. 1c–f). However, compared with the *E. coli* 6S RNA, the transition temperature representing cooperative melting of the secondary structure was lower and differed slightly for the individual cyanobacterial 6S RNAs. The characteristic melting temperatures derived from the TGGE gels (indicated by arrows in Fig. 1) varied between 28 °C (*Prochlorococcus*) and 36 °C (*Nostoc*) and, interestingly, the order of melting temperatures correlated with the optimal growth temperature of the different bacteria tested. In the case of *Synechococcus* (Fig. 1e) and *Synechocystis* (Fig. 1d), additional bands are visible on the high-temperature side of the gel, which merge with the main band. These bands likely indicate co-existing structures of the 6S RNA molecules, which disappear at higher temperature. As opposed to the rather discontinuous mobility transitions of 6S RNAs from *E. coli*, *Synechocystis*, *Synechococcus* and *Nostoc*, the transition for *Prochlorococcus* was continuous, indicating an ordered, more reversible melting process. This is consistent with the prediction of a different closing stem structure for *Prochlorococcus* 6S RNA that prevents the complete disruption of the 5′ and 3′ ends in one step, and rather causes a consecutive melting of the stem structures involved. While a general common secondary structure appears to be conserved for 6S RNAs, the results also indicate subtle structural differences, possibly reflecting specific adaptation to the individual lifestyles of different organisms.

Structural probing analysis of 6S RNAs from *Synechocystis*, *Synechococcus* and *Nostoc*

Limited enzymic hydrolysis and spontaneous cleavage (in-line probing) of 6S RNAs labelled with [^{32}P]pCp at the 3′ ends was employed to verify and compare the secondary structures of the different cyanobacterial 6S RNAs (Soukup & Breaker, 1999; Wagner, 2006). Enzymic reactions were performed with guanosine-specific RNase T1, which preferentially cleaves non-base-paired structures, and the double strand-specific RNase V1 from cobra venom was used to map helical and base-paired regions. Single-stranded structures were additionally identified by the in-line probing method based on their reduced chemical stability (Soukup & Breaker, 1999). Results are shown in Fig. 2, where the probing patterns of 6S RNAs from *Synechocystis*, *Synechococcus* and *Nostoc* after separation on

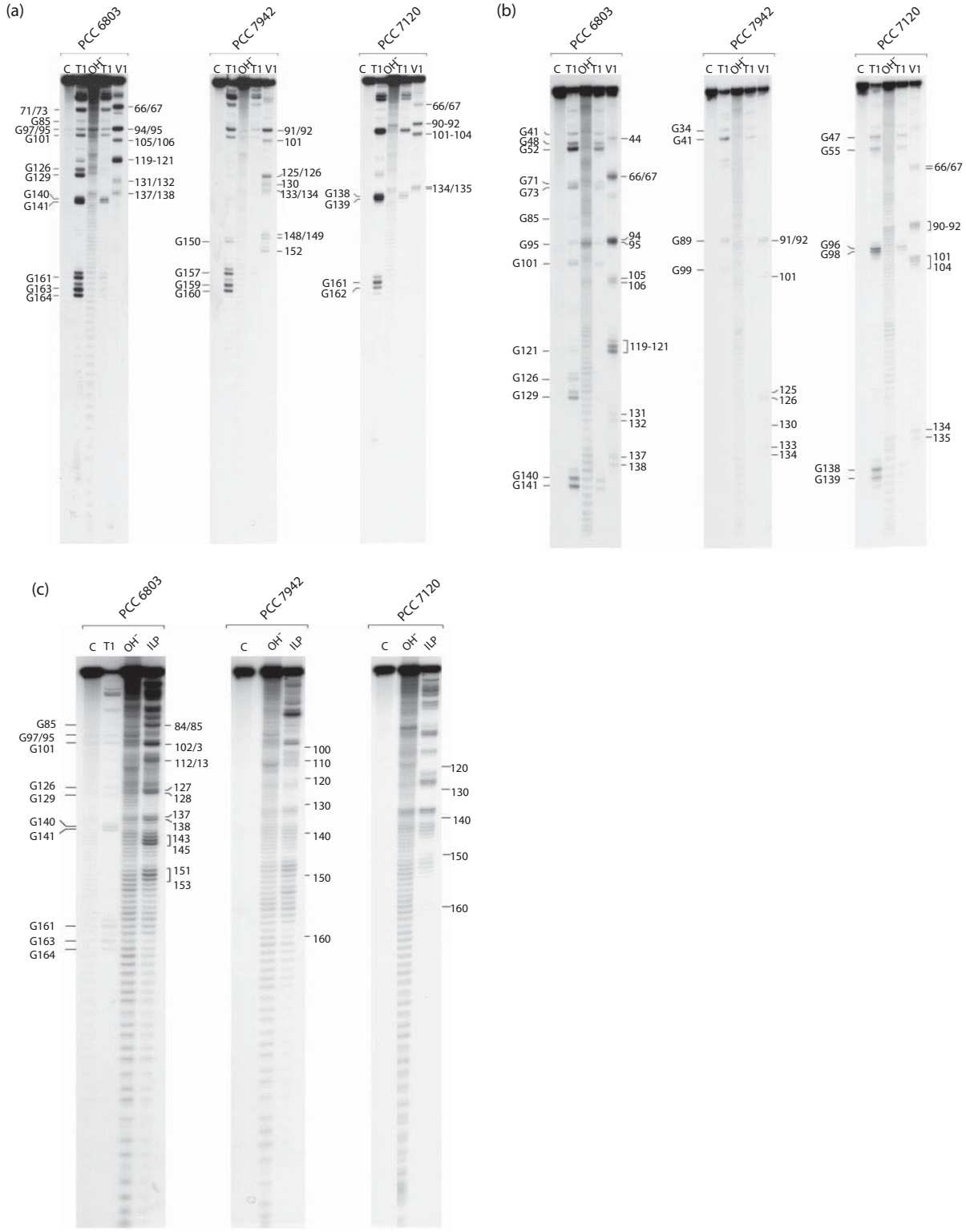
(a)
PCC 6803
PCC 7942
PCC 7120
C T1 OH- T1 V1
71/73
G85
G97/95
G101
66/67
94/95
105/106
119-121
G126
G129
131/132
G140
G141
137/138
G161
G163
G164
91/92
101
125/126
130
133/134
G150
148/149
152
G157
G159
G160
G138
G139
134/135
G161
G162
90-92
101-104
(b)
PCC 6803
PCC 7942
PCC 7120
C T1 OH- T1 V1
G41
G48
G52
44
G71
G73
66/67
G85
G95
G101
94
95
105
106
119-121
G121
G126
G129
131
132
137
138
G140
G141
G34
G41
G89
G99
91/92
101
125
126
130
133
134
G47
G55
66/67
G96
G98
90-92
101
104
134
135
G138
G139
(c)
PCC 6803
PCC 7942
PCC 7120
C T1 OH- ILP
C OH- ILP
G85
G97/95
G101
84/85
102/3
112/13
G126
G129
127
128
G140
G141
137
138
143
145
151
153
G161
G163
G164
100
110
120
130
140
150
160
120
130
140
150
160

Fig. 2. Structural probing of 6S RNAs from *Synechocystis*, *Synechococcus* and *Nostoc*. Results from enzymic secondary structure probing are shown. (a) Short gel electrophoretic separation of 6S RNA samples from *Synechocystis* (PCC 6803), *Synechococcus* (PCC 7942) and *Nostoc* (PCC 7120) (from left to right) after limited enzymic hydrolysis. T1, RNA after hydrolysis with guanosine-specific RNase T1 (left, 20 mU; right, 10 mU); V1, cobra venom RNase (double strand-specific); OH^-, alkaline ladder; C, unreacted control RNA. Characteristic sequence positions are depicted at the margin of each panel (left, RNase T1; right, V1). (b) For a better resolution of the 5′ sequence a longer gel electrophoretic separation of the same analysis as in (a) is shown. (c) Results from in-line probing (ILP) are presented. In C and OH^-, unreacted control RNAs and samples after alkaline hydrolysis are separated, respectively. The left panel *Synechocystis* (PCC 6803) contains a T1 lane to indicate relevant guanosine positions, and characteristic positions prone to in-line attack are marked in the right margin. In the mid and right panels, sequence length positions for the different *Synechococcus* (PCC 7942) and *Nostoc* (PCC 7120) 6S RNA hydrolysis products are indicated.

denaturing gels are presented. For better resolution a short (Fig. 2a) and a long separation (Fig. 2b) of the enzymic probing analyses are shown. The in-line probing results are depicted in Fig. 2(c). The results from structural probing have been used as constraints for secondary structure predictions by mfold (Zuker, 2003). Clearly, all three cyanobacterial 6S RNAs exhibit great structural homology, with two irregular helices flanking a largely single-stranded central domain (Fig. S3) consistent with the TGGE melting pattern (Fig. 1). The experimentally derived structures are also very similar to recently published suboptimal secondary structures, allowing a better view of the conserved elements (Pánek *et al.*, 2011). One interesting point of the probing results deserves mention: in all cases the 3′ central domain (3′-CD) exhibits ambiguous structural elements, with overlapping sites accessible for both single (RNase T1 and ILP) and double strand-specific probes (RNase V1). Similar probing results have also been observed for RNA from *E. coli* (Barrick *et al.*, 2005). We take this as evidence for the occurrence of co-existing structures with only minor differences in stability. Indications for co-existing structures were already apparent from the TGGE experiments (see Fig. 1 above). Comparison of the structures reveals a second interesting point. All three structures indicate that the start position for pRNA synthesis is located in the unstructured part (5′ central domain) of the molecules. Accordingly, a multiple sequence alignment of the different 6S RNA structures (Fig. S4) unmasked regions of sequence conservation. Interestingly, the parts of the structures encoding pRNAs exhibit a significant degree of conservation.

Cyanobacterial 6S RNAs bind specifically to RNA polymerase from *E. coli*

It is known that 6S RNA from *E. coli* specifically interacts with the σ^{70} holoenzyme of RNA polymerase, which is responsible for transcription of the housekeeping genes during exponential growth. Contact sites on the RNA have been identified for *E. coli* (Gildehaus *et al.*, 2007) and the RNA polymerase β, β' and σ^{70} subunits have been shown to be in contact with the 6S RNA from *E. coli* and *Haemophilus influenzae* (Gildehaus *et al.*, 2007; Wassarman & Storz, 2000). Moreover, a detailed analysis has identified sites within the σ^{70} subunit which likely interact with *E. coli* 6S RNA (Klocko & Wassarman, 2009). No direct interaction could be shown with the isolated sigma factors and only weak, possibly non-specific, binding was observed to the RNA polymerase core enzyme. Generally, bacterial RNA polymerases are highly conserved with respect to structures and function. RNA polymerases from cyanobacteria, however, are known to contain an additional γ subunit, which represents a split β' gene (Schneider *et al.*, 1987; Xie *et al.*, 1989). Based on *in vitro* transcription studies it has also been reported that the two enzymes from *Calothrix* PCC 7601 and *E. coli* are not completely interchangeable (Schyns *et al.*, 1998). However, despite subtle differences in the RNA polymerase architecture, a general recognition of heterologous *E. coli* or *Nostoc* promoters and transcription initiation could be demonstrated for the different enzymes (Schneider *et al.*, 1987). Encouraged by the latter observation and considering the general functional conservation of RNA polymerases among bacteria we performed heterologous binding experiments with the different cyanobacterial 6S RNAs and the purified RNA polymerase holoenzyme from *E. coli*. Binding assays were performed with 3′-^{32}P end-labelled 6S RNA and increasing concentrations of RNA polymerase holoenzyme Eσ^{70} under standard conditions (see Methods). Complex formation was analysed by gel retardation, as described previously (Wurm *et al.*, 2010), and the results are presented in Fig. 3. Since direct 3′ end-labelling of the *Prochlorococcus* 6S RNA turned out to be inefficient we analysed binding of this RNA species by a competition assay (Fig. 3b). 6S RNAs from *Synechocystis*, *Synechococcus* and *Nostoc* were able to form specific complexes with *E. coli* RNA polymerase with affinities close to that of the homologous *E. coli* 6S RNA (Fig. 3a). Binding of 6S RNA from *Prochlorococcus* to RNA polymerase could also be demonstrated by efficient competition for pre-formed RNA polymerase complexes with 6S RNA from *Synechocystis* (Fig. 3b). The presence of heparin in all binding experiments assured the specificity of the complexes formed. It is also evident from Fig. 3 that more than one complex is formed, particularly for 6S RNAs from *Synechocystis* and *Synechococcus*. Although we cannot exclude the putative existence of multiple conformations of RNA–holoenzyme complexes, formation of more than one complex on native polyacrylamide gels has also been

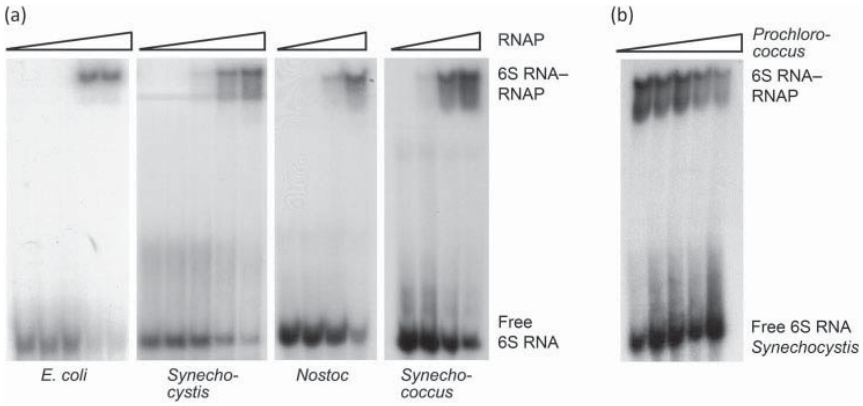

Fig. 3. 6S RNAs from different cyanobacteria bind specifically to RNA polymerase from *E. coli*. (a) Gel retardation analysis (5 % polyacrylamide) of radiolabelled 6S RNA from *E. coli* and three cyanobacterial representatives (*Synechocystis*, *Nostoc* and *Synechococcus*) at increasing concentrations of *E. coli* RNA polymerase holoenzyme (0, 5, 15, 50 nM and additionally 100 nM for *E. coli* and *Synechocystis* 6S RNA). The positions of free RNAs and the 6S RNA–RNA polymerase complexes are indicated in the right margin. (b) Binding competition analysis of pre-formed radiolabelled *Synechocystis* 6S RNA–RNA polymerase (50 nM) complexes with increasing concentrations (0, 15, 50, 100 and 200 nM) of non-labelled *Prochlorococcus* 6S RNA on a retardation gel.

reported for RNA polymerase and 6S RNA from *E. coli*, and in that case it was shown that the band with the higher mobility represented core RNA polymerase–6S RNA complexes (Gildehaus *et al.*, 2007). Since the RNA polymerase preparation contained some free core enzyme it is likely that the two complex bands observed also represent core and holoenzyme complexes. In summary, the experiment demonstrates that all four investigated cyanobacterial 6S RNAs are capable of forming specific complexes with *E. coli* RNA polymerase in much the same way as the homologous RNA, underlining their potential involvement in transcription regulation.

Cyanobacterial 6S RNAs inhibit transcription *in vitro*

It has been shown that 6S RNA from *E. coli* is able to inhibit *in vitro* transcription from a variety of promoters (Gildehaus *et al.*, 2007). Therefore we compared the ability of the different cyanobacterial 6S RNAs to interfere specifically with transcription under the same conditions. Transcription reactions were performed with a multi-promoter template harbouring a set of different *E. coli* promoters, which differ in regulatory properties and promoter strength (*rrnB* P1, *tac*, *bolA*, RNA 1 and *hisL*). Each promoter gives rise to a transcript of defined length due to the *rrnB* tandem terminators, which are positioned at a defined downstream site. The results from multiple-round *in vitro* transcription reactions performed in the presence of increasing concentrations of the respective 6S RNAs are shown in Fig. 4. The specificity of 6S RNAs regulating transcription was tested in a control reaction, where instead of 6S RNA, increasing amounts of tRNA were added. The analyses revealed similar inhibition patterns for all four cyanobacterial 6S RNAs in comparison with the *E. coli* 6S RNA, with slightly weaker inhibition for 6S RNA from *Prochlorococcus* and *Synechococcus*. The amount of 6S RNA to reach half-maximal inhibition varied slightly for the different 6S RNAs and was also not identical for the individual promoters tested. The observed differences in the degree of inhibition for the different cyanobacterial 6S RNAs can be explained by subtle differences in the affinities of the RNAs for *E. coli* RNA polymerase, but may also reflect an unidentified promoter-specific component, a property which is also known for *E. coli* 6S RNA (Cavanagh *et al.*, 2008; Gildehaus *et al.*, 2007; Neußer *et al.*, 2010). The addition of increasing concentrations of tRNA did not affect the transcription of any promoters notably, underlining the specificity of the 6S RNAs to act as transcriptional repressors. In summary, we conclude that cyanobacterial 6S RNAs, like their *E. coli* counterpart, are able to act as specific transcriptional inhibitors. Moreover, as demonstrated for *E. coli*, inhibition seems to depend on specific promoter properties.

Cyanobacterial 6S RNAs serve as templates for the *de novo* synthesis of small pRNAs

The most striking property of 6S RNA is its function as an RNA polymerase template, directing the synthesis of small RNAs, which themselves serve as regulators of 6S RNA activity (Gildehaus *et al.*, 2007; Wassarman & Saecker, 2006; Wurm *et al.*, 2010). 6S RNA-directed *de novo* transcription of small RNAs (pRNAs) occurs in the cell at high concentrations of substrate NTPs, for instance, when cells recover from stationary phase after a nutritional

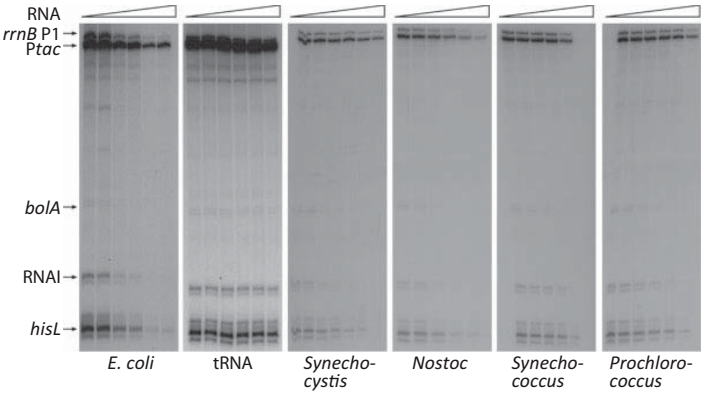

Fig. 4. Inhibition of transcription by cyanobacterial 6S RNAs. (a) Gel electrophoretic separation of multiple-round *in vitro* transcription products obtained in the presence of increasing amounts of 6S RNAs (0, 10, 50, 100, 250 and 500 nM) from different species. Transcription reactions were performed with *E. coli* RNA polymerase and a multi-promoter vector (Methods). Transcription products originating from the different promoters are depicted in the left margin.

upshift. The reaction has been analysed in detail in *E. coli*, but 6S RNA-directed pRNA transcripts have also been reported in other bacteria, such as *B. subtilis* and *Helicobacter pylori*, mainly based on deep sequencing approaches (Beckmann *et al.*, 2011; Irnov *et al.*, 2010; Sharma *et al.*, 2010). The existence of 6S RNA-templated small RNAs has also been observed from whole-transcriptome sequencing analysis of several different cyanobacteria. For instance, a potential pRNA transcript, slightly larger (~30 nt) than the ones observed in *E. coli*, was detected by genome-wide mapping of transcription start sites in *Synechocystis* (Mitschke *et al.*, 2011). In principle, the small RNAs may also arise as antisense transcription products directed from a possible convergent promoter. In fact, a sequence with reasonable similarity to cyanobacterial promoters can be found on the *ssaA* antisense strand in *Synechocystis*. To verify that the observed small RNA derives from a 6S RNA-templated transcription we performed *in vitro* reactions with purified RNA polymerase, NTP substrates and cyanobacterial 6S RNAs in the absence of any DNA under conditions that lead to the well-characterized synthesis of pRNAs in *E. coli*. In Fig. 5, the generation of small 6S RNA-derived transcripts at increasing RNA polymerase concentrations is exemplified for 6S RNAs from *E. coli* and *Synechocystis*. In the case of *E. coli* 6S RNA the characteristic products of 15 to 20 nt starting from sequence position U44 can be seen (Wurm *et al.*, 2010). A similar reaction pattern is apparent for *Synechocystis* 6S RNA, although a series of longer transcripts, up to 30 nt, consistent with the results from genome-wide sequencing, is formed (Fig. 5a). We take this as evidence that the *E. coli* RNA polymerase can substitute for the homologous enzyme in this reaction. Considering the length of the pRNA transcripts and the deep sequencing data (Mitschke *et al.*, 2011), the deduced start site of the transcript matches with the single-stranded U47 and reads into the irregular helix of the closing stem (Fig. 5b).

To confirm that the *in vitro*-generated products are indeed identical to the genuine pRNA sequence we tested the identity of the sequences by hybridization to specific DNA

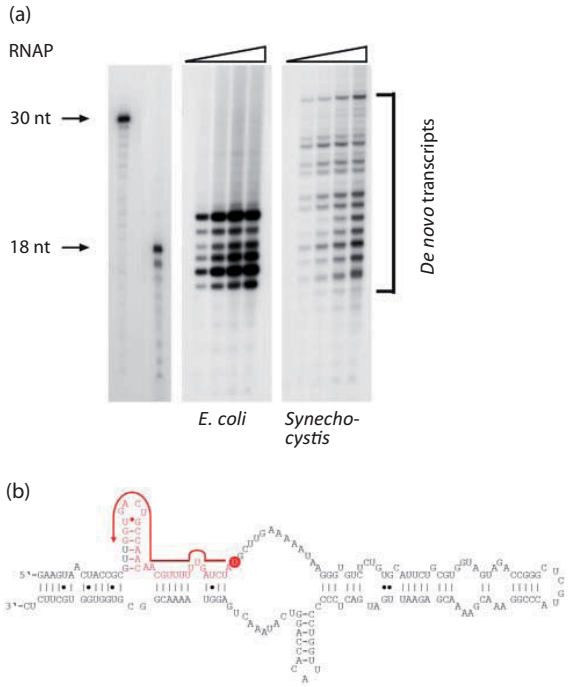

Fig. 5. Cyanobacterial 6S RNAs serve as templates for the synthesis of small pRNAs. (a) 6S RNA-templated synthesis of pRNAs in the absence of DNA with increasing concentrations of *E. coli* RNA polymerase (0, 50, 100, 200 and 500 nM). *E. coli* and *Synechocystis* 6S RNA at 300 nM each was employed as indicated. An NTP mix (300 μM each of ATP, GTP, UTP and 5 μM CTP) containing 133 nM [α-^{32}P]CTP was used for product labelling. Bands representing *de novo* transcription products are indicated on the right. Size markers are shown next to the left panel. (b) Secondary structure arrangement of *Synechocystis* 6S RNA, with the start point and direction of pRNA transcription indicated by an arrow.

oligonucleotides. Results for the products obtained from *Synechocystis* and *Synechococcus* clearly confirmed the correctness of the *in vitro*-generated pRNAs (Fig. S5). Experiments performed with the other cyanobacterial 6S RNAs revealed that in all cases small RNAs were formed, although they differed in yield and length distribution (Fig. S6). The results also demonstrate that the small RNAs identified by deep sequencing are very likely products derived from RNA-templated transcription and not from any antisense promoter. Moreover, we conclude that formation of 6S RNA-templated pRNAs seems to be a common mechanism not only in γ-proteobacteria and firmicutes but also in the phylogenetically distant cyanobacteria. The length difference noted and a possible specific influence of the pRNA sequences are matters for more detailed future studies.

6S RNA-directed *de novo* synthesis of small pRNAs causes disintegration of RNA polymerase–cyanobacterial 6S RNA complexes

It has been demonstrated that synthesis of pRNAs in *E. coli* is a key reaction to disintegrate the stable RNA polymerase–6S RNA complexes, which sequester almost all RNA polymerase molecules in the cell during stationary phase. Rapid recovery from this inhibition is necessary when the nutritional conditions improve and active transcription of housekeeping genes is required. The synthesis of pRNAs is triggered in the cell by an increase in substrate NTPs as a consequence of nutritional upshift (Wassarman & Saecker, 2006; Wurm *et al.*, 2010). The situation can be mimicked *in vitro*, and RNA polymerase–6S RNA complexes start to transcribe small RNAs when the NTP concentration is raised above 10 μM (Wurm *et al.*, 2010). Hence, we analysed the stability of pre-formed inhibitory complexes between RNA polymerase and cyanobacterial 6S RNAs under conditions of increasing concentrations of substrate NTPs. As has been demonstrated before for *E. coli*, not only do increasing NTP concentrations give rise to small RNA synthesis but also a concomitant decay of the RNA polymerase 6S RNA complexes can be observed for cyanobacterial 6S RNAs from *Synechocystis*, *Synechococcus* and *Nostoc* (Fig. 6). It is also apparent that the small RNAs formed during the 6S RNA-directed transcription remain stably associated with the template 6S RNA and migrate as an RNA–RNA complex during gel electrophoresis, in the same way as that shown for *E. coli* (Wurm *et al.*, 2010). The results show that synthesis of pRNAs in cyanobacteria reverses the inhibitory effect of the 6S RNA template. Furthermore, the data indicate a common mechanism for all 6S RNAs, possibly involving similar structural changes that trigger the disintegration of the inhibitory complex.

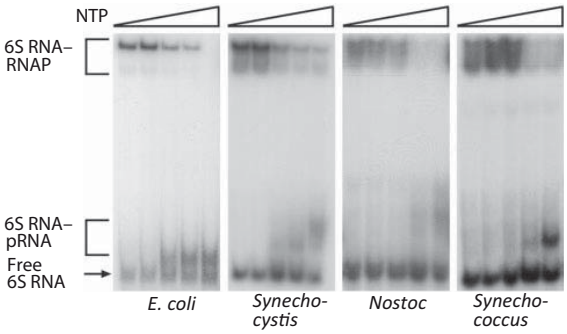

Fig. 6. 6S RNA–RNA polymerase complex decay at high NTP concentrations. Complexes between RNA polymerase (50 nM) and 15 nM of each radiolabelled 6S RNA from *E. coli*, *Synechocystis*, *Nostoc* and *Synechococcus* (indicated below the gel) were incubated with increasing concentrations of all four NTPs (0, 5, 50, 100 and 500 nM). Reaction mixtures were separated on 5 % native polyacrylamide gels. Bands representing the free 6S RNAs, the hybrid of the complementary pRNAs and the 6S RNA, as well as the 6S RNA–RNA polymerase complexes are indicated in the left margin.

Construction and phenotypic characterization of a *Synechocystis* 6S RNA deletion mutant

Although 6S RNA affects transcription of many genes *in vivo* (Neußer *et al.*, 2010), deletion of the 6S RNA gene (*ssrS*) in *E. coli* does not reveal a notable phenotype when analysed under rich growth conditions, and only subtle differences could be detected when mutants were observed under long-term stress or starvation (Trotochaud & Wassarman, 2004, 2006), indicating that 6S RNA improves the fitness of cells under stress conditions. To test whether similar observations can be made for 6S RNA deletions in cyanobacteria, we constructed a *Synechocystis* 6S RNA deletion strain. Deletion of the *Synechocystis ssaA* gene was achieved by homologous recombination with a kanamycin-resistance cassette flanked by upstream and downstram sequences of the *ssaA* gene (Fig. S7). Two positive clones (del6S-K5 and del6S-K7) were verified by PCR and Northern blot analysis and further used for growth characterization. No significant change in growth behaviour was detected due to the *ssaA* deletion, and both mutants exhibited similar growth curves in liquid cultures, with marginally faster growth compared with the wild-type (Fig. S8a). A difference in fitness was apparent, however, when the two *ssaA* mutants were grown on agar plates after serial dilutions (Fig. S8b). The number of living cells taken from an early exponential culture (OD_{750} 0.2) appeared to be drastically reduced for the two deletion mutants, and this was visible after transfer to an agar plate (Fig. S8b, left panel). Likewise, during later growth (OD_{750} 0.6), serial dilution revealed that both deletion mutants were still significantly reduced in the number of living cells (Fig. S8b, right panel). Possibly, cells which are growing as a layer on an agar surface are directly exposed to the light, such that the standard light conditions (80 μmol photons m^{-2} s^{-1}) can become light-stress. In contrast, cells in a liquid culture may shadow each other. We conclude from this preliminary

observation that, as observed for *E. coli*, cyanobacterial 6S RNAs may function to provide better fitness under certain growth conditions, in this case light.

DISCUSSION

In this study we have analysed the functions of a selection of cyanobacterial 6S RNAs and compared the results with the known properties of 6S RNA from *E. coli*, for which detailed functional information has already been collected. The secondary structures among different 6S RNA molecules, which are predicted under conditions that allow suboptimal structures according to Pánek *et al.* (2011), already suggested a certain functional conservation for these RNA regulators. TGGE analyses demonstrated that the cyanobacterial 6S RNAs share the characteristic thermodynamic melting transition with the *E. coli* homologue, consistent with a common overall secondary structure. The results from structural probing analyses of three cyanobacterial 6S RNAs largely supported the predicted structures (Fig. S3). Distinct sequence variations between the individual RNAs result in slightly different melting temperatures of the major transition, and may indicate a specialized adaptation to the optimal growth temperature and a different lifestyle. It is tempting to speculate that in addition to differences in thermal stability small structural variations may also contribute to specific stability within the cell. This could be an explanation for the differences in steady-state concentrations of 6S RNAs from *Synechocystis* and *Synechococcus* during heterologous expression in *E. coli* (Fig. S9). Since both RNAs are expressed from identical vectors with the same copy number per cell, we infer that the difference in concentration is very likely the result of a structure-dependent difference in turnover at the growth temperature for *E. coli* (37 °C).

All tested 6S RNAs were able to bind specifically to the *E. coli* RNA polymerase holoenzyme, and to inhibit *in vitro* transcription from a set of *E. coli* promoters. It is interesting to note in this respect that the first systematic studies of transcription initiation sites (TISs) for cyanobacteria revealed general features of the cyanobacterial promoter architecture not too divergent from *E. coli*: a conserved −10 region (TAnnnT) about 6 bp upstream of the TIS, which is a purine in most cases. Also, elements with similarity to the enterobacterial −35 box (5′-TTGnnn-3′) have been detected (Mitschke *et al.*, 2011; Vogel *et al.*, 2003).

Most notably, we demonstrated that all tested cyanobacterial 6S RNAs were able to serve as templates for the synthesis of small pRNAs. We could show, furthermore, that the latter reaction induced the decay of the inhibitory complex between 6S RNAs and RNA polymerase. This reaction has been shown to be of physiological importance for *E. coli* in re-establishing a functional population of RNA polymerase during outgrowth from stationary phase. Even so, the 6S RNA interaction with cyanobacterial RNA polymerase should be tested in the future because of the presence of a split subunit β' encoded by two separate genes, *rpoC1* and *rpoC2* (Xie *et al.*, 1989). Thus, future experiments using RNA polymerase from cyanobacteria might uncover further details of gene transcription in these organisms.

The subtle structural differences among the diverse cyanobacterial 6S RNAs are reflected in a corresponding modulation of the activity for the characteristic functions analysed in this study. In several of our assays, the 6S RNA from *Nostoc* exhibited a higher degree of functional homology with *E. coli*. This is noticeable for the similarity of the TGGE pattern, the efficiency in inhibiting transcription from DNA promoters, and the specificity of the pRNA products. 6S RNA from *Prochlorococcus*, however, which deviates considerably in length, gives rise to a noticeably different secondary structure prediction and only displays similar folding with the other 6S RNAs when suboptimal structures are considered. It is not surprising that 6S RNA from *Prochlorococcus* shows the largest functional deviation with respect to the other cyanobacterial 6S RNAs. This was observed, for instance, in the melting transition and the reduced capacity to inhibit *in vitro* transcription from the strong P*tac* or *rrnB* P1 promoters. The somewhat aberrant structure may also explain the failure of 3′ end-labelling *Prochlorococcus* 6S RNA by a ligation reaction. One might speculate that the specific structure and length of *Prochlorococcus* 6S RNA could be an adaptation to its particular niche, the upper layer of the ocean. Moreover, the 6S RNA expression pattern is very distinct for marine *Prochlorococcus* and *Synechococcus* strains, and thus might correlate with their habitat. In a previous study, all *Prochlorococcus* strains investigated, including MED4, that are adapted to high-light conditions exhibited two signals for 6S RNA, at approximately 200 and 300 nt, whereas RNA from the low-light-adapted *Prochlorococcus* and *Synechococcus* strains analysed gave only a single signal at approximately 180 nt (Axmann *et al.*, 2007).

A particularly interesting observation is the striking genetic organization of many cyanobacterial 6S RNA genes directly adjacent to the *purK* gene, which encodes an enzyme involved in purine metabolism (Fig. S1). A similar genetic link is found in many enterobacteria and γ- and ε-proteobacteria, where 6S RNA genes are often co-transcribed with genes involved in purine metabolism (Sharma *et al.*, 2010). This genetic co-localization obviously represents a functional link, at least in *E. coli*, where a differential expression for several enzymes involved in the biosynthesis and salvage of purines has been reported in a 6S RNA-deficient mutant (Neußer *et al.*, 2010). It has been shown that *E. coli* 6S RNA is functionally connected not only to purine metabolism but also to the basal concentration of the global regulator ppGpp (Cavanagh *et al.*, 2010; Neußer *et al.*, 2010), which reflects a stress signal and mirrors changes in the nutritional status of the cell. In cyanobacteria, ppGpp is known to

accumulate in response to a sudden reduction in the incident light intensity (Akinyanju & Smith, 1982), which might thus suggest a coupling between regulation by light and/or the circadian clock and ppGpp accumulation. It is tempting to speculate, therefore, that 6S RNA in cyanobacteria might also be linked to the light–dark cycle of these organisms (Axmann *et al.*, 2007), controlling metabolic and genetic functions. This would add another facet to the spectrum of 6S RNA regulation. Further studies in this direction are required to answer this interesting question.

ACKNOWLEDGEMENTS

We like to thank P. Schoengraf (Institut für Unfallchirurgische Forschung und Mechanik, Universitätsklinik Ulm, Germany) for the generous gift of vector pSH666-2 and K. Shanmugarajah (Molecular Biology of Bacteria, Heinrich-Heine-University, Düsseldorf, Germany) for constructing *E. coli* Δ*ssrS* strain KS-1. Special thanks are given to G. Steger for his expert help with sequence aligning and secondary structure analysis. This work was supported by the Deutsche Forschungsgemeinschaft (SPP 1258) to R. W., and by the German Ministry for Education and Research (BMBF) through the FORSYS partner program (grant no. 0315294) to A. R., B. H. and I. M. A.

REFERENCES

Akinyanju, J. A. & Smith, R. J. (1982). Energy deprivation and guanosine 5′-diphosphate 3′-diphosphate synthesis in cyanobacteria. *J Bacteriol* **149**, 681–684.

Axmann, I. M., Kensche, P., Vogel, J., Kohl, S., Herzel, H. & Hess, W. R. (2005). Identification of cyanobacterial non-coding RNAs by comparative genome analysis. *Genome Biol* **6**, R73.

Axmann, I. M., Holtzendorff, J., Voß, B., Kensche, P. & Hess, W. R. (2007). Two distinct types of 6S RNA in *Prochlorococcus*. *Gene* **406**, 69–78.

Barrick, J. E., Sudarsan, N., Weinberg, Z., Ruzzo, W. L. & Breaker, R. R. (2005). 6S RNA is a widespread regulator of eubacterial RNA polymerase that resembles an open promoter. *RNA* **11**, 774–784.

Beckmann, B. M., Burenina, O. Y., Hoch, P. G., Kubareva, E. A., Sharma, C. M. & Hartmann, R. K. (2011). *In vivo* and *in vitro* analysis of 6S RNA-templated short transcripts in *Bacillus subtilis*. *RNA Biol* **8**, 839–849.

Beidler, J. L., Hilliard, P. R. & Rill, R. L. (1982). Ultrasensitive staining of nucleic acids with silver. *Anal Biochem* **126**, 374–380.

Brow, J. W. & Ellis, J. C. (2005). Comparative analysis of RNA secondary structures: 6S RNA. In *Handbook of RNA Biochemistry*. Edited by R. K. Hartmann, A. Bindereif, A. Schön & E. Westhof. Weinheim: Wiley-VCH Verlag.

Burgess, R. R. & Jendrisak, J. J. (1975). Procedure for the rapid, large-scale purification of *Escherichia coli* DNA-dependent RNA polymerase involving polymin P precipitation and DNA-cellulose chromatography. *Biochemistry* **14**, 4634–4638.

Cavanagh, A. T., Klocko, A. D., Liu, X. & Wassarman, K. M. (2008). Promoter specificity for 6S RNA regulation of transcription is determined by core promoter sequences and competition for region 4.2 of σ^{70}. *Mol Microbiol* **67**, 1242–1256.

Cavanagh, A. T., Chandrangsu, P. & Wassarman, K. M. (2010). 6S RNA regulation of *relA* alters ppGpp levels in early stationary phase. *Microbiology* **156**, 3791–3800.

Datsenko, K. A. & Wanner, B. L. (2000). One-step inactivation of chromosomal genes in *Escherichia coli* K-12 using PCR products. *Proc Natl Acad Sci U S A* **97**, 6640–6645.

Ermakova, S. Y., Elanskaya, I. V., Kallies, K. U., Weihe, A., Börner, T. & Shestakov, S. V. (1993). Cloning and sequencing of mutant *psbB* genes of the cyanobacterium *Synechocystis* PCC 6803. *Photosynth Res* **37**, 139–146.

Faucher, S. P., Friedlander, G., Livny, J., Margalit, H. & Shuman, H. A. (2010). *Legionella pneumophila* 6S RNA optimizes intracellular multiplication. *Proc Natl Acad Sci U S A* **107**, 7533–7538.

Geißen, R., Steuten, B., Polen, T. & Wagner, R. (2010). *E. coli* 6S RNA: a universal transcriptional regulator within the centre of growth adaptation. *RNA Biol* **7**, 564–568.

Gildehaus, N., Neusser, T., Wurm, R. & Wagner, R. (2007). Studies on the function of the riboregulator 6S RNA from *E. coli*: RNA polymerase binding, inhibition of *in vitro* transcription and synthesis of RNA-directed *de novo* transcripts. *Nucleic Acids Res* **35**, 1885–1896.

Gonzalez, N., Wiggs, J. & Chamberlin, M. J. (1977). A simple procedure for resolution of *Escherichia coli* RNA polymerase holoenzyme from core polymerase. *Arch Biochem Biophys* **182**, 404–408.

Hindley, J. (1967). Fractionation of ^{32}P-labelled ribonucleic acids on polyacrylamide gels and their characterization by fingerprinting. *J Mol Biol* **30**, 125–136.

Irnov, I., Sharma, C. M., Vogel, J. & Winkler, W. C. (2010). Identification of regulatory RNAs in *Bacillus subtilis*. *Nucleic Acids Res* **38**, 6637–6651.

Jeanguenin, L., Lara-Núñez, A., Pribat, A., Mageroy, M. H., Gregory, J. F., III, Rice, K. C., de Crécy-Lagard, V. & Hanson, A. D. (2010). Moonlighting glutamate formiminotransferases can functionally replace 5-formyltetrahydrofolate cycloligase. *J Biol Chem* **285**, 41557–41566.

Klocko, A. D. & Wassarman, K. M. (2009). 6S RNA binding to Eσ^{70} requires a positively charged surface of σ^{70} region 4.2. *Mol Microbiol* **73**, 152–164.

Kugel, J. F. & Goodrich, J. A. (2007). An RNA transcriptional regulator templates its own regulatory RNA. *Nat Chem Biol* **3**, 89–90.

Lee, S. Y., Bailey, S. C. & Apirion, D. (1978). Small stable RNAs from *Escherichia coli*: evidence for the existence of new molecules and for a new ribonucleoprotein particle containing 6S RNA. *J Bacteriol* **133**, 1015–1023.

Mitschke, J., Georg, J., Scholz, I., Sharma, C. M., Dienst, D., Bantscheff, J., Voss, B., Steglich, C., Wilde, A. & other authors (2011). An experimentally anchored map of transcriptional start sites in the model cyanobacterium *Synechocystis* sp. PCC6803. *Proc Natl Acad Sci U S A* **108**, 2124–2129.

Neußer, T., Polen, T., Geissen, R. & Wagner, R. (2010). Depletion of the non-coding regulatory 6S RNA in *E. coli* causes a surprising reduction in the expression of the translation machinery. *BMC Genomics* **11**, 165–178.

Pánek, J., Krásny, L., Bobek, J., Jezková, E., Korelusová, J. & Vohradsky, J. (2011). The suboptimal structures find the optimal RNAs: homology search for bacterial non-coding RNAs using suboptimal RNA structures. *Nucleic Acids Res* **39**, 3418–3426.

Rippka, R., Deruelles, J., Waterbury, J., Herdman, M. & Stanier, R. (1979). Generic assignments, strain histories and properties of pure cultures of cyanobacteria. *J Gen Microbiol* **111**, 1–61.

Rosenbaum, V. & Riesner, D. (1987). Temperature-gradient gel electrophoresis. Thermodynamic analysis of nucleic acids and proteins in purified form and in cellular extracts. *Biophys Chem* **26**, 235–246.

Schneider, G. J., Tumer, N. E., Richaud, C., Borbely, G. & Haselkorn, R. (1987). Purification and characterization of RNA polymerase from the cyanobacterium *Anabaena* 7120. *J Biol Chem* **262**, 14633–14639.

Schopf, J. W. (1993). Microfossils of the Early Archean Apex chert: new evidence of the antiquity of life. *Science* **260**, 640–646.

Schyns, G., Jia, L., Coursin, T., Tandeau de Marsac, N. & Houmard, J. (1998). Promoter recognition by a cyanobacterial RNA polymerase: *in vitro* studies with the *Calothrix* sp. PCC 7601 transcriptional factors RcaA and RcaD. *Plant Mol Biol* **36**, 649–659.

Sharma, C. M., Hoffmann, S., Darfeuille, F., Reignier, J., Findeiß, S., Sittka, A., Chabas, S., Reiche, K., Hackermüller, J. & other authors (2010). The primary transcriptome of the major human pathogen *Helicobacter pylori*. *Nature* **464**, 250–255.

Soukup, G. A. & Breaker, R. R. (1999). Relationship between internucleotide linkage geometry and the stability of RNA. *RNA* **5**, 1308–1325.

Trotochaud, A. E. & Wassarman, K. M. (2004). 6S RNA function enhances long-term cell survival. *J Bacteriol* **186**, 4978–4985.

Trotochaud, A. E. & Wassarman, K. M. (2005). A highly conserved 6S RNA structure is required for regulation of transcription. *Nat Struct Mol Biol* **12**, 313–319.

Trotochaud, A. E. & Wassarman, K. M. (2006). 6S RNA regulation of *pspF* transcription leads to altered cell survival at high pH. *J Bacteriol* **188**, 3936–3943.

Vogel, J., Axmann, I. M., Herzel, H. & Hess, W. R. (2003). Experimental and computational analysis of transcriptional start sites in the cyanobacterium *Prochlorococcus* MED4. *Nucleic Acids Res* **31**, 2890–2899.

Wagner, R. (2006). Protein-Nucleinsäure Wechselwirkungen. In *Bioanalytik*. Edited by F. Lottspeich & J. W. Engels. Heidelberg: Elsevier GmbH, Spektrum-Akademischer Verlag.

Wassarman, K. M. (2007). 6S RNA: a small RNA regulator of transcription. *Curr Opin Microbiol* **10**, 164–168.

Wassarman, K. M. & Saecker, R. M. (2006). Synthesis-mediated release of a small RNA inhibitor of RNA polymerase. *Science* **314**, 1601–1603.

Wassarman, K. M. & Storz, G. (2000). 6S RNA regulates *E. coli* RNA polymerase activity. *Cell* **101**, 613–623.

Watanabe, T., Sugiura, M. & Sugita, M. (1997). A novel small stable RNA, 6Sa RNA, from the cyanobacterium *Synechococcus* sp. strain PCC6301. *FEBS Lett* **416**, 302–306.

Wurm, R., Neußer, T. & Wagner, R. (2010). 6S RNA-dependent inhibition of RNA polymerase is released by RNA-dependent synthesis of small *de novo* products. *Biol Chem* **391**, 187–196.

Xie, W. Q., Jäger, K. & Potts, M. (1989). Cyanobacterial RNA polymerase genes *rpoC1* and *rpoC2* correspond to *rpoC* of *Escherichia coli*. *J Bacteriol* **171**, 1967–1973.

Zuker, M. (2003). Mfold web server for nucleic acid folding and hybridization prediction. *Nucleic Acids Res* **31**, 3406–3415.

Edited by: C.-C. Zhang

3.1.1 Supplemental material: Rediger *et al.* 2012

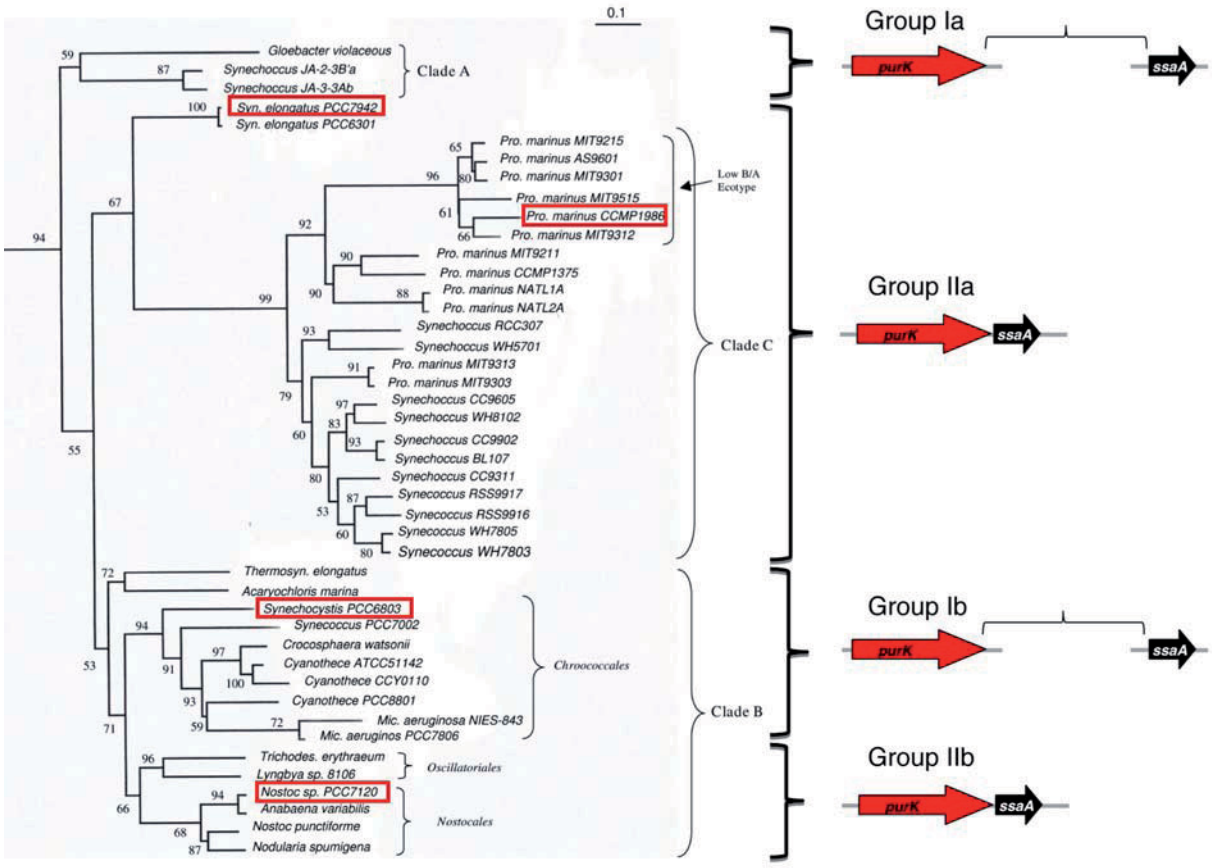

Figure S1: Phylogenetic relationship of cyanobacteria used in this study. A maximum-likelihood distance tree for sequenced cyanobacteria based on concatenated sequences of conserved proteins is shown (taken from (Gupta and Mathews 2010)). Information about phylogenetic relationship is overlaid with genome information about localisation of 6S RNA and *purK* gene suggesting different groups, I and II. Group II exhibits co-localization of 6S RNA and *purK*, group I does not. Example species (in red boxes) corresponding to either sub-group Ia, Ib, IIa or IIb are taken for further experiments.

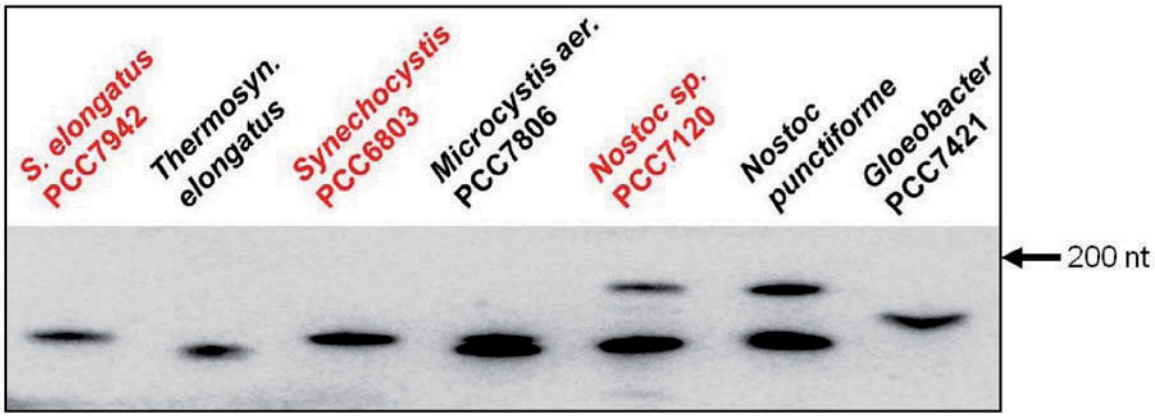

Figure S2: Detection of 6S RNA in diverse cyanobacteria. Total RNA (10 µg) from *Synechococcus* PCC 7942, *Thermosynechococcus elongatus* BP1, *Synechocystis* PCC 6803, *Microcystis aeruginosa* PCC 7806, *Nostoc* PCC 7120, Nostoc *punctiforme* and *Gloeobacter violaceus* PCC 7421 were separated on a 10% polyacrylamide gel followed by Northern blot hybridization with DNA oligonucleotides. Example species corresponding to either group Ia, Ib or IIb (Fig. S1) are shown in red.

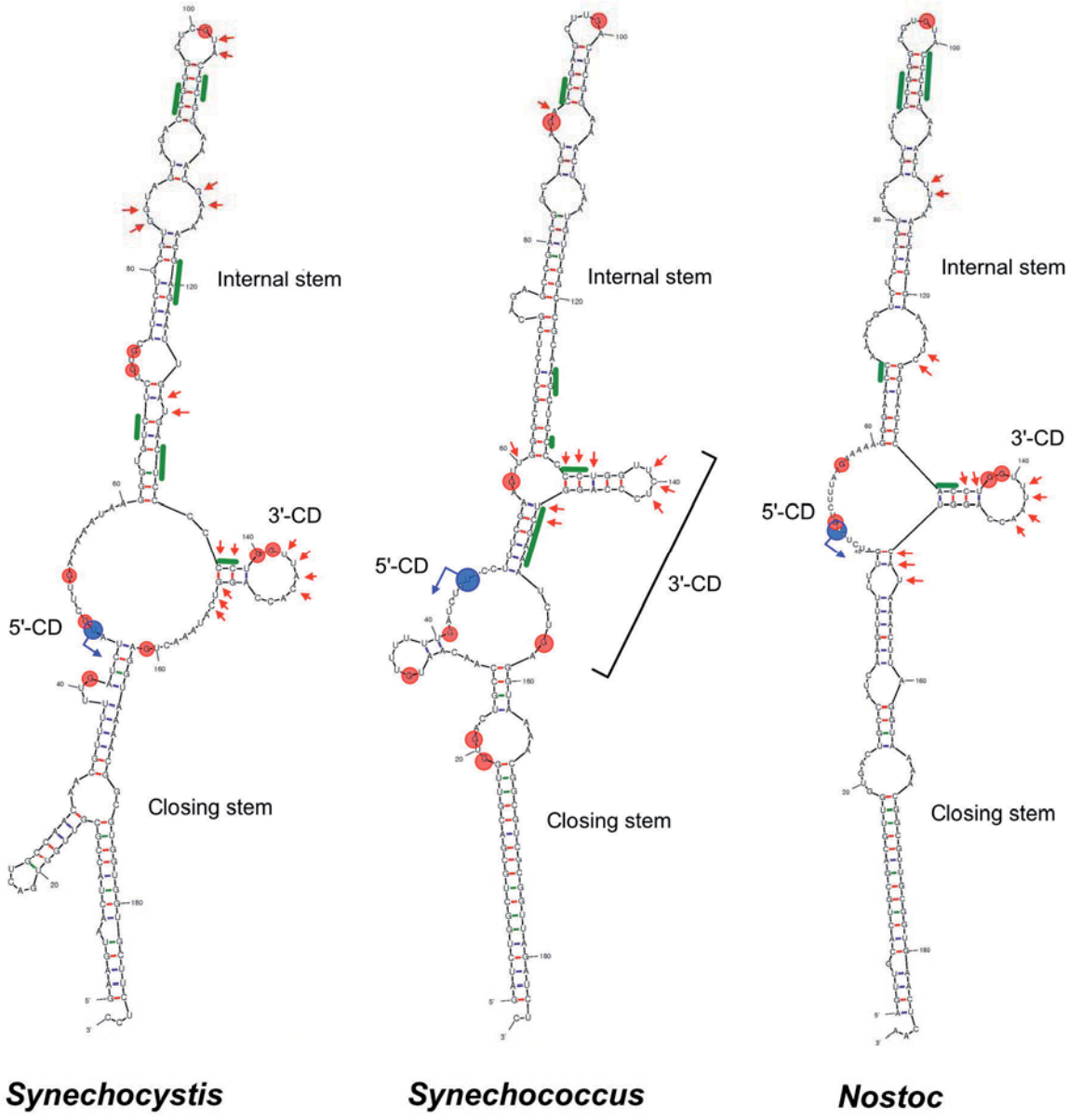

Figure S3: Deduced secondary structure models according to enzymatic and chemical probing and predictions for different cyanobacterial 6S RNAs. Secondary structures for *Synechocystis*, *Synechococcus* and *Nostoc* 6S RNAs have been arranged by mfold with constraints according to the enzymatic and chemical probing results. Single-strand guanosines according to RNase T1 accessibility are indicated by red circles. Helical base-paired regions recognized by RNase V1 are depicted as green bars. Nucleotide positions preferentially cleaved by in-line attack are indicated by red arrows. The location of the closing stem, internal stem and the 3'- or 5'-central domains, indicated 3'-CD or 5'-CD, respectively, is given. The start positions for pRNA synthesis are indicated by blue circles with an arrow pointing in the direction of transcription.

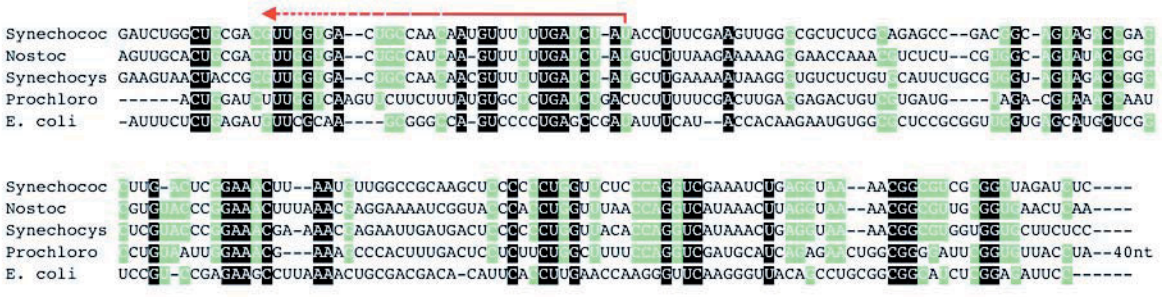

Figure S4: Multiple sequence alignment of 6S RNA sequences from the four cyanobacteria and *E. coli*. Sequences were aligned using CLUSTALW. The pRNA start position and direction of transcription is indicated by an arrow on top of the alignment. The exceptional extension at the 3'-end of *Prochlorococcus* (as shown by a previous study (Axmann *et al.* 2005), see Figure 7) folding back to a unique stem structure at the 3'-end is shortened here.

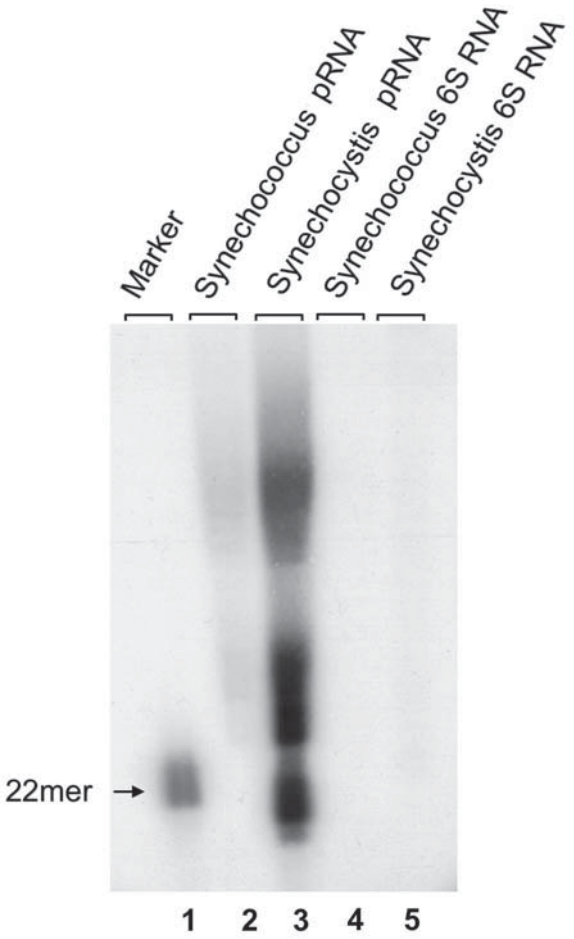

Figure S5: Identification of cyanobacterial pRNAs with a sequence-specific probe. pRNAs from *Synechocystis* and *Synechococcus* were prepared by *in vitro* transcription with 200 nM RNA polymerase and 300 µM of each NTP. Transcripts were purified and separated on a 15 % denaturing polyacrylamide gel. After Northern transfer pRNAs were specifically detected with the DNA oligonucleotide CApRNA ($^{5'}$-CCA ACA ACG TTT TTT GAT CTA T-$^{3'}$), complementary to the first 22 nucleotides. Due to the high sequence conservation in the pRNA-templated region of cyanobacterial 6S RNA this probe has a perfect match with *Synechocystis* pRNA but one mismatch with *Synechococcus* pRNA. Note that the efficiency of hybridization is clearly reduced in the case of *Synechococcus* pRNA (compare lanes 2 and 3), which can be explained by lower transcription yields with *E. coli* RNA polymerase and *Synechococcus* 6S RNA as a template (see Fig. S6). Moreover, a one base-pair mismatch between the CApRNA oligonucleotide and the *Synechococcus* pRNA lowers hybridization efficiency. As negative controls no hybridization of *E. coli* pRNA-specific ADN1 oligonucleotide against cyanobacterial pRNAs or hybridization of CApRNA against *E. coli* pRNAs could be detected (not shown). A 22 nucleotide length marker has been separated in lane 1.

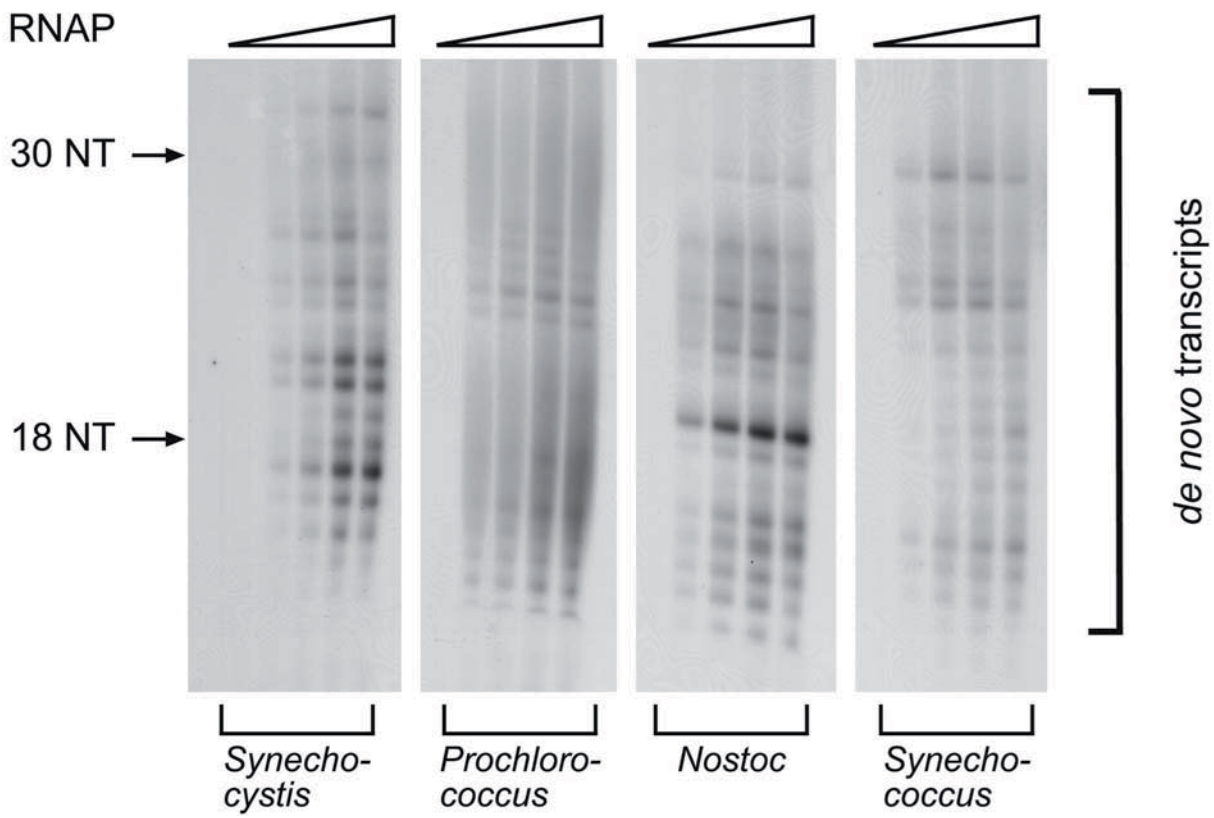

Figure S6: Formation of pRNAs from diverse cyanobacteria. 6S RNAs (300 nM each) from *Synechocystis*, *Prochlorococcus*, *Nostoc* and *Synechococcus*, respectively were incubated with increasing concentrations of *E. coli* RNA polymerase (0, 50 nM, 100 nM, 200 nM and 500 nM) and an NTP mix (300 µM each ATP, GTP, UTP and 5 µM CTP) containing 133 nM [α-^{32}P] CTP for product labeling. The positions of *de novo* transcription products and size markers are indicated.

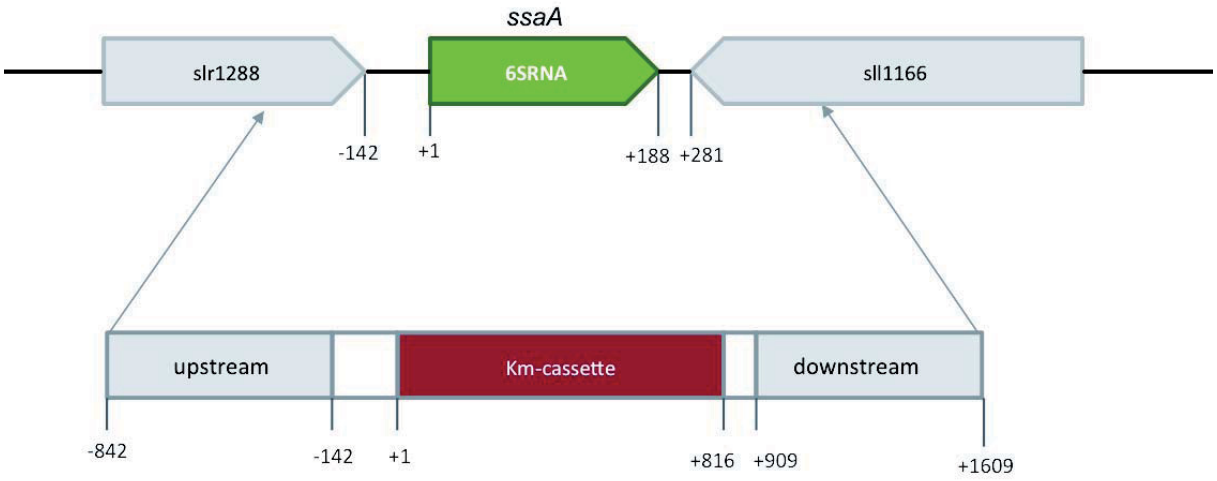

Figure S7: Scheme for construction of *Synechocystis ssaA* deletion mutants. Deletion of the *Synechocystis* 6S RNA gene (*ssaA*) was achieved by homologous recombination employing a kanamycin resistance cassette flanked by sequences 700 bp upstream and downstram of the *ssaA* gene. Sequence positions are indicated relative to the 5'- end of the mature *Synechocystis* 6S RNA.

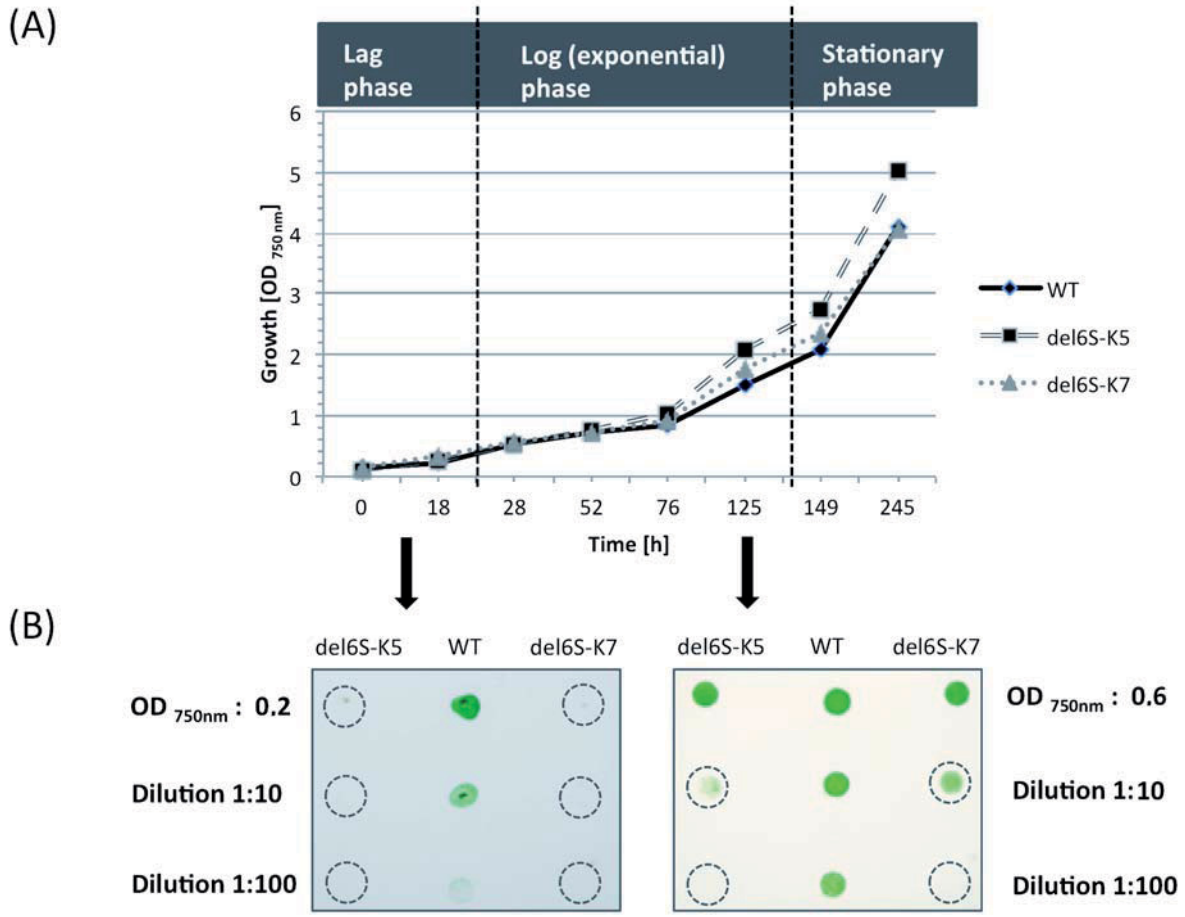

Figure S8: Phenotypic characterization of *Synechocystis ssaA* deletion mutants. The wild-type strain of *Synechocystis* (WT) and two 6S RNA deletion mutants (del6S-K5 and del6S-K7) were cultured under continuous illumination with white light of 80 µmol photons $m^{-2}s^{-1}$ for 4 days. Growth characteristics for WT and mutant strains were determined by following the growth curves in BG11 liquid medium (A) or after spotting serial dilutions on solid agar plates (B).

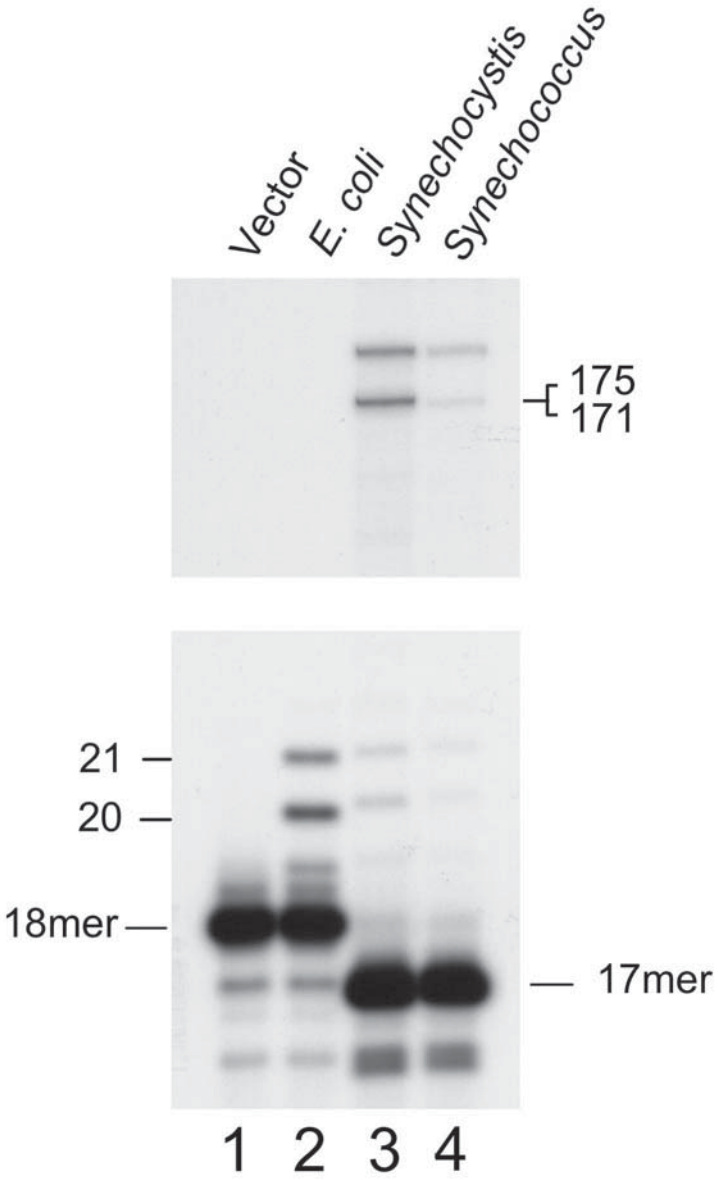

Figure S9: Expression of cyanobacterial 6S RNAs in *E. coli*. The expression vectors pKK-6S, pKK-6803-6S and pKK-7942-6S encoding 6S RNAs from *E. coli*, *Synechocystis* and *Synechococcus*, respectively, were transformed into the 6S RNA-deficient *E. coli* MG1655 strain KS-1. Cells were grown in YT-medium to early stationary phase (OD = ~2.4) and collected. Total RNA was isolated (Neußer *et al.* 2008). The primer extension reaction was performed with 1 µg total RNA employing AMV reverse transcriptase (Promega, Mannheim, Germany) and ^{32}P-labelled oligonucleotide c6S ($^{5'}$-TTG CGA ACA TCT CAG AGA-$^{3'}$) for transformants carrying the empty vector pKK223-3 and pKK-6S or the CA6SRNA oligonucleotide ($^{5'}$-ACG CCG TTT TAC CTC AG-$^{3'}$) in case of cyanobacterial 6S RNAs expressing transformants. Reaction products were separated on a 15% denaturing polyacrylamide gel and visualized by autoradiography.

3.2 The pRNA-mediated structural rearrangement of 6S RNA

In the subsequent article, entitled “A conformational switch is responsible for the reversal of the 6S RNA-dependent RNA polymerase inhibition in *Escherichia coli*”, details of the mechanism of 6S RNA release from RNA polymerase have been explored. As reported previously the synthesis of small pRNAs by the 6S RNA-RNAP complex is triggered by a nutritional upshift *in vivo* or high NTP concentration *in vitro*. This leads to a disintegration of the complex with RNAP and to the formation of stable 6S-pRNA hybrids. These hybrids were subjected to a comparative enzymatic and chemical probing analysis in order to discover structural transitions from the free 6S RNA to the 6S-pRNA duplex. Indeed, a new hairpin structure can be formed consisting of sequences from the single-stranded 3’ central domain and the unmasked sequence of the downstream closing stem due to the annealing of the pRNA. The formation of this altered structure participates in a series of events that leads to the ejection of the σ^{70} subunit and finally to the decay of 6S-pRNA-core polymerase intermediates.

DE GRUYTER DOI 10.1515/hsz-2012-0237 — Biol. Chem., 2012; 393(12): 1513–1522

Benedikt Steuten and Rolf Wagner*

A conformational switch is responsible for the reversal of the 6S RNA-dependent RNA polymerase inhibition in *Escherichia coli*

Abstract: 6S RNA is a bacterial transcriptional regulator, which accumulates during stationary phase and inhibits transcription from many promoters due to stable association with σ^{70}-containing RNA polymerase. This inhibitory RNA polymerase~6S RNA complex dissociates during nutritional upshift, when cells undergo outgrowth from stationary phase, releasing active RNA polymerase ready for transcription. The release reaction depends on a characteristic property of 6S RNAs, namely to act as template for the *de novo* synthesis of small RNAs, termed pRNAs. Here, we used limited hydrolysis with structure-specific RNases and in-line probing of isolated 6S RNA and 6S RNA~pRNA complexes to investigate the molecular details leading to the release reaction. Our results indicate that pRNA transcription induces the refolding of the 6S RNA secondary structure by disrupting part of the closing stem (conserved sequence regions CRI and CRIV) and formation of a new hairpin (conserved sequence regions CRIII and CRIV). Comparison of the dimethylsulfate modification pattern of 6S RNA in living cells at stationary growth and during outgrowth confirmed the conformational change observed *in vitro*. Based on our results, a model describing the individual steps of the release reaction is presented.

Keywords: pRNA; regulatory RNA; RNA secondary structure; structural probing.

***Corresponding author: Rolf Wagner,** Molecular Biology of Bacteria, Heinrich-Heine-University Düsseldorf, Universitätsstr. 1, D-40225 Düsseldorf, Germany,
e-mail: r.wagner@rz.uni-duesseldorf.de
Benedikt Steuten: Molecular Biology of Bacteria, Heinrich-Heine-University Düsseldorf, Universitätsstr. 1, D-40225 Düsseldorf, Germany

Introduction

Escherichia coli 6S RNA is a small regulatory RNA with widespread distribution in bacteria (Wassarman, 2007). Unlike most bacterial sRNAs with regulatory functions that predominantly affect post-transcriptional or translational events, 6S RNA acts as a transcriptional regulator (Wassarman and Storz, 2000; Waters and Storz, 2009). By virtue of its characteristic secondary structure, 6S RNA is capable of interacting specifically with the σ^{70}-containing RNA polymerase holoenzyme ($E\sigma^{70}$), which results in the down-regulation of a large number of promoters (Trotochaud and Wassarman, 2004, 2006; Neußer et al., 2010). A preliminary characterization of the interacting surfaces between RNA polymerase and 6S RNA by cross-linking has revealed that regions from the 6S RNA central domain are in contact with RNA polymerase subunits β/β′ and σ^{70} (Gildehaus et al., 2007). Moreover mutagenesis studies demonstrated that sequences within σ^{70} region 4.2, overlapping but not identical with DNA promoter binding sites, are crucial for 6S RNA recognition (Klocko and Wassarman, 2009). During stationary growth conditions, when cellular 6S RNA levels reach a maximum, an efficient sequestration of RNA polymerase holoenzymes occurs through stable complex formation. Hence, 6S RNA is considered to facilitate the shift in transcription specificity between exponential and stationary growth phase. The inactivation of $E\sigma^{70}$ holoenzyme by 6S RNA complex formation is not irreversible but is rapidly released when the nutritional conditions improve and cells undergo outgrowth into exponential phase again (Wassarman and Saecker, 2006; Gildehaus et al., 2007; Wurm et al., 2010). It has been shown that, under these conditions, small *de novo* transcripts (pRNAs), between 10 and 22 nucleotides in length, are synthesized resulting from a 6S RNA-templated reaction. The 6S RNA-directed synthesis of such small pRNA transcripts is a specific property shown for 6S RNAs from many different species, including *Bacillus subtilis*, *Helicobacter pylori* (Sharma et al., 2010; Beckmann et al., 2011; Cavanagh et al., 2011) or diverse cyanobacteria (Rediger et al., 2012). The 6S RNA-templated synthesis of pRNAs can also be observed *in vitro* with binary RNA polymerase~6S RNA complexes in the presence of high NTP concentrations, and it has been shown that this reaction directly triggers the decay of the inhibitory RNA polymerase~6S RNA complex (Wassarman and Saecker, 2006; Gildehaus et al., 2007; Wurm et al., 2010).

Hence, 6S RNA is considered to encode its own regulatory RNA, releasing stationary phase repression of Eσ^{70}-dependent transcription (Kugel and Goodrich, 2006). Although it seems clear that a conformational change within the RNA polymerase~6S RNA complex ultimately leads to the dissociation of the inhibitory complex, the molecular details of the reaction are not known. In particular, we wished to determine whether specific secondary structural elements or conserved primary sequence regions, CRI to CRIV (Brown and Ellis, 2005), are involved in the dynamic change that ultimately leads to destabilization of the RNA polymerase complex.

Here, we describe studies aimed to explore structural details of a potential 6S RNA conformational change as a result of the pRNA transcription reaction. As it is known that the synthesized pRNA is stably bound by 6S RNA following the transcription reaction (Wurm et al., 2010), we used chemical and enzymatic probing analyses to characterize the structural differences of free and pRNA-bound 6S RNA. We show here that pRNA transcription is accompanied by defined conformational changes within the 6S RNA secondary structure involving phylogenetically conserved sequence elements. Results from the *in vitro* structural probing were verified by a structural analysis of 6S RNA *in vivo* under conditions of pRNA synthesis. The results of our study enable a molecular understanding of the structural details that lead to the pRNA-mediated reversal of the transcriptional inhibition by 6S RNA.

Results

6S RNA cannot bind to RNA polymerase following pRNA synthesis

As shown previously, 6S RNA spontaneously forms stable binary complexes when incubated with the RNA polymerase holoenzyme Eσ^{70} *in vitro* (see also Figure 1A). These stable RNA polymerase~6S RNA complexes dissociate rapidly when pRNA synthesis is induced by high NTP concentrations *in vitro* or following a nutritional upshift from stationary growth *in vivo* (Wassarman and Saecker, 2006; Wurm et al., 2010). During pRNA synthesis, it was observed that the resulting transcripts remained stably bound to the 6S RNA template due to perfect sequence complementarity (Figure 1B). To form a perfect complementary hybrid between the pRNA and the 6S RNA template sequence, the native 6S RNA secondary structure, which forms the non-perfectly paired closing stem structure, has to be disrupted. We surmised that the resulting conformational change of the hybrid pRNA~6S RNA renders the 6S RNA into a structure that is inadequate for RNA polymerase binding. To test this assumption, we analyzed preformed 6S RNA~pRNA hybrids in an RNA polymerase binding reaction. The experiment clearly showed that, in contrast to native 6S RNA, the preformed 6S~pRNA hybrids fail to form stable complexes with RNA polymerase (Figure 1, compare A and C). We conclude that, due to steric constraints or blocked interacting surfaces, RNA polymerase cannot accommodate the altered secondary structure resulting from the conformational change induced by pRNA~6S RNA hybridization.

Enzymatic and chemical probing of 6S RNA and 6S~pRNA complexes

When analyzed by temperature-gradient gelelectrophoresis (TGGE), 6S RNA~pRNA hybrids exhibited an altered temperature-dependent transition compared to isolated 6S RNA, consistent with a distinctly different secondary structure (data not shown). To characterize this potential structural difference in detail, we performed enzymatic and chemical probing experiments. Limited enzymatic cleavage reactions were performed with RNase T1, which specifically attacks single-stranded guanines and with RNase V1, a double-strand-specific nuclease isolated from cobra venom. In addition, we employed the in-line probing method (Regulski and Breaker, 2008), which takes advantage of the natural instability of single-stranded

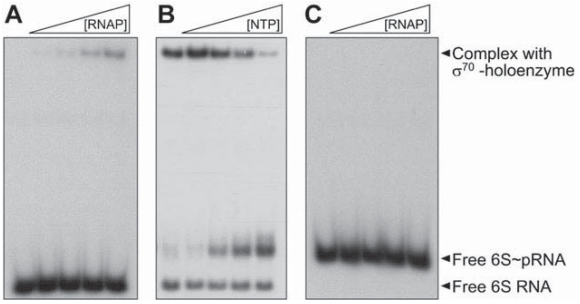

Figure 1 Preformed 6S~pRNA hybrids fail to form stable complexes with RNA polymerase.
Mobility shift assays with RNA polymerase and radiolabeled 6S RNA are shown. Probes were separated on 5% native polyacrylamide gels and visualized by autoradiography. (A) 6S RNA incubated with increasing RNA polymerase concentrations (0–60 nM). (B) 6S RNA incubated with 50 nM RNA polymerase and increasing NTP concentrations (0–500 μM). (C) Preformed 6S~pRNA hybrids incubated with increasing RNA polymerase concentrations (0–60 nM). Complexes and free RNA positions are depicted at the right margin.

RNA sequences. For the structural probing experiments, 6S RNA was labeled at its 3′ ends by ligation with [^{32}P]-pCp and, after a round of de- and renaturation, subjected to the probing reactions either alone or hybridized with a chemically synthesized 20 nucleotide pRNA. Hydrolyzed RNA samples were separated on denaturing polyacrylamide gels, and cleavage sites were identified by autoradiography. A typical example of the experiments is shown in Figure 2. Based on the data for the free 6S RNA (Figure 2A), a secondary structure was derived (Figure 3A) in accordance with the proposed *E. coli* 6S RNA structure published previously (Barrick et al., 2005). Comparison of the probing data for the native structure and the 6S RNA~pRNA hybrid revealed a number of clear differences. The perfect pairing of pRNA to the 6S RNA template, comprising sequence positions 25–44, causes a change in the imperfectly paired closing stem structure consisting of the conserved sequence regions CRI and CRIV as well as flanking sequence elements (Figure 3B). A corresponding change in the product pattern of the double-strand-specific RNase V1 is visible in the upper part of the gel above the labeled sequence position G68 (Figure 2A). Additionally, a reduced reactivity at position A123 and a newly accessible site between positions 132 and 135 are apparent for the pRNA-hybridized sample (Figure 2A). These differences in reactivity are consistent with a change in the base-pairing of the downstream part of the internal stem and the formation of a new base-paired region, likely involving region CRIII of the central domain (Figure 3B). The structural changes are supported by the RNase T1 hydrolysis pattern, which shows new single-stranded sites at positions G68 and G119/G122 consistent with the disruption of the paired downstream region of the internal stem for the pRNA~6S RNA complex sample. In contrast, position G136, accessible to RNase T1 in the free 6S RNA, becomes shielded in the complexed sample. Moreover, new single-strand-specific cuts are observed at positions G143, G153 and G159, indicating that the upstream part of the imperfectly paired closing stem structure, comprising regions CRIV and CRI, becomes accessible in the pRNA~6S RNA complex (Figure 3B). The accessibility of the bulged guanosines G79/G80 in the internal stem is also reduced in the pRNA~6S RNA complex. This may indicate an extended conformational change, including a large part of the internal stem. As

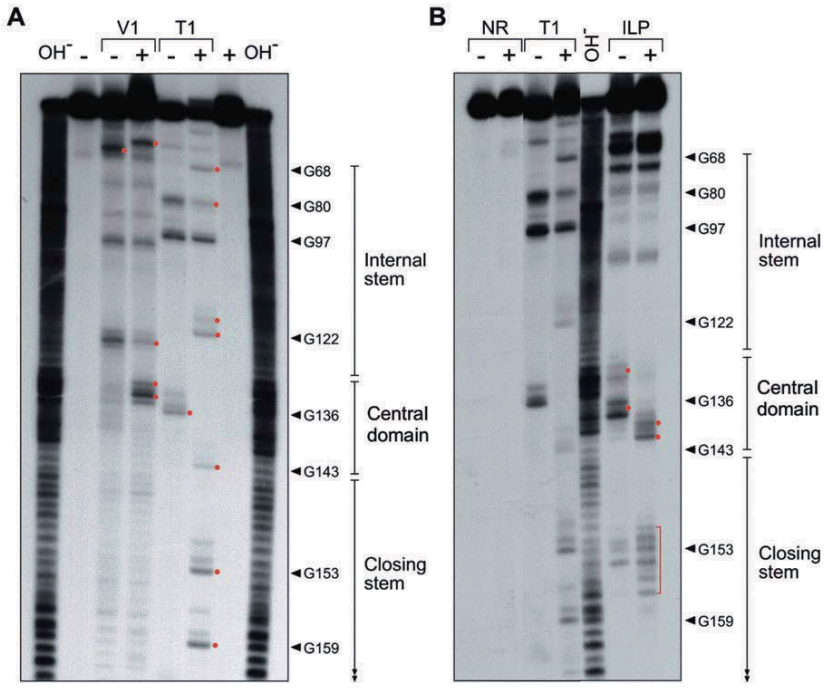

Figure 2 Enzymatic and chemical probing of 6S RNA and 6S~pRNA complexes.
Separation of RNA fragments on a 12% denaturing polyacrylamide gel is shown. Radiolabeled 6S RNA was denatured for 3 min at 68°C and slowly renatured in the absence (-) or presence (+) of a 1.5-fold molar excess of pRNA prior to the structural probing reaction. (A) 6S RNA and 6S~pRNA hybrids were treated with RNase T1 and RNase V1. (B) In-line probing of 6S RNA and 6S~pRNA hybrids. NR denotes no reaction. OH^- indicates a random RNA ladder obtained by alkaline hydrolysis. Cleavage positions and corresponding 6S RNA secondary structure regions are indicated at the right margin of each panel. Red dots and a red line indicate differential band intensities representing nucleotide positions relevant for structural changes.

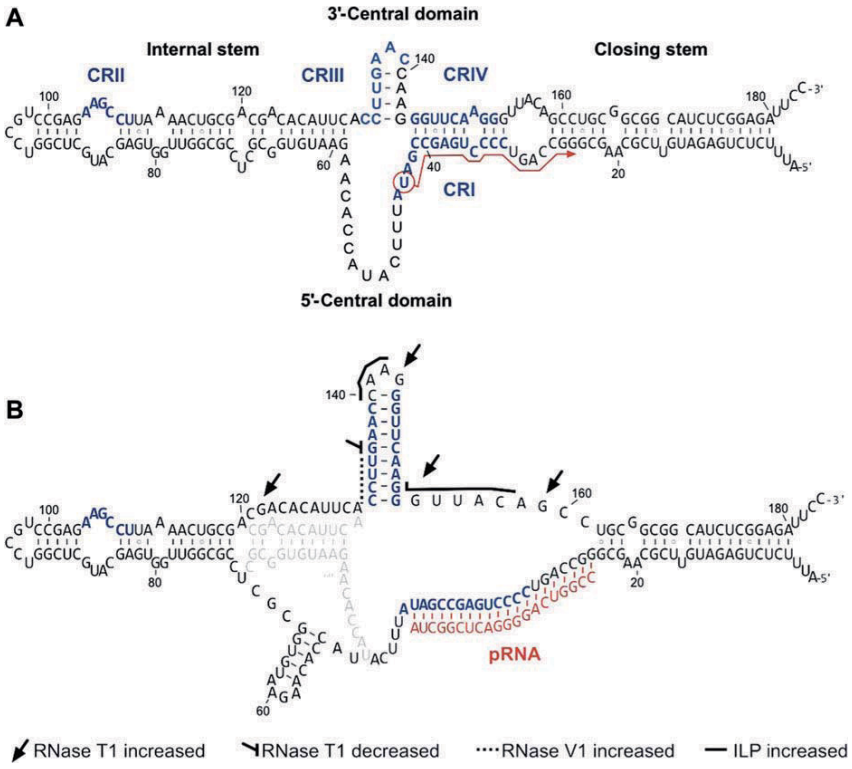

Figure 3 Secondary structure prediction of the 6S~pRNA complex.
The common secondary structure prediction of 6S RNA (A) and the prediction for the 6S~pRNA hybrid (B), based on the probing results, are shown. The common designation of the 6S RNA secondary structure elements is given on the top. The main secondary structural elements, internal stem, 3′- and 5′- central domain and closing stem, are indicated in (A). The conserved primary sequence regions (CRI to IV) according to Brown and Ellis (2005) are shown in blue, the region of pRNA synthesis is displayed by a red arrow (A) and the pRNA sequence is marked in red (B). Alternative RNA folding of the internal stem region of the 6S~pRNA hybrid is indicated in light gray (B). Key symbols summarizing the probing results are explained on the bottom.

we neither see additional changes directly upstream and downstream to guanosines G79/G80 nor in the opposite strand, we surmise that this altered accessibility rather reflects a local structural distortion, possibly resulting from a change in the conformation of the bulged guanosines. A likely explanation for the reduced T1 accessibility could be an enhanced stacking of the two purines triggered by a change in the helical geometry as a result of the partial disruption of internal stem structure directly flanking the central domain.

In support of the enzymatic cleavage pattern, very similar differences were obtained by in-line probing analysis (Figure 2B). Self-cleavage positions characteristic for single stranded regions are shifted from A131/C132 and G136 to C139 in the free 6S RNA to positions C140 to A142 in the pRNA~6S RNA complex. In addition, the single-stranded region of the closing stem G152 to U154 is extended to both sites in the pRNA~6S RNA complex, now comprising nucleotides G151 to C157 (Figure 2B). Together, the changes in reactivity are consistent with a structural rearrangement, whereupon hybridization of the pRNA to position G25 to U44 of the 6S RNA template triggers the disruption of sequence CRIV of the adjacent closing stem from interactions with CRI. CRIV, which shows almost perfect complementarity with CRIII, is now free to form a new stable hairpin structure. Moreover, the part of the internal stem region flanking the central domain becomes distorted, presumably rendering sequence 119–131 single-stranded and giving rise to a potential new hairpin involving sequences 53–66.

The major structural features, resulting from 6S RNA~pRNA complex formation, are outlined in Figure 3B and can be characterized in the following way: (i) A 20-bp, perfectly paired helical element between pRNA and 6S RNA sequence region 22–44 substitutes the irregular helix of the closing stem formed by the conserved sequence elements CRI and CRIV (Figure 3A). (ii) A new hairpin structure with 9 continuous base pairs is formed

by the conserved complementary sequence regions CRIV and CRIII. (iii) The internal stem structure flanking the central domain becomes refolded, likely resulting in a single-stranded region (positions 119–131) and two single-stranded regions (45–52 and 67–71) separated by a small (5-bp) hairpin (positions 53–66) (Figure 3B). It is feasible that the dramatic change in overall structure will no longer be accommodated in a functional RNA polymerase complex. Particularly formation of the new 9-bp hairpin between CRIII and CRIV might create a steric clash with the RNA polymerase active site causing rapid dissociation of the RNA polymerase~6S RNA complex and likely rendering the RNA molecule prone for enzymatic degradation.

Verification of the observed structural change *in vivo*

To test whether the structural changes observed by *in vitro* structural probing are also valid in living cells, we performed chemical probing analysis under *in vivo* conditions. We used dimethylsulfate (DMS) modification, which allows the detection of non-paired adenine and cytosine residues in nucleic acids of living cells (Balzer and Wagner, 1998). Methylation of single-stranded RNA residues was identified by primer extension analysis of total RNA (Wells et al., 2000). Specific conditions were selected to ensure the predominant presence of either free or pRNA-bound 6S RNA for comparison. We chose stationary cells, where pRNA synthesis is negligible as a source for free 6S RNA. To monitor pRNA~6S RNA complexes, we modified cells after a short outgrowth period following a nutritional upshift from stationary phase. Under this condition, a major proportion of the 6S RNA undergoes a burst of pRNA synthesis resulting in high levels of pRNA~6S RNA hybrids (Wurm et al., 2010). The existence of free and pRNA-complexed 6S RNA was verified before by Northern blotting of a total RNA sample after gel purification (Supplementary Figure S1). The analysis demonstrated that, at stationary growth, only free 6S RNA is visible, whereas immediately after nutritional upshift, pRNA~6S RNA hybrids are transiently formed, reaching maximal concentration between 2 and 5 min. Methylated nucleotide positions of 6S RNA samples, either isolated from stationary phase cells or after outgrowth (2 min after nutritional upshift, see Methods), were identified by reverse transcription. A comparison of the 6S RNA methylation pattern of the different samples is shown in Figure 4. For better comparison of the band intensities, the densitometric profiles of the autoradiogram from all RNA samples are shown next to the gel, revealing subtle changes for a

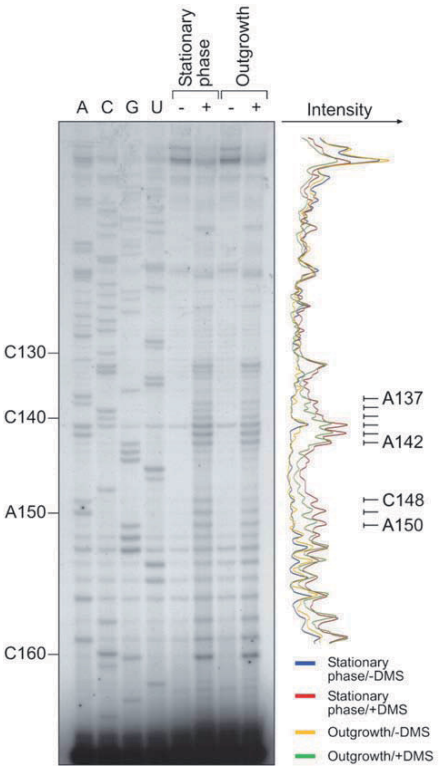

Figure 4 *In vivo* footprint of 6S~pRNA complexes.
A representative autoradiogram of a primer extension reaction with a 6S RNA specific oligonucleotide is shown. The cDNA products were separated on a 15% polyacrylamide gel. Total RNA was isolated from cells in stationary phase or after short-time outgrowth from stationary phase. The absence (-) or addition (+) of DMS to the culture is indicated at the top. 6S RNA sequence positions are marked on the left. On the right, a densitometric scan of the band intensities for DMS-reacted free 6S RNA (red) and modified 6S RNA~pRNA (green) are depicted. Also indicated are control lanes for non-modified 6S RNA before (blue) and after upshift (yellow), respectively. Sequence positions of protection of the outgrowth sample, compared to the sample at stationary phase, are indicated on the right margin. The color code and the symbol key are given on the right bottom.

number of nucleotides. As a significant amount of free 6S RNA is present also during outgrowth (Figure S1), the differences in the methylation pattern are not as pronounced as for the purified samples analyzed *in vitro*. The same difference in methylation pattern has been reproduced, however, in several experiments, clearly demonstrating that *in vivo* modification is reduced after outgrowth for nucleotides C148 to G151, and a somewhat weaker reduction can be seen for positions A137 to A142. This change in reactivity is consistent with the formation of a stable hairpin consisting of sequence elements CRIII and CRIV (reduced reactivity of A137 to A142 and C148 to A150).

Overall, the reactivity changes observed *in vivo* support the conformational rearrangement demonstrated by the *in vitro* structural probing analysis above. In summary, we conclude that the same or very similar structural changes determined on the basis of the *in vitro* probing results do also take place *in vivo*.

Initial steps of the 6S RNA~RNA polymerase complex decay

As demonstrated in Figure 1 and consistent with previous studies (Wassarman and Saecker, 2006; Gildehaus et al., 2007; Wurm et al., 2010), the 6S RNA-directed synthesis of pRNAs causes an immediate decay of the inhibitory RNA polymerase~6S RNA complex. Although it is clear that the transcribed pRNA remains hybridized to the 6S RNA template sequence (Figure 1B), any further mechanistic details leading to the complex decay are not precisely known. From recent studies, we surmised, however, that the dissociation of the σ^{70} subunit is likely to be the initial step in the complex breakdown (Wurm et al., 2010). To test this assumption, we analyzed the decay of 6S RNA~RNA polymerase complexes under conditions of pRNA synthesis employing native discontinuous polyacrylamide gels, which enable the separation of RNA polymerase core and holoenzyme complexes (Severinova et al., 1996). Synthesis of pRNAs was induced by the addition of increasing amounts of NTPs to Eσ^{70} RNA polymerase holoenzyme, which had been complexed with 6S RNA before. The reaction was allowed to proceed for 10 min at 30°C, after which the samples were separated on a native discontinuous polyacrylamide gel. Heparin, which is usually added to suppress non-specific binding, was omitted from this reaction to enable the separation of transient RNA polymerase core~6S RNA intermediates known to be destabilized by high heparin concentrations. The result shown in Figure 5 demonstrates that increasing NTP concentrations cause a successive disruption of the Eσ^{70} RNA polymerase holoenzyme complex with the concomitant formation of an intermediate RNA polymerase core~6S RNA complex. We take this as evidence that the complex decay is initiated by a loss of the σ^{70} subunit as the pivotal step.

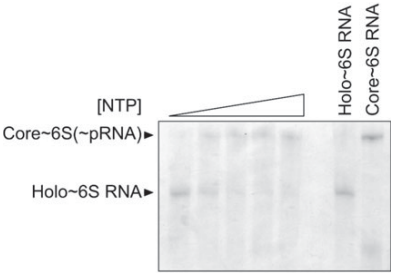

Figure 5 Release of the σ^{70} subunit from RNA polymerase~6S RNA complex following pRNA-synthesis.
The result of a native discontinuous polyacrylamide gel, stained with Coomassie Blue, is shown. RNA polymerase~6S RNA complexes were incubated with increasing NTP concentrations (0–1 mM) in the absence of the competitor heparin. 6S RNA complexes with either RNA polymerase holo or core enzyme are indicated at the left margin. The 6S RNA~core complex likely contains hybridized pRNA.

Discussion

It has been documented in the past, both for *E. coli* and *Bacillus subtilis*, that RNA-templated pRNA synthesis triggers the recovery from transcriptional inactivity after 6S RNA-dependent inhibition during outgrowth (Wassarman and Saecker, 2006; Wurm et al., 2010; Beckmann et al., 2011; Cavanagh et al., 2011). It was also shown that pRNAs exceeding a length of about 14 nucleotides form stable hybrids with the 6S RNA template. Here, we have demonstrated for *E. coli* that, in contrast to free 6S RNA, such pre-formed 6S RNA~pRNA hybrids are unable to bind to RNA polymerase holoenzyme. Subsequent *in vitro* structural probing analyses revealed that the formation of 6S RNA~pRNA hybrids resulted in distinct conformational changes that disrupt the characteristic 6S RNA central domain structure necessary for RNA polymerase interaction. The main features of this conformational change are the formation of a stable hairpin structure (sequence positions 132–152 comprising conserved elements CRII and CRIV) that replace the short helical structure of the 3′-half of the central domain (positions 132–143). This structural change is also supported by the *in vivo* methylation largely confirming the *in vitro* experiments. Additional changes comprise the likely formation of a small hairpin (sequence positions 53–66), altering the single-stranded structure of the 5′-half of the central domain (positions 42–58). Moreover, the helical structure of the internal stem flanking the central domain becomes disrupted (Figure 3B).

A likely mechanism for the release of 6S RNA-mediated transcriptional repression

Based on the results of this investigation and previous findings, we suggest the following likely scenario of the pRNA-directed decay of the inhibitory RNA polymerase

complex. The activity of $E\sigma^{70}$ RNA polymerase is largely restricted during stationary growth due to the fact that most of the molecules are in stable association with 6S RNA. When growth conditions improve (mimicked *in vitro* by high NTP concentrations), RNA polymerase~6S RNA complexes initiate the transcription of pRNAs. As with natural transcription complexes, the growing RNA chain remains at first hybridized to the template nucleic acid. Under normal transcription conditions, with DNA as a template, the stability of this heteroduplex between the growing RNA chain and the template DNA strand does not exceed the stability of the double-stranded DNA. Driven by the free energy of the DNA double-strand formation, the RNA strand is displaced from the template strand after 8–9 nucleotides, and the non-complexed RNA leaves the transcribing complex through the exit tunnel (Vassylyev et al., 2007). In contrast, with 6S RNA as a template, the transcribed pRNA forms a perfectly double-stranded complex with the complementary 6S RNA sequence over the full pRNA length. This double strand is significantly more stable than the corresponding secondary structure of the 6S RNA template region, which is interrupted by a bulged mismatch and an internal loop. Hence, the pRNA is not released from the template sequence after 9 nucleotides, as is normally the case during DNA-templated transcription. Stable association of the pRNA with the 6S RNA sequence (CRI and part of the 5′ closing stem) releases the opposite strand (CRIV and part of the 3′ closing stem), which now forms a thermodynamic favorable new hairpin consisting of sequences CRI and CRIV. Additional changes may occur within the internal stem region flanking the central domain (Figure 3B). Quite obviously, this structural change either sequesters sequence elements important for RNA polymerase complex formation and/or causes a steric clash with structural elements of the $E\sigma^{70}$ holoenzyme. As a result, σ^{70} dissociates from the RNA polymerase complex, leaving as intermediate a 6S RNA~pRNA hybrid transiently associated to the core RNA polymerase. *In vivo* 6S RNA~pRNA complexes without RNA polymerase protection are degraded rapidly, whereas core RNA polymerase and the σ^{70} subunit are free for a new round of mRNA transcription supporting outgrowth from stationary phase.

Known interactions of RNA polymerase with RNA molecules

A number of RNA molecules are known to undergo specific interactions with RNA polymerase during the transcription cycle. Well-characterized interactions include the nut sites of potential antiterminators (Nodwell and Greenblatt, 1991), hairpin loops of class I pauses (Artsimovitch and Landick, 2000) or bacteriophage HK022 *putL* RNA (Komissarova et al., 2008). The *putL* RNA, for example, is known to bind to the surface of RNAP close to the exit channel, where it regulates pausing and antitermination. Interestingly, *putL* RNA shows structural similarity with 6S RNA (irregular stem region). A highly conserved zinc-binding domain close to the N-terminus of the β′ subunit is known to bind growing RNA products upstream of the catalytic center and the RNA–DNA hybrid (King et al., 2004). It is tempting to speculate that this RNA-binding motif could be involved in 6S RNA binding to the outside surface of RNA polymerase. It may otherwise also represent a domain for pRNA interaction.

In *B. subtilis*, two 6S RNAs, 6S-1 and 6S-2, are expressed, of which only 6S-1 serves as template for pRNAs (Beckmann et al., 2011). In a recent publication (Beckmann et al., 2012), the pRNA-mediated release of *B. subtilis* RNA polymerase bound to 6S-1 RNA has been analyzed in detail. The authors demonstrated that a structural rearrangement occurs involving nucleotides in the 5′ region of the central domain and the sequences released by complex formation of the pRNA and that this structural change decreases the affinity between 6S-1 RNA and the *B. subtilis* RNA polymerase holoenzyme. The authors also showed that the length of the pRNAs plays a crucial role for the efficiency of the release reaction between 6S RNA and RNA polymerase, and on the basis of a bioinformatics approach they propose that all bacterial 6S RNAs are potentially capable of a pRNA-induced structural rearrangement. It should be noted that their proposed structural rearrangement is fully consistent with the results presented in this study.

What distinguishes pRNA synthesis from DNA-templated transcription?

The occurrence of short abortive transcripts (2–15 nucleotides) is a common phenomenon for normal transcription initiation, and the products are supposed to have a functional importance in gene regulation (Goldman et al., 2009). Abortive transcripts may act as antisense molecules or act as transcription primers (Goldman et al., 2011). The synthesis of pRNAs, at least the shorter fraction up to 14 nucleotides, has many parallels to abortive transcription, although we do not presently know if they fulfill any function. The longer pRNAs, up to 22 nucleotides, differ clearly in several aspects with abortive or productive transcripts. Their 5′ end does not unwind from

the template but the complete pRNA remains in perfectly annealed double-stranded conformation over its entire length with the 6S RNA. As a consequence, pRNAs will never enter the RNA polymerase exit tunnel. For natural transcripts to enter the exit tunnel, they must displace σ^{70} linker region 3.2, which in turn weakens the interaction of σ region 4 with the β flap and provides the first step for the dissociation of σ^{70} from the initiation complex (Murakami and Darst, 2003). In case of pRNA synthesis, one might ask why the growing RNA remains hybridized to the template for more than the common 8–9 nucleotides and what is the molecular trigger to dissociate σ^{70} from the 6S RNA~RNA polymerase complex? A possible reason for the long (up to 22 nucleotides) pRNA~6S RNA hybrid might result from the favorable energy difference between the perfect pRNA~6S RNA double helix compared to the irregular secondary structure of the 6S RNA closing stem helix. The pRNA~6S RNA helix, comprising two helical turns, is likely too large and rigid to fit within the interior architecture of the RNA polymerase initiation complex and possibly clashes with the lid or β flap structure of RNA polymerase. On the other hand, even longer pRNA transcripts (more than 30 nucleotides, data not shown) are transcribed with cyanobacterial 6S RNAs bound to *E. coli* RNA polymerase, suggesting that part of the 6S RNA closing stem, together with the annealed pRNA, may be located in the RNA polymerase cleft that normally takes up the upstream DNA. Destabilization of the RNA polymerase~6S RNA complex and dissociation of σ^{70} may therefore alternatively be triggered by the new 6S RNA helix formed by conserved sequences CRIII and CRIV. Remarkably, the primary sequences involved in the structural change are conserved in many 6S RNAs, indicating that the folding mechanism may be a general phenomenon. Clearly, more structural details of the complex architecture are required to give a high-resolution answer to this question.

Materials and methods

Oligonucleotides used

The following oligonucleotides were used for analysis: The RNA oligonucleotide pRNA (5′-AUC GGC UCA GGG GAC UGG CC-3′), complementary to the 6S RNA positions 25–44, was used for the formation of 6S~pRNA hybrids in binding and structural probing studies. For the primer extension analysis of *in vivo* modified 6S RNA with DMS the DNA oligonucleotide 6S-B (5′-CCT GGA ATC TCC GAG ATG CCG C-3′), complementary to the 6S RNA sequence 166–184, was used. The DNA oligonucleotide was purchased from Thermo Scientific, Ulm, Germany and the RNA oligonucleotide was from Microsynth, Balgach, Switzerland.

In vitro transcription of 6S RNA with T7 RNA polymerase

6S RNA for *in vitro* studies was generated by run-off transcription from linearized plasmid pUC18-T7-6S with T7 RNA polymerase (Gildehaus et al., 2007). 6S RNA was radiolabeled at the 3′-end by ligation with [5′-^{32}P]-pCp (Göringer et al., 1984).

Binding studies with RNA polymerase

For complex formation, 15 nM radiolabeled 6S RNA or 6S~pRNA hybrids were incubated with increasing amounts of Eσ^{70} RNA polymerase holoenzyme (0–60 nM) for 10 min at 30°C in 50 mM Tris-acetate, pH 8.0, 10 mM Mg-acetate, 0.5 mM DTT, 0.5 mM EDTA, 80 mM K-glutamate. Reactions were performed in the presence of heparin (final concentration 100 ng/µl) to prevent non-specific binding. To mimic outgrowth conditions, increasing amounts of NTPs (0–500 µM) were added, and transcribing complexes were incubated for 10 min at 30°C (Wurm et al., 2010). Complexes were separated on 5% native polyacrylamide gels.

Enzymatic and chemical probing

For the enzymatic hydrolysis, ~120 nM radiolabeled, purified 6S RNA or 6S~pRNA hybrids were incubated with 10 mU RNase V1 (Pharmacia, Erlangen, Germany) in 20 mM Tris-HCl, pH 7.2, 200 mM NaCl and 10 mM $MgCl_2$ or 20 mU RNase T1 (Sankyo, Tokyo, Japan) in 50 mM Tris-HCl, pH 7.5 and 1 mM EDTA for 10 min at 30°C. After phenol/chloroform extraction and ethanol precipitation, the cleavage products were separated on 12% denaturing polyacrylamide gels.

The in-line probing reactions contained ~250 nM radiolabeled, purified 6S RNA or 6S~pRNA hybrids, 50 mM Tris-HCl pH 8.5 and 20 mM $MgCl_2$ and were incubated for 42 h at 23°C (Soukup and Breaker, 1999). After ethanol precipitation, the samples were loaded on 12% denaturing polyacrylamide gels.

RNA sequencing ladders were generated by alkaline hydrolysis with ~250 nM radiolabeled 6S RNA incubated in the presence of 2 µg tRNA as carrier in 50 mM Na_2CO_3/$NaHCO_3$, pH 9.5 for 5 min at 95°C.

In vivo DMS modification of 6S RNA

Cultures (100 ml) of *E. coli* wild-type MG1655 were grown at 37°C to stationary phase (OD_{600}=1.0–1.3) in M9 minimal media (Miller, 1972) supplemented with 0.2% glucose. The nutritional upshift was performed as described previously (Wurm et al., 2010). After 2 min, 10 ml samples were taken from outgrowing and stationary cells, supplemented with 200 µl DMS (99.8% p.a. Sigma-Aldrich, Munich, Germany; 1:4 dilution in 95% ethanol) and incubated for an additional 2 min at 37°C. The reaction was stopped by addition of 10 ml frozen TME buffer (100 mM Tris-HCl, pH 7.5, 300 mM 2-mercaptoethanol, 5 mM EDTA) (Mayford and Weisblum, 1989; Wells et al., 2000). Cells were then pelleted and subjected to total RNA extraction by the hot phenol method as described previously (Liebig and Wagner, 1995; Neußer et al., 2008).

Primer extension reactions

Primer extension reactions were performed with 2 µg total RNA employing the [^{32}P]-labeled oligonucleotide 6S-B and AMV reverse transcriptase (Promega, Mannheim, Germany) as described (Neußer, et al., 2008). Reaction products were separated on 15% denaturing polyacrylamide gels and visualized by autoradiography.

Native, discontinuous PAGE

To separate high molecular weight complexes of 6S RNA with holo or core RNA polymerase, a native, discontinuous polyacrylamide gel was used, consisting of 4% stacking gel (125 mM Tris-HCl, pH 6.8, 4% v/v glycerol) and a 5% running gel (375 mM Tris-HCl, pH 8.8, 4% v/v glycerol) (Severinova et al., 1996).

Acknowledgements: We thank R. Wurm for providing purified *E. coli* RNA polymerase. We wish to acknowledge the expert help of G. Steger with respect to RNA secondary structure predictions. The work was supported by a Priority Program of the Deutsche Forschungsgemeinschaft (SPP 1258).

Received March 7, 2012; accepted July 5, 2012

References

Artsimovitch, I. and Landick, R. (2000). Pausing by bacterial RNA polymerase is mediated by mechanistically distinct classes of signals. Proc. Natl. Acad. Sci. USA *97*, 7090–7095.

Balzer, M. and Wagner, R. (1998). Mutation in the leader region of ribosomal RNA operons cause structurally defective 30S ribosomes as revealed by *in vivo* structural probing. J. Mol. Biol. *276*, 547–557.

Barrick, J.E., Sudarsan, N.,Weinberg, Z., Ruzzo, W.L., and Breaker, R.R. (2005). RNA *11*, 774–784.

Beckmann, B.M., Burenina, O.Y., Hoch, P.G., Kubareva, E.A., Sharma, C.M., and Hartmann, R.K. (2011). *In vivo* and *in vitro* analysis of 6S RNA-templated short transcripts in *Bacillus subtilis*. RNA Biol. *8*, 839–849.

Beckmann, B.M., Hoch, P.G., Marz, M., Willkomm, D.K., Salas, M., and Harmann, R.K. (2012). A pRNA-induced structural rearrangement triggers 6S-1 RNA release from RNA polymerase in *Bacillus subtilis*. EMBO J. doi:10.1038/emboj.2012.23.

Brown, J.W. and Ellis, J.C. (2005). Comparative analysis of RNA secondary structures: 6S RNA. In: Handbook of RNA Biochemistry, R.K. Hartmann, A. Bindereif, A. Schön, E. Westhof, eds. (Weinheim: Wiley-VCH Verlag GmbH & Co.), pp. 491–512.

Cavanagh, A.T., Sperger, J.M., and Wassarman, K.M. (2011). Regulation of 6S RNA by pRNA synthesis is required for efficient recovery from stationary phase in *E. coli* and *B. subtilis*. Nucleic Acids Res., doi:10.1093/nar/gkr1003.

Gildehaus, N., Neusser, T., Wurm, R., and Wagner, R. (2007). Studies on the function of the riboregulator 6S RNA from *E. coli*: RNA polymerase binding, inhibition of in vitro transcription and synthesis of RNA-directed de novo transcripts. Nucleic Acids Res. *35*, 1885–1896.

Goldman, S.R., Ebright, R.H., and Nickels, B.E. (2009). Direct detection of abortive RNA transcripts *in vivo*. Science *324*, 927–928.

Goldman, S.R., Sharp, J.S., Vvedenskaya, I.O., Livny, J., Dove, S.L., and Nickels, B.E. (2011). NanoRNAs prime transcription initiation *in vivo*. Mol. Cell *42*, 817–825.

Göringer, H.U., Bertram, S., and Wagner, R. (1984). The effect of tRNA binding on the structure of 5S RNA in *E. coli*. A chemical modification study. J. Biol. Chem. *259*, 491–496.

King, R.A., Markov, D., Sen, R., Severinov, K., and Weisberg, R.A. (2004). A conserved zinc binding domain in the largest subunit of DNA-dependent RNA polymerase modulates intrinsic transcription termination and antitermination but does not stabilize the elongation complex. J. Mol. Biol. *342*, 1143–1154.

Klocko, A.D. and Wassarman, K.M. (2009). 6S RNA binding to Eσ^{70} requires a positively charged surface of σ^{70} region 4.2. Mol. Microbiol. *73*, 152–164.

Komissarova, N., Velikodvorskaya, T., Sen, R., King, R.A., Banik-Maiti, S., and Weisberg, R.A. (2008). Inhibition of a transcriptional pause by RNA anchoring to RNA polymerase. Mol. Cell *31*, 683–694.

Kugel, J.F. and Goodrich, J.A. (2006). Beating the heat: a translation factor and an RNA mobilize the heat shock transcription factor HSF1. Mol. Cell *22*, 153–154.

Liebig, B. and Wagner, R. (1995). Effects of different growth conditions on the *in vivo* activity of the tandem *Escherichia coli* ribosomal RNA promoters P1 and P2. Mol. Gen. Genet. *249*, 328–335.

Mayford, M. and Weisblum, B. (1989). Conformational alterations in the *ermC* transcript *in vivo* during induction. EMBO J. *8*, 4307–4314.

Miller, J. H. (1972). Experiments in Molecular Genetics. (New York: Cold Spring Harbor Laboratory Press).

Murakami, K.S. and Darst, S.A. (2003). Bacterial RNA polymerases: the whole story. Curr. Opin. Struct. Biol. *13*, 31–39.

Neußer, T., Gildehaus, N., Wurm, R., and Wagner, R. (2008). Studies on the expression of 6S RNA from *E. coli*: involvement of regulators important for stress and growth adaptation. Biol. Chem. *389*, 285–297.

Neußer, T., Polen, T., Geißen, R., and Wagner, R. (2010). Depletion of the non-coding regulatory 6S RNA in *E. coli* causes a surprising reduction in the expression of the translation machinery. BMC Genomics *11*, 165–178.

Nodwell, J.R. and Greenblatt, J. (1991). The *nut* site of bacteriophage λ is made of RNA and is bound by transcription antitermination factors on the surface of RNA polymerase. Genes Dev. *5*, 2141–2151.

Rediger, A., Geißen, R., Steuten, B., Heilmann, B., Wagner, R., and Axmann, I. M. (2012). 6S RNA – an old issue became blue-green. Microbiol., doi:10.1099/mic.0.058958-0.

Regulski, E.E. and Breaker, R.R. (2008). In-line probing analysis of riboswitches. Methods Mol. Biol. *419*, 53–67.

Severinova, E., Severinov, K., Fenyö, D., Marr, M., Brody, E.N., Roberts, J.W., Chait, B.T., and Darst, S.A. (1996). Domain organization of the *Escherichia coli* RNA polymerase σ^{70} subunit. J. Mol. Biol. *263*, 637–647.

Sharma, C.M., Hoffmann, S., Darfeuille, F., Reignier, J., Findeiss, S., Sittka, A., Chabas, S., Reiche, K., Hackermuller, J., Reinhardt, R., et al. (2010). The primary transcriptome of the major human pathogen *Helicobacter pylori*. Nature *464*, 250–255.

Soukup, G.A. and Breaker, R.R. (1999). Relationship between internucleotide linkage geometry and the stability of RNA. RNA *5*, 1308–1325.

Trotochaud, A.E. and Wassarman, K.M. (2004). 6S RNA function enhances long-term cell survival. J. Bacteriol. *186*, 4978–4985.

Trotochaud, A.E. and Wassarman, K.M. (2006). 6S RNA regulation of *pspF* transcription leads to altered cell survival at high pH. J. Bacteriol. *188*, 3936–3943.

Vassylyev, D.G., Vassylyeva, M.N., Perederina, A., Tahirov, T.H., and Artsimovitch, I. (2007). Structural basis for transcription elongation by bacterial RNA polymerase. Nature *448*, 157–162.

Wassarman, K.M. (2007). 6S RNA: a small RNA regulator of transcription. Curr. Opin. Microbiol. *10*, 164–168.

Wassarman, K.M. and Storz, G. (2000). 6S RNA regulates *E. coli* RNA polymerase activity. Cell *101*, 613–623.

Wassarman, K.M. and Saecker, R.M. (2006). Synthesis-mediated release of a small RNA inhibitor of RNA polymerase. Science *314*, 1601–1603.

Waters, L.S. and Storz, G. (2009). Regulatory RNAs in bacteria. Cell *136*, 615–628.

Wells, S.E., Hughes, J.M., Igel, A.H., and Ares, M., Jr. (2000). Use of dimethyl sulfate to probe RNA structure *in vivo*. Methods Enzymol. *318*, 479–493.

Wurm, R., Neußer, T., and Wagner, R. (2010). 6S RNA-dependent inhibition of RNA polymerase is released by RNA-dependent synthesis of small *de novo* products. Biol. Chem. *39*, 187–196.

3.2.1 Supplemental material: Steuten and Wagner 2012

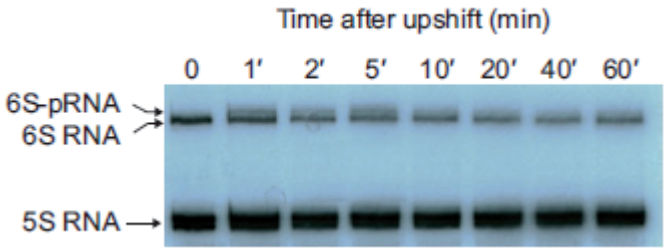

Figure S1: *In vivo* presence of 6S RNA~pRNA hybrids after outgrowth from stationary phase. The autoradiogram of a Northern blot of total RNA samples (5 µg each) on a 10 % acrylamide gel is shown. *E. coli* MG1655 were grown in YT-media to stationary phase (OD600 = ~5). Outgrowth from stationary phase was achieved by a 1:5 dilution in fresh YT-media supplemented with 0.2 % glucose. Total RNA was isolated from cells in stationary phase (0) and at time intervals (1, 2, 5, 10, 20, 40 and 60 minutes) following outgrowth from stationary phase. 6S RNA or 6S~pRNA hybrids were detected with the 6S RNA-specific oligonucleotide c6S (5'TTG CGA ACA TCT CAG AGA3'), complementary to positions 4 to 21 of 6S RNA. The positions of free 6S RNA and 6S RNA~pRNA complexes are indicated at the left margin. 5S RNA was used as internal standard and visualized with the 5S RNA-specific oligonucleotide 5S-PE (5'ACC ACC GCG CTA CTG CCG3'), complementary to positions 8 to 25 of 5S RNA. An upshift period of 2 minutes was selected before the addition of DMS.

3.3 A spatial assignment of 6S RNA to the three-dimensional structure of the RNAP holoenzyme

The third article with the title “Mapping the spatial neighborhood of the regulatory 6S RNA bound to the *Escherichia coli* RNA polymerase holoenzyme” extends the previous structural studies to a more complete and precise three-dimensional view. Owing to the difficulty to obtain three-dimensional information by X-ray diffraction or NMR imaging techniques for 6S RNA or the 6S-RNAP complex we used the chemical nuclease FeBABE to map proximal sites between 6S RNA and its major σ^{70} interaction surface within the RNAP. Several RNA-protein sites could be localized enabling the construction of a three-dimensional model of the 6S RNA-Eσ^{70} complex. Based on this data we suggested new direct interaction sites between 6S RNA and its protein counterpart. A preliminary mutational analysis of specific 6S RNA regions revealed strong importance on binding.

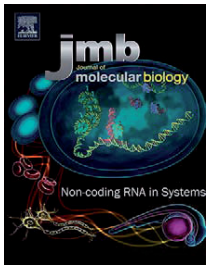

Mapping the Spatial Neighborhood of the Regulatory 6S RNA Bound to *Escherichia coli* RNA Polymerase Holoenzyme

Benedikt Steuten[1], Piotr Setny[2], Martin Zacharias[2] and Rolf Wagner[1]

1 - Molecular Biology of Bacteria, *Heinrich-Heine Universität Düsseldorf, Universitätsstrasse 1, D-40225 Düsseldorf, Germany*
2 - Physics Department T38, *Biomolecular Dynamics, Technische Universität München, James-Franck-Strasse 1, D-85748 Garchingen, Germany*

Correspondence to Rolf Wagner: *r.wagner@rz.uni-duesseldorf.de*
http://dx.doi.org/10.1016/j.jmb.2013.07.008
Edited by A. Pyle

Abstract

Bacterial 6S RNA interacts specifically with RNA polymerase acting as transcriptional regulator. Until now, no detailed characterization of the spatial arrangement of the non-coding RNA within the three-dimensional structure of RNA polymerase has been performed. Here we present results obtained with the chemical nuclease FeBABE tethered to distinct positions of RNA polymerase σ^{70} subunit. 6S RNA complexes were formed with a collection of RNA polymerases, where the cleavage reagent had been fused to σ^{70} single-cysteine variants close to regions involved in promoter recognition. FeBABE-induced cleavage sites within the 6S RNA structure were identified, indicating close spatial neighborhood between σ^{70} single-cysteine side chains and defined positions of the 6S RNA structure. Our analysis demonstrates close proximity between the 6S RNA internal hairpin and σ^{70} domain 4.2, normally involved in recognition of −35 promoter DNA. Defined sections of the internal 6S RNA stem structure flanking the central bubble are positioned near conserved σ^{70} domains 3.1, 2.3 and 2.1, which are implicated in binding and melting DNA promoters between the −10 and −35 elements. Moreover, we show that U44 of 6S RNA is located near RNA polymerase active site (σ^{70} domain 3.2), fully consistent with its function as starting nucleotide in RNA-directed pRNA transcription. No neighboring contacts were detected between 6S RNA and σ^{70} region 1.2 or between σ^{70} and the 6S RNA closing stem structure (residues 1–41 and 144–184). Results were used to dock a structural model of 6S RNA to the known three-dimensional structure of *Escherichia coli* σ^{70} RNA polymerase holoenzyme.

Introduction

Small non-coding RNAs (sRNAs or ncRNAs) have recently been recognized as regulatory elements in all kingdoms of life, where they affect various steps of gene expression. In *Escherichia coli*, more than 80 different regulatory sRNAs are known to be expressed, many of which are induced upon stress or changing environmental conditions [1,2]. The majority of these RNAs act by base pairing with target mRNAs affecting translation or mRNA stability. Others affect cell physiology by forming complexes with proteins or mimicking the structure of other nucleic acids in the cell [3]. 6S RNA is rather an exception, as it belongs to the rare group of sRNAs directly affecting transcription by binding to RNA polymerase. In *E. coli*, 6S RNA accumulates to high intracellular levels during the growth cycle [4,5] and contributes to transcriptional adaptation between exponential growth and stationary phase [4,6–8]. Although first identified in the late sixties [9], 6S RNA is now known for more than a decade as a transcriptional regulator that specifically interacts with the holoenzyme of RNA polymerase [5,10,11]. This interaction causes a complex change of the transcriptional initiation efficiency from many but not all promoters [7,12–14].

All bacterial 6S RNAs display a characteristic secondary structure consisting of two irregular helical stem regions (internal stem and closing stem) flanking a central bubble, which is more or less single stranded [11,15]. This highly conserved RNA secondary structure, resembling an open DNA promoter, appears to be the primary determinant for

specific binding of 6S RNA to the RNA polymerase [11,16]. Not only is 6S RNA recognized by RNA polymerase like a DNA promoter but it actually serves as a template under certain growth conditions, giving rise to the synthesis of small specific transcription products, termed pRNAs [17,18]. The synthesis of these small RNAs is not restricted to *E. coli* but has been shown to occur in a number of different bacteria as well, where it causes the release of 6S RNA-dependent transcriptional inhibition [19–22]. Whether the small pRNA transcripts have additional functions of their own is not yet known.

While we have a rather profound knowledge on RNA polymerase interactions with DNA promoters and several high-resolution structures of RNA polymerase sigma factor, alone or as a part of a holoenzyme, both in free or in DNA complexed form have been solved [23–27], comparably detailed structural information with respect to 6S RNA–RNA polymerase complexes is not available. Based on structural probing and sequence comparison, reliable information on the secondary structure of 6S RNA exists, whereas high-resolution methods to solve the three-dimensional structure of 6S RNA free or in complex with RNA polymerase are not applicable at present due to the size of the molecule or lack of suitable crystals. So far, cross-linking and mutagenesis experiments together with functional information have only yielded restricted information on the 6S RNA–RNA polymerase contact sites [5,10,18,28]. From these studies, it is quite obvious to conclude that position U44 within the central domain of 6S RNA must be positioned within the active site of RNA polymerase made up by defined β and β′ subunit domains because this nucleotide serves as the start position for 6S RNA-templated pRNA synthesis [10,17]. Clearly, as for DNA promoters, the σ^{70} subunit plays a pivotal role in the binding and recognition of 6S RNA and no stable complexes are formed in the absence of σ^{70}. Consistent with this notion, the σ^{70} subunit, but also both β and β′ subunits, has been cross-linked to 6S RNA in independent studies [5,10]. The role of σ^{70} in binding 6S RNA is further highlighted by mutagenesis studies, which revealed that an expanded positively charged binding surface within region 4.2 of the σ^{70} subunit, overlapping but distinct from the −35 promoter recognition element, appears to be responsible for the binding of 6S RNA [28]. Despite this information, we only have a rather crude picture of 6S RNA–RNA polymerase contact sites. We wished to extend this information by identifying 6S RNA nucleotide positions in close proximity to predefined positions of the σ^{70} RNA polymerase holoenzyme. Potential contact sites should be identified by the chemical nuclease Fe(III) (*S*)-1-(*p*-bromoacetamidobenzyl)-ethylenediaminetetraacetic acid (FeBABE) conjugated to single cysteines within defined functional domains of σ^{70} [29]. To achieve this, we took advantage of a set of σ^{70} single-cysteine mutants that had successfully been employed to unravel the architecture of RNA polymerase–DNA promoter complexes [30]. Complexes between 6S RNA and reconstituted RNA polymerase holoenzymes with σ^{70} single-cysteine mutants tethered to the cleavage reagent FeBABE were formed, and cleavage sites within the 6S RNA sequence were subsequently identified. The cleavage distance of FeBABE-generated hydroxyl radicals has been determined to be ≈12 Å from the Cys sulfur plus the 3- to 4-Å diffusion distance of the hydroxyl radicals [30]. Within this range, the results allowed us to position distinct 6S RNA structural sites in proximity to defined parts of the three-dimensional RNA polymerase holoenzyme structure. Based on the results, a three-dimensional model of the 6S RNA–RNA polymerase complex has been constructed. The model suggests the mechanism of transcription inhibition by direct competition of the 6S RNA to fully occupy the complete binding region for DNA in a similar spatial arrangement.

Results

Isolation of single-cysteine σ^{70} variants and characterization of their 6S RNA binding capacity

E. coli single-cysteine σ^{70} mutants had previously been employed in the positioning of DNA promoter sites within RNA polymerase structure [30]. The Meares laboratory kindly provided a set of such constructs for the expression of σ^{70} mutants C132, K376C, R422C, K496C, S517C and D581C. The single-cysteine σ^{70} proteins were expressed, purified and conjugated to the chemical nuclease (FeBABE) *via* the sulfhydryl-reactive bromoacetamidobenzyl moiety. Consistent with earlier observations [30], conjugation efficiencies for the different variants ranged between 20% and 60%. The modified σ^{70} subunits were reconstituted with purified core RNA polymerase, and the resulting holoenzymes with the chemical nuclease attached to different functional σ^{70} domains (Fig. 1) were analyzed for their capacity to bind *E. coli* 6S RNA. All σ^{70} variants proved to be active in 6S RNA binding, and comparative binding assays revealed only marginal differences in the binding capacity of 6S RNA, whether or not FeBABE had been conjugated (Fig. 2).

To further verify the functionality of the reconstituted RNA polymerase mutants, we tested the capability for the 6S RNA-dependent synthesis of pRNAs. To this aim, we incubated complexes between the different holoenzymes and 6S RNA in the presence of high substrate NTP concentrations to allow pRNA transcription. The resulting

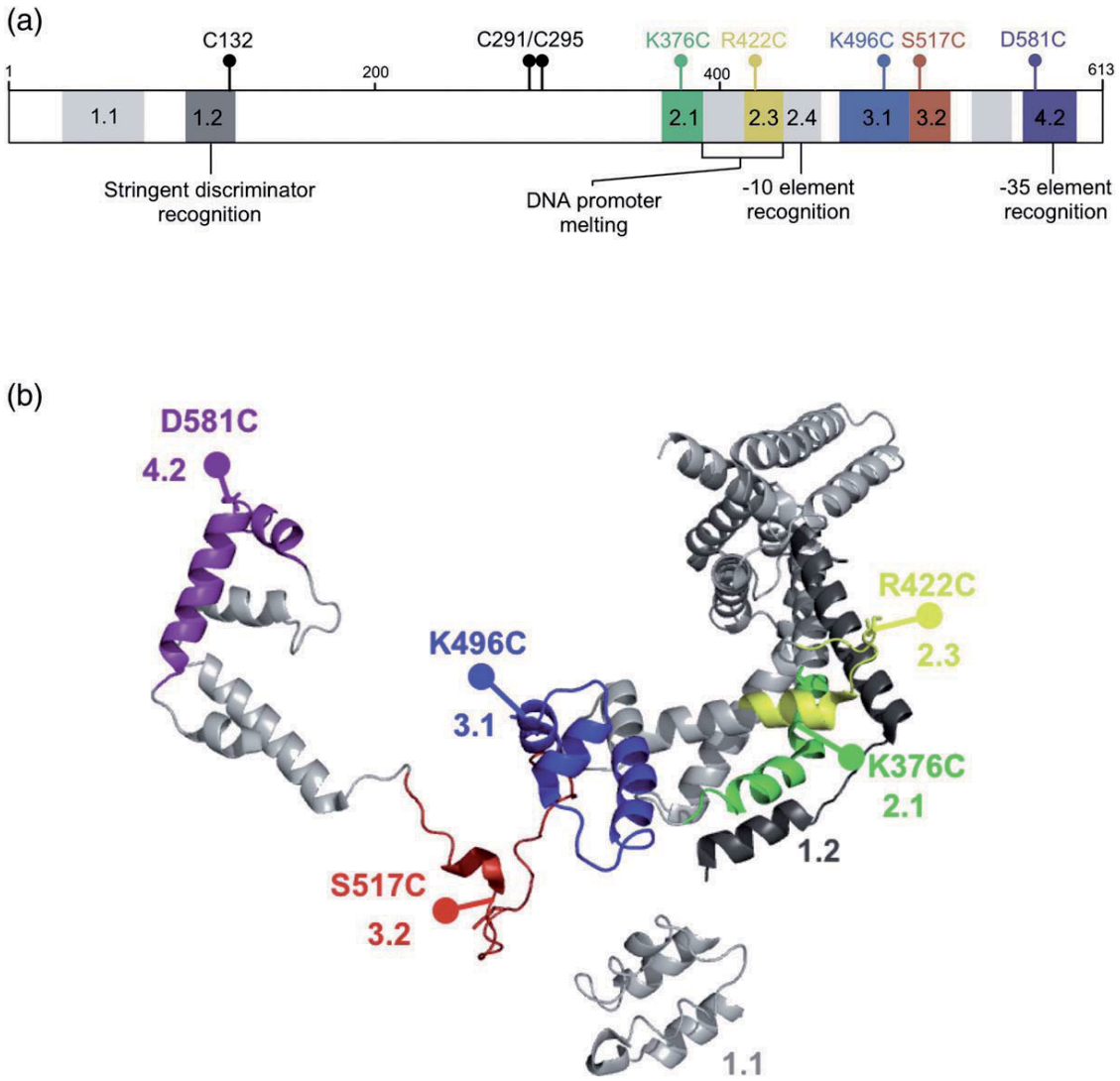

Fig. 1. Scheme indicating *E. coli* σ^{70} amino acid positions conjugated to the cleavage reagent FeBABE. (a) The linear domain organization of the σ^{70} subunit is shown [31]. Positions of single-cysteine substitutions are labeled and marked by colored symbols. Subdomains are numbered and presented in different colors. Black labels indicate natural cysteines. Functions during promoter recognition assigned to individual subdomains are given below the scheme. (b) Location of the single-cysteine substitutions within the three-dimensional structure of *E. coli* σ^{70} subunit (PDB ID: 4IGC) [27]. The colors of the subdomains and the labeled cysteines are the same as in (a).

transcription products were then identified by denaturing gel electrophoresis (Fig. 3) [18]. In all cases, 6S RNA-directed transcription of pRNAs occurred, indicating that neither the cysteine replacements nor the conjugation to the chemical nuclease FeBABE did substantially affect the basic functionality of the different RNA polymerase holoenzymes. Despite a certain difference in the overall yield of pRNAs (Fig. 3), we like to note that the transcription pattern of the individual pRNA products looked very similar, whether or not FeBABE was conjugated to the different sigma variants indicating that all variants were able to recognize 6S RNA as a template for pRNA transcription.

Identification of 6S RNA sites bound to specific σ^{70} structural domains

For the identification of 6S RNA positions in close contact with RNA polymerase holoenzyme, we formed complexes with 6S RNAs end-labeled with 3′-[^{32}P] as well as 5′-[^{32}P] and the different reconstituted RNA polymerases with FeBABE

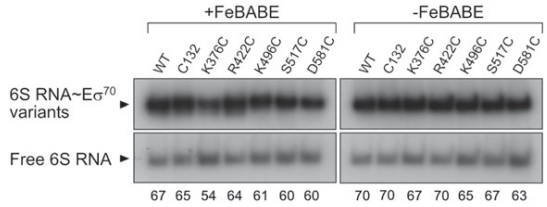

Fig. 2. Binding of FeBABE-tethered RNA polymerase holoenzymes to 6S RNA. Binding of [^{32}P]6S RNA to RNA polymerase holoenzymes reconstituted with different σ^{70} variants was analyzed by gel retardation. Bands corresponding to free 6S RNA and the 6S RNA–Eσ^{70} holoenzyme complexes are indicated at the left margin. Single-cysteine variants are indicated above the lanes. WT denotes reconstitution with wild-type σ^{70}. Lanes marked by –FeBABE/+FeBABE represent Eσ^{70} holoenzymes before and after conjugation with the chemical nuclease FeBABE, respectively. Numbers below the gel lanes indicate the percent complex formed for each variant.

attached to six distinct single-cysteine variants (C132, K376C, R422C, K496C, S517C and D581C). Note that wild-type σ^{70} has three Cys residues (C132, C291 and C295) of which C291 and C295 were changed to Ser in all singe-cysteine variants [30]. We additionally employed a reconstituted wild-type enzyme where all three native cysteines (C132, C291 and C295) had been conjugated to FeBABE in the reaction. Moreover, RNA polymerase reconstituted with unmodified wild-type σ^{70} without FeBABE conjugation was used as negative control. Complexes were treated with sodium ascorbate and hydrogen peroxide to initiate the cleavage reaction and samples were quenched by addition of thiourea after 3 min of incubation at 30 °C. The reacted RNAs were precipitated with ethanol, and cleavage products were subsequently analyzed on denaturing polyacrylamide gels. Gel bands representing cleaved RNA fragments were identified by autoradiography (Fig. 4).

Cleavage sites could be consistently identified as bands in both 3′- and 5′-labeled 6S RNA samples, although cleavage intensity seemed to be somewhat weaker with the 3′-labeled sample. Interestingly, often two distant cleavage sites could be identified within one RNA sample. The single-cysteine variant C132 did not result in 6S RNA cleavage, and FeBABE conjugation to wild-type σ^{70}, which, next to C132, has two natural cysteines (C291 and C295), did also not give rise to any cleavage. Since all the other RNA polymerase variants resulted in distinct cleavage products, we take the absence of any cleavage with FeBABE tethered to C132, where the chemical nuclease is located adjacent to σ^{70} domain 1.2, as an indication that this domain is not in close contact to bound 6S RNA or at least is more distant than the critical range for FeBABE-catalyzed cleavage (≈15 Å) [30,32]. The same conclusion applies to C291 and C295, which are both positioned in a non-conserved region of the σ^{70} subunit.

We summarize below the cleavage results that were reproducibly obtained in at least three independent experiments. Amino acid C376 is located within σ^{70} domain 2.1, which had previously been shown to be close to the –10 region and not far from the transcription start site of the non-template DNA strand within an open RNA polymerase–*lac*UV5 promoter complex [30]. The K376C variant caused distinct cleavage at positions 124–126 and 65–67. These distant cleavage positions are very close in the secondary structure, where they face opposite sites of the same helical element, flanking the central 6S RNA domain.

Residue 422 within domain 2.3 of σ^{70} is close to the recognition helix that is known to be in contact with the –10 element of non-template promoter DNA. This part of σ^{70} is also considered to take part in promoter melting [33]. The R422C variant gave rise to cleavage between positions 126–133, with slightly stronger signals for the 126 and 133 positions. An additional signal could also be seen at positions 63–65 (more prominently on the 5′-labeled RNA sample; Fig. 4). Again, the centers of cleavage are distant in the primary sequence of 6S RNA but face neighboring sites of the same helical arrangement based on the 6S RNA secondary or derived tertiary structure (Fig. 5).

σ^{70} position 496 is located in domain 3.1, which, in RNA polymerase–promoter complexes, is known to stretch across the –10 and the –35 promoter elements [30]. In terms of structural analogy, the identified 6S RNA sequence region could be regarded as analogous to the spacer element of DNA promoters. FeBABE conjugation to the K496C variant of σ^{70} resulted in two distinct cleavage

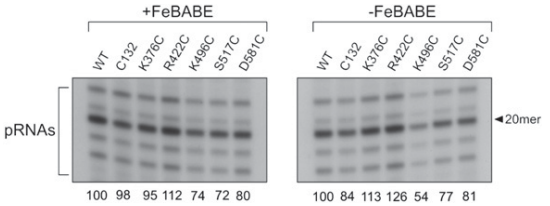

Fig. 3. 6S RNA-directed pRNA synthesis with FeBABE-tethered RNA polymerase holoenzymes. RNA polymerase holoenzymes with different σ^{70} variants were analyzed for their capability to synthesize 6S RNA-directed pRNAs. [^{32}P]pRNA products were separated on denaturing polyacrylamide gels. The position of a 20mer length marker is indicated by an arrowhead. σ^{70} variants for reconstitution are given above the lanes. WT denotes reconstitution with wild-type σ^{70}. Lanes marked by –FeBABE/+FeBABE denote holoenzymes before or after conjugation with FeBABE, respectively. Numbers below the gel lanes indicate the overall yield of pRNA transcripts relative to the wild-type σ^{70}, which was set to 100%.

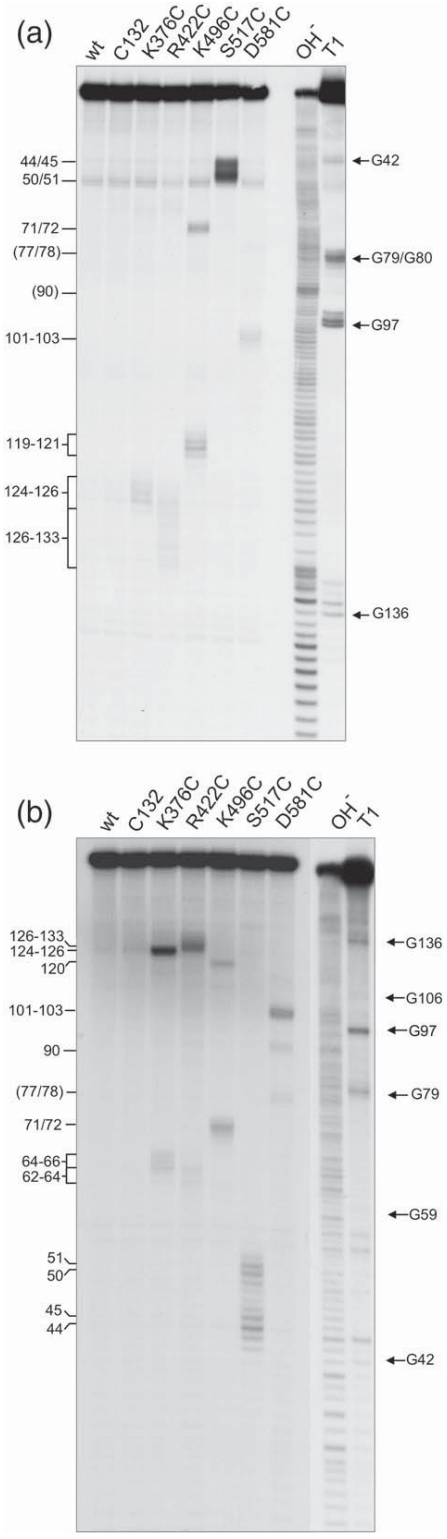

positions: 71/72 and 119–121. Both sequence elements face each other on adjacent strands of the helically arranged 6S RNA structure (Fig. 5). As noted above, the close spatial neighborhood nicely supports the specificity of the FeBABE footprinting analysis.

The σ^{70} variant D581C, with the FeBABE reagent within domain 4.2, which is known to interact with the −35 element of DNA promoters, gave rise to cleavages at positions 77/78, 90 and 101–103. In a three-dimensional model of the terminal 6S RNA hairpin helix (Fig. 5), positions 101–103 and 90 are close to each other while position 77/78 is more distant and not on the same site of the helical RNA arrangement. The distance in the derived tertiary structure between positions 77/78 and 90 is about 40 Å, making it rather unlikely that both cleavages occur in one and the same conformer of the RNA polymerase–6S RNA complex. Since the cleavage site at 77/78 is of rather low intensity in both 5′- and 3′-labeled RNA molecules, it might result from a minor structural population or could possibly be explained by a conformational dynamic of the 6S RNA–RNA polymerase complex (see Discussion).

Of special interest are cleavage sites observed with the σ^{70} variant S517C. This residue is located in domain 3.2, also termed “σ-finger” [39], which has been shown to be close to the +1 position of the DNA promoter template strand and as such points deep into the RNA polymerase active-site structure [30]. Cleavage sites within 6S RNA resulting from this σ variant could be mapped between positions 44/45 and 50/51, which is in perfect accordance with U44 as start site for the 6S RNA-directed transcription of pRNA [10,17]. According to structural probing data, this part of the 6S RNA sequence is clearly single stranded and not involved in any stable higher-order structural element, making predictions about its precise three-dimensional arrangement extremely difficult. Within the constraints of RNA polymerase structure, however, it may be folded similarly as the coding and non-coding DNA strands of open RNA

Fig. 4. Identification of FeBABE-induced cleavage sites within 6S RNA bound to different reconstituted RNA polymerase holoenzymes. Examples from analyses of end-labeled 6S RNA cleavage products resulting from the chemical nuclease FeBABE conjugated to different RNA polymerase Eσ^{70} holoenzymes on denaturing polyacrylamide gels are shown. (a) Cleavage products obtained with 3′-labeled 6S RNA. (b) Cleavage products obtained with 5′-labeled 6S RNA. Numbers on the left margin indicate nucleotide positions resulting from FeBABE cleavage. The different σ^{70} variants are given above the lanes. Products from alkaline hydrolysis (OH^-) and a lane with limited RNase T1 cleavage products (T1) are shown on the right side of each gel with characteristic G positions indicated.

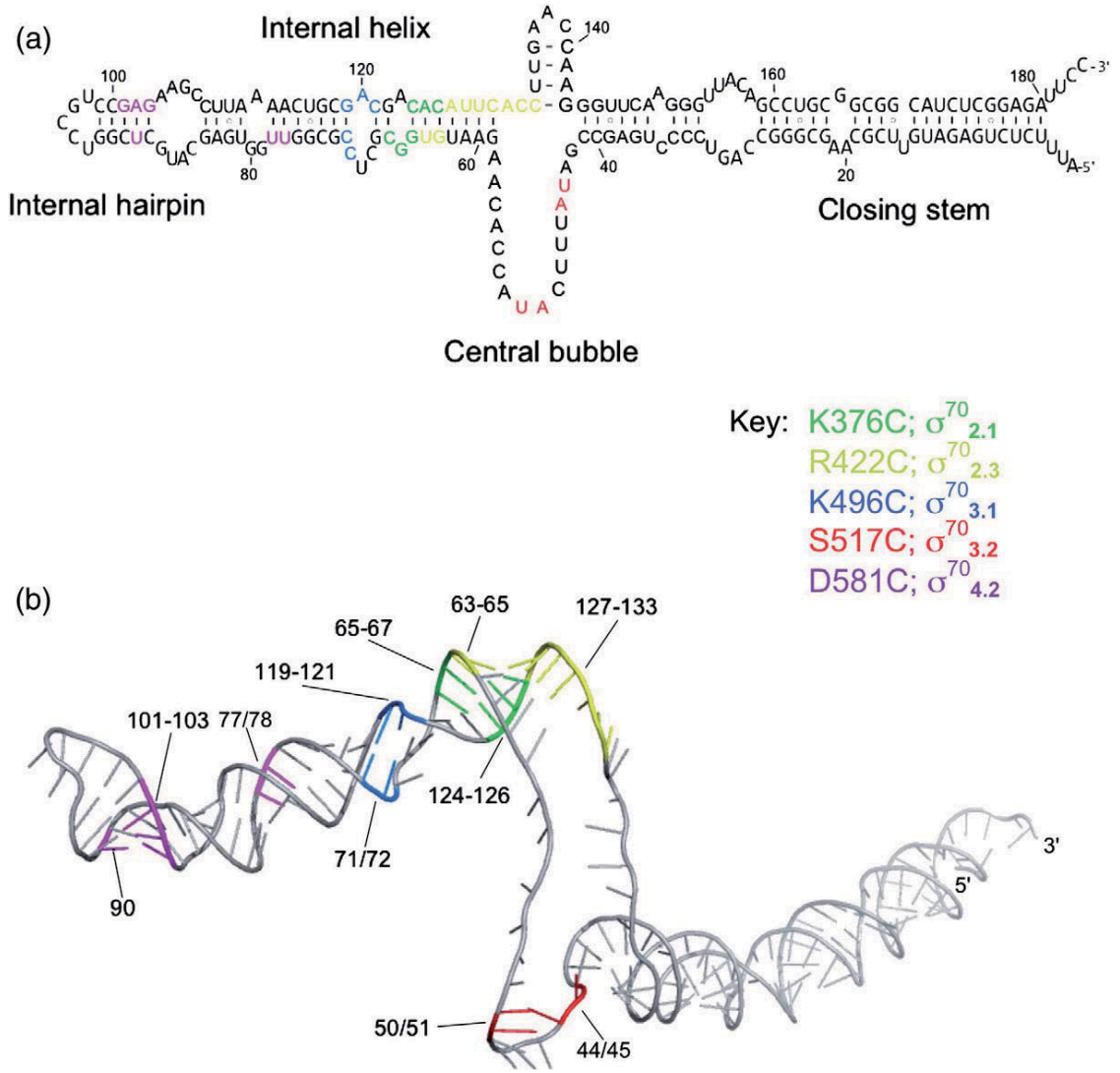

Fig. 5. Schematic arrangement of FeBABE-induced cleavage sites within the 6S RNA structure. (a) The 6S RNA secondary structure as recently determined is shown [34]. Secondary structural elements (Closing stem, Central bubble, Internal helix and Internal hairpin) are indicated, and the 6S RNA 5′- and 3′-ends are marked. Nucleotides identified as FeBABE-induced cleavage sites with the single-cysteine substitution variants are shown in different color: green, K376C ($\sigma^{70}_{2.1}$); yellow, R422C ($\sigma^{70}_{2.3}$); blue, K496C ($\sigma^{70}_{3.1}$); red, S517C ($\sigma^{70}_{3.2}$); magenta, D581C ($\sigma^{70}_{4.2}$). (b) Location of the different cleavage sites within a three-dimensional model of the 6S RNA is presented according to tertiary structure predictions for the helical segments with the program 3dRNA [35] based on the established secondary structure [34] and overall arrangement as a result from the docking and modeling data [36–38]. The same color code is used as in (a). Numbers indicate cleavage sequence positions.

polymerase promoter complexes, which have been fitted within the three-dimensional structure of RNA polymerase based on structural studies [24,40].

In summary, the cleavage data demonstrate that extended helical regions of the 6S RNA internal stem–loop structure (position C56 to C133) are proximal to σ^{70} domains 2.1, 2.3, 3.1 and 4.2, all of which have been implicated in the binding and melting of DNA promoter elements. The 6S RNA position U44, which has been characterized as start site for pRNA transcription, is located close to σ^{70} domain 3.2, known to be close to the RNA polymerase active center. None of the 6S RNA sequence elements could be detected in close proximity to σ^{70} position C132, adjacent to domain 1.2, or the two neighboring cysteines C291/C295 in the non-conserved domain of σ^{70}. Interestingly, all three amino acids occupy positions in RNA polymerase open promoter complexes outside the major channel that takes up the downstream DNA.

Notably, the complete 6S RNA closing stem structure (sequence positions 1–40 and 144–184) has not been a target for the cleavage reagent, indicating that this part of the structure is very likely distant from the RNA polymerase σ^{70} interface. Consistent with previous cross-linking studies [10], it is still likely, however, that this part of the 6S RNA is close to domains of the β/β′ subunits.

A three-dimensional model of a 6S RNA–RNA polymerase complex

We used the collected cleavage data and a low-resolution model of RNA polymerase σ^{70} holoenzyme in complex with Class I CAP-dependent DNA promoter (PDB ID: 3IYD) [40] as a template for nucleic acid positioning. We docked a computer-derived model of a full 6S RNA assembled from fragments according to the program 3dRNA [35] into the recent crystal structure of RNA polymerase σ^{70} holoenzyme (PDB ID: 4IGC) [27]. In the resulting binding mode, 6S RNA fits into RNA polymerase structure without producing conformational strain or sterical clashes that, given the size and complexity of protein–RNA interface, confirms the relevance of the assumed RNA tertiary structure. The geometry of the complex represents the gathered cleavage data. All regions in 6S RNA that are subject to cleavage are found in direct vicinities of the respective FeBABE nuclease sites (Fig. 6a).

The model indicates that the helical part of the internal stem region (along residues 59–93) structurally corresponds to the upstream promoter region from position −43 to position −12. It is of suitable size and geometry to maintain contacts with RNA polymerase both in the −10 promoter melting region and in the σ 4.2 region in a way analogous to the −35 DNA element.

A single-stranded central bubble region, comprising residues 42–58 in 6S RNA, closely follows the geometry and position of the transcription bubble in a DNA promoter (positions −11 to 5). Notably, two cleavage sites (U44/A45 and A50/U51), targeted by S517C-tethered FeBABE, are positioned within the polymerase active site symmetrically on both sides of the substituted amino acid embedded in a protein loop. Any shift in the nucleotide sequence in this area would result in worse agreement with cleavage data.

The 131–143 region in 6S RNA that, according to the secondary structure model of isolated RNA, is supposed to form a short hairpin loop [34] most likely adopts an unfolded conformation in the RNA–polymerase complex. As this region is four nucleotides shorter than the corresponding region in a DNA promoter, it is expected to maintain a relatively more straightened configuration than its DNA counterpart (Fig. 6b). A considerable width of the polymerase channel in this area apparently permits such structural variations.

Finally according to our model, the location of the closing stem in 6S RNA (along residues 1–41 and 144–184) corresponds to the placement of the downstream promoter region. Accordingly, its binding most likely requires the repositioning of σ 1.1 domain that occupies the binding channel in the holoenzyme structure (this domain had to be removed from the polymerase crystal structure prior to docking simulations).

Effects of 6S RNA mutations on RNA polymerase binding

As a result of the cleavage and docking analysis, we were able to identify 6S RNA regions that potentially interact with σ^{70} regions known to contain nucleic acid binding motifs. The helix–turn–helix motif of σ^{70} region 4.2 faces the major groove of 6S RNA at an internal bulge loop (residues 85–88 and 104–107). Such bulge loops or termini of helices can interrupt regular A-form helices and widen the deep major groove, thereby increasing the accessibility for protein interactions [41]. A second example for such a possible interaction is the α-helical part of σ^{70} region 3.0, shown to interact with the extended −10 sequence elements of promoter DNA [24]. This region seems to be proximal to bulged residues of the 6S RNA internal stem (residues 66–71 and 120–123). To test whether these bulge loops represent 6S RNA binding modules for $E\sigma^{70}$, we constructed 6S RNA mutants where the two bulge loops above were replaced, single or combined, by paired helical structures. The resulting mutant 6S RNAs CB1 (C85G/A86C/G88U), CB2 (G66U/ΔC69/Δ71C) and CB1-2 (C85G/A86C/G88U/G66U/ΔC69/Δ71C) (Supplemental Fig. S2a) were expressed, purified, labeled and tested for $E\sigma^{70}$ binding. It turned out that the loss of each of the two bulge loops had dramatic consequences on complex formation. Compared to wild-type 6S RNA, binding of CB1 was reduced by more than 98%. Binding of CB2 was reduced by roughly 60% while the absence of both bulges in CB1-2 resulted in complete loss of binding (Supplemental Fig. S2b). Next we asked if binding might be restored by compensatory mutations of the opposite strand of 6S RNA mutants reforming the original bulge structures with a different sequence. We focused on CB1, which displayed the strongest binding defect and constructed mutant 6S RNA CB3 (C85G/A86C/G88U; A104U/A105U/C107A, Supplemental Fig. S2a). These base exchanges were chosen as a result of a best fit from secondary and tertiary structure predictions [35,42] in comparison to the wild-type 6S RNA sequence. Unexpectedly, the compensatory CB3 mutation did not restore the ability to bind to $E\sigma^{70}$, however indicating that this bulge loop *per se* is not sufficient for correct recognition (Supplemental Fig. S2b).

Discussion

In this study, we have identified 6S RNA regions not previously known to be in close contact to the σ^{70} subunit of RNA polymerase holoenzyme. The results allow assigning spatial relationships between distinct sequence positions of the *E. coli* 6S RNA internal stem–loop region and known functional elements of RNA polymerase involved in the binding and conversion of closed to open promoter complexes. Interestingly, most of the FeBABE-induced cleavage sites identified in this study map at distant sites in the primary structure of 6S RNA but are located in close spatial proximity given the three-dimensional helical arrangement (Fig. 5). This fact nicely reflects the specificity of the cleavage reaction and is fully consistent with the deduced 6S RNA tertiary structure. Moreover, and in accordance with its function as initiating nucleotide for 6S RNA-directed pRNA transcription, position U44 was mapped in the vicinity of the RNA polymerase active center. It should be noted that the vicinity of position U44 had already been shown to be close to the active site by a previous study with RNA polymerase in which magnesium had been replaced by iron [17].

With the exception of the C132 variant RNA polymerase, where the chemical nuclease has been tethered to σ^{70} domain 1.2, all tested single-cysteine constructs induced distinct cleavages in the 6S RNA structure. The possibility of unsuccessful conjugation of the FeBABE reagent to this variant can be excluded based on the determination of free sulfhydryl groups before and after conjugation. Hence, we take the absence of cleavage products as clear indication that no part of the 6S RNA is close (in the range of 15 Å) to position 132 of σ^{70}. It should be noted that domain 1.2 has been shown to contact single-stranded regions of the non-template strand of stringent regulated promoters [43]. However, the contacting amino acids are located more C-terminal and did not include C132 [39]. We also did not find cleavages in 6S RNA with wild-type σ^{70}, where, beside C132, the natural cysteine positions 291 and 295 tethered to FeBABE are located in a non-conserved region between subdomains 1.2 and 2.1 (Fig. 4). This is consistent with the RNA polymerase holoenzyme structure, where all three cysteine side chains are located distant from the path occupied by nucleic acids. A large part of the 6S RNA structure, namely, the complete closing stem–helix (sequences 1–40 and 144–184), is also likely out of the range of the chemical nuclease tethered to σ^{70}. In analogy with downstream DNA promoter binding, we infer that this part of the molecule might be embedded in the RNA polymerase major cleft formed by the β and β′ domains that takes up the downstream promoter DNA.

Using UV-cross-linking 6S RNA sites in direct contact to σ^{70} and β/β′ had been determined before, yet the identified sequence positions were not assigned to distinct proteins or protein domains [10]. With the analyses reported here, we are now able to assign distinct 6S RNA sites, such as the internal stem–loop (positions 90 and 101–103) and the adjacent helical region flanking the central bubble (residues 63–72 and 119–133) to neighboring protein domains of the σ^{70} subunit. Moreover, identification of the close proximity of 6S RNA position U44, the +1 position for pRNA transcription, to σ^{70} subdomain 3.2, which reaches deeply into the RNA polymerase active center, explains the template property of the regulatory RNA.

Four of the previously identified cross-link sites [10] (6S RNA positions 125, 127, 131 and 136) fit perfectly well with the assignment to σ^{70} regions identified in this study. Hence, the three remaining sites (142, 150 and 159) located in or adjacent to the closing stem–helix, which appears to be distant from the σ^{70} subunit according to the proposed model, are likely reflecting close proximity to the β/β′ subunits. In fact, the docking results are consistent with all three 6S RNA positions in close vicinity to the β lobe and β′ jaw structures. However, we do not consider this part of the 6S RNA sequence, which corresponds to the downstream element by analogy to promoter DNA, as essential for RNA polymerase binding. Similar conclusions had been reached by a mutagenesis study with truncated 6S RNA molecules [16]. In contrast, the previously predicted 6S RNA site, functionally replacing the −35 elements of DNA promoters, is in rather good agreement with the site assigned to be in close proximity to domain 4.2 [16].

From previous attempts to identify RNA polymerase sites, which are interacting with or which are in close contact with 6S RNA, we know that the σ^{70} subregion 4.2 is critical for binding 6S RNA [12]. Moreover, amino acid replacement studies revealed that positively charged side chains of the domain 4.2 recognition helix are responsible for 6S RNA binding through charge–charge interactions [28]. This study also indicated that an expanded binding surface of σ^{70} domain 4.2 comprising residues more

Fig. 6. (a) Three-dimensional model of 6S RNA bound to Eσ^{70} RNA polymerase holoenzyme. 6S RNA has been docked to the RNA polymerase holoenzyme (Materials and Methods). Single-cysteine positions in σ^{70} are shown as colored spheres. Cleavage sites within the 6S RNA structure are colored accordingly (same color code as in Figs. 1 and 5). (b) Superimposition of the three-dimensional structures of promoter DNA and 6S RNA derived from the respective complexes with RNA polymerase as shown in (a). Cyan, DNA promoter; green, 6S RNA. The DNA structure is arranged according to 3IYD [40].

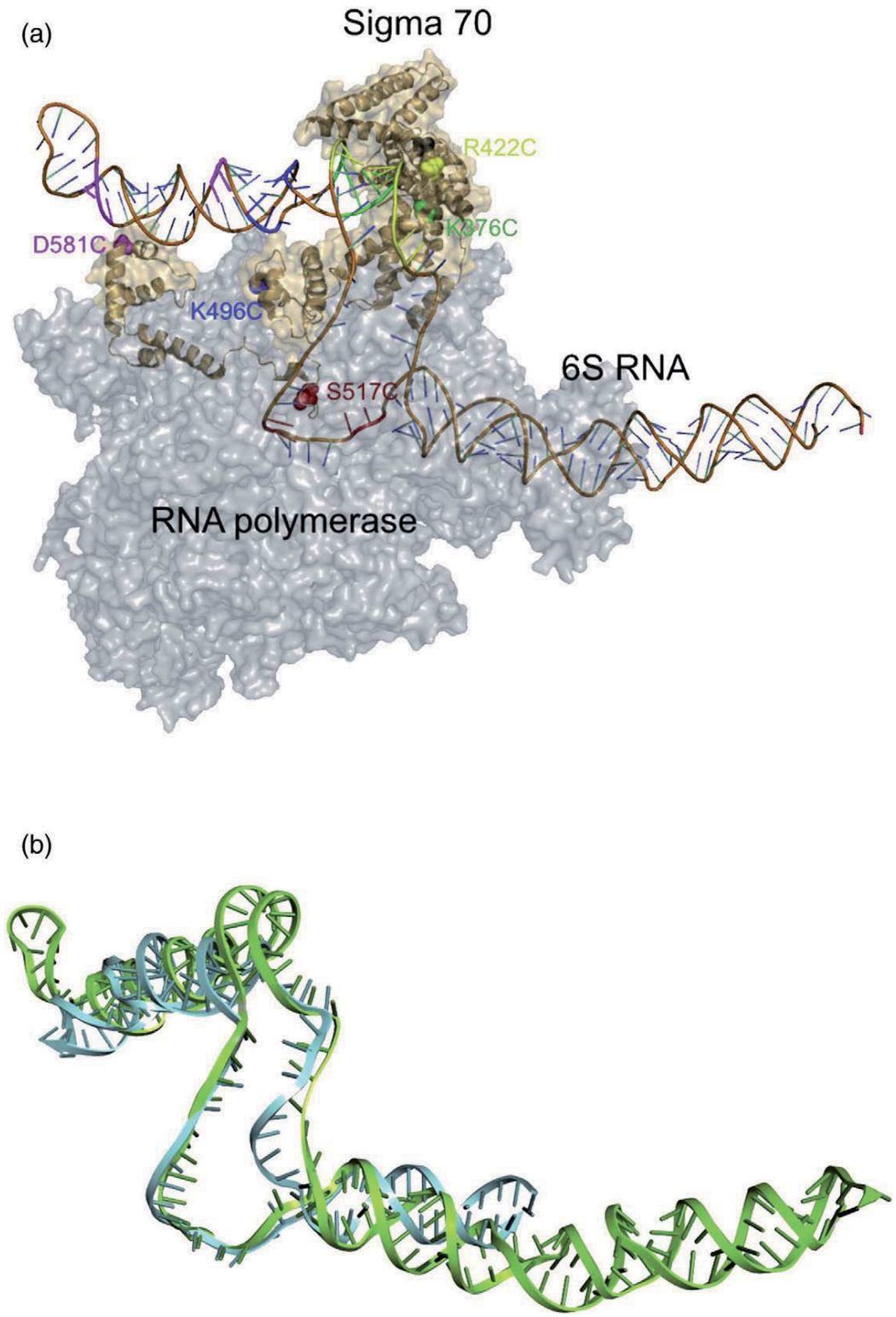

Fig. 6 (*legend on previous page*)

C-terminal in the recognition helix of region 4.2 was necessary for efficient 6S RNA binding. A direct interaction between 6S RNA and a more C-terminal extension of this σ^{70} domain is difficult to reconcile, however, with the results from the present study. Taken together, our study underlines the importance of σ^{70} domain 4.2 and adds domains 2.1, 2.3, 3.1 and 3.2 as spatially neighbored to 6S RNA.

In contrast to the known isomerization steps from closed to open RNA polymerase complexes, typical for DNA promoters, it is assumed that 6S RNA by virtue of its permanently unstructured single-stranded central domain is recognized as open promoter without any major structural transition. In line with this conjecture, neither previous attempts to identify any possible structural dynamics of the 6S RNA during RNA polymerase binding indicated gross conformational heterogeneity nor did we obtain evidence that the RNA undergoes structural changes that could be detected by footprint methods [34]. The only hint pointing to a possible structural dynamic or heterogeneity that we obtained from the FeBABE-induced cleavage experiments might be the simultaneous cleavage at three distinct sites (77/78, 90 and 101–103) induced with the D581C variant. While positions 90 and 101–103 are adjacent on the helical arrangement and close to D581C, position 77/78 is almost on the opposite face of the helix and at the far side of the chemical nuclease in our model (Figs. 5 and 6a). It seems rather unlikely that, in a rigid complex structure, all three 6S RNA positions are simultaneously in reach of the cleavage reagent. The result might be explained, however, by a dynamic complex structure. It is known that σ^{70} domain 4.2, which harbors D581C, interacts with the β flap domain. This interaction undergoes a dynamic change at the transition between the open initiation complex and promoter clearance [44]. Hence, a certain RNA polymerase population, which undergoes such a conformational change, might be a possible explanation for the distant cleavage positions observed.

Our attempts to monitor possible changes of the FeBABE-induced cleavage upon conditions of partial or full-length pRNA synthesis failed due to rapid dissociation of the σ subunit even in the presence of limiting NTPs. Hence, with this method, we could not determine possible structural alterations under conditions of provoked pRNA synthesis.

Comparison of the 6S RNA model docked to RNA polymerase with holoenzyme–DNA complexes [40,45] reveals subtle differences in the three-dimensional arrangement of the two different nucleic acids (Fig. 6b; Supplemental Fig. S1). Both types of nucleic acids have been arranged to follow a similar path within the three-dimensional architecture of RNA polymerase but apparently exhibit distinct but small differences in structure. Deviations can be discerned for the helical elements flanking the single-stranded (melted) region, not only due to the difference between A-form RNA and B-form DNA structures but also because of the occurrence of numerous little bubbles and bulges characteristic for the helical parts of the 6S RNA structure. A further functional indication for subtle recognition differences between DNA promoters and 6S RNA may possibly be reflected by reduced binding of *lac*UV5 promoter DNA to σ^{70} with FeBABE tethered to R422C [30] while 6S RNA is normally recognized by the same σ^{70} variant. Interestingly, the structures of the R422C cleavage sites differ notably (Fig. 6b; Supplemental Fig. S1). Moreover, some additional small differences may be noted comparing *lac*UV5 promoter DNA cleavage obtained in the above study [30] with the same σ variants and 6S RNA. Variant K496C causes a very prominent and rather extended cleavage in the DNA suggesting more extensive and closer contacts of σ^{70} domain 3.1 with the promoter DNA. Moreover, variant S517C (σ^{70} domain 3.2) cleaves both template and non-template strands of promoter DNA, while 6S RNA is only cleaved twice within a short sequence region. This might indicate that the non-template strand of the *lac*UV5 promoter and the corresponding 6S RNA sequence element (residues 131–143) do not share the same path.

The recognition of DNA promoters involves direct interactions of amino acid side chains between the σ^{70} domain 4.2 recognition helix and the backbone and conserved bases of both template and non-template strands of −35 promoter elements [23]. The part of the 6S RNA structure identified in this study to be closest to the recognition helix of σ^{70} domain 4.2 (positions 90 and 101–103) is flanking a four-nucleotide internal bubble within the internal stem structure. The cleavage reagent is located in the loop region of the helix–turn–helix DNA binding motif (D581C). A second example for cleavages adjacent to an internal bubble is apparent for the sites 71/72 and 119–121 induced by the K496C variant. It is reasonable to assume that such structures of the 6S RNA do exist exclusively neither in a regular A-form RNA-helix nor in a B-form DNA-helix conformation. Moreover, no sequence similarity with any conserved −35 promoter sequences exists for the respective 6S RNA region. Hence, the type of interaction between 6S RNA and σ^{70} domain 4.2 almost certainly deviates from standard helix–turn–helix recognition and base-specific interactions of the σ^{70} domain 4.2 recognition helix and canonic sequences of −35 promoters. To further explore the functional importance of the 6S RNA bulge loops of the internal stem region in $E\sigma^{70}$ recognition, we analyzed mutant 6S RNAs CB1, CB2 and CB1-2 in which one, two or both bulge regions, respectively, had been replaced by corresponding double-stranded sequences. It turned out that each bulge is important for binding and that the replacement of both structural elements causes a complete loss in binding activity (Supplemental Fig. S2). Initially,

this result indicates a structural rather than sequence-dependent recognition mechanism. However, the fact that a compensatory 6S RNA mutation (CB3) restoring the terminal bulge loop did not restore $E\sigma^{70}$ binding reveals that recognition is not solely dependent on secondary structure but apparently has a sequence-dependent component. In a previous study, several single-base residues (e.g., C85A or A86G) in the closed bulge mutants (CB1 and CB3) were altered as single-base substitutions and displayed decreased binding [16]. Since CB1 mutant RNA exhibits a stronger binding defect than each of the C85A or A86G mutations in the above study, one might conclude that the important residues in this region need to be single stranded. The results obtained with the CB2 mutant revealed that the bulged region proximal to the central domain additionally contributes to RNA polymerase binding. Our model would predict that σ^{70} region 3.0, which is in direct neighborhood to this sequence element (Fig. 6a), might be involved in the recognition of this structure.

While our study has yielded rather precise information on the spatial relationship between a selection of σ^{70} amino acid side chains and defined sequence elements of 6S RNA, it should be noted that only a limited number of single-cysteine substitutions were analyzed and that close contacts to other parts of the molecule cannot be excluded. Moreover, as a note of caution, the presented model should not be over-interpreted with respect to the details of RNA–protein atomic contacts. It does not reflect, for instance, global rearrangement of the RNA polymerase upon RNA binding. Nevertheless, our experimentally derived three-dimensional structure of 6S RNA bound to RNA polymerase should be helpful for the understanding of 6S RNA function and inspire further high-resolution studies on this unique riboregulator.

Materials and Methods

Preparation of FeBABE tethered to single-cysteine σ^{70} variant proteins

Overexpression, purification and conjugation with FeBABE of wild-type and mutant σ^{70} proteins were performed as described previously [46]. Conjugation efficiency was determined by measuring dithionitrobenzoic acid (Ellman's reagent) reactivity with free sulfhydryl groups before and after conjugation with FeBABE [47]. Yields for the different mutants varied between 20% and 60% roughly in accordance with recently determined conjugation efficiencies [30].

In vitro transcription assay

To monitor the transcriptional activity of holoenzymes reconstituted with mutant σ^{70} proteins with and without the FeBABE conjugate, we performed *in vitro* transcription reactions with 6S RNA as template. We incubated 300 nM 6S RNA with 50 nM core RNA polymerase together with a 5-fold molar excess of each of the σ^{70} variants, either with or without FeBABE in 50 mM Tris–acetate (pH 8.0), 10 mM Mg acetate, 0.5 mM DTT, 0.5 mM ethylenediaminetetraacetic acid (EDTA) and 80 mM K glutamate. The reaction was started by addition of 65 μM each of ATP, CTP and UTP and 6.32 μM GTP containing 4 μCi [α-^{32}P]GTP and allowed to proceed for 10 min at 30 °C. New rounds of initiation were then inhibited with chase solution (2 mM each NTP and 2 mg/ml heparin), and after another incubation for 10 min at 30 °C, transcription products were separated on denaturing polyacrylamide gels.

RNA polymerase–6S RNA complex formation

In a total volume of 40 μl, 15 nM 3′- or 5′-radiolabeled 6S RNA, which had been purified on denaturing polyacrylamide gels, was incubated with 50 nM core RNA polymerase and a 5-fold molar excess of σ^{70} variants in 50 mM Tris–acetate (pH 8.0), 10 mM Mg acetate, 0.5 mM DTT, 0.5 mM EDTA and 80 mM K glutamate for 10 min at 30 °C. To avoid nonspecific complexes, we added heparin (200 ng/μl final concentration) followed by incubation for 5 min at 30 °C. An aliquot was analyzed by gel retardation for successful complex formation, whereas the rest of the sample was used for cleavage reactions.

Cleavage reaction of 6S RNA

Cleavage of 6S RNA in complex with FeBABE-tethered σ^{70} holoenzyme variants was started by sequential addition of sodium ascorbate (2 mM final concentration) and hydrogen peroxide (5 mM final concentration), and the reaction was allowed to proceed for 3 min at 30 °C. The reaction was quenched with 100 mM thiourea and 20 mM EDTA, and following ethanol precipitation, we separated the cleavage products on denaturing polyacrylamide gels.

Construction of 6S RNA mutants

For the construction of CB1 6S RNA, the oligonucleotides 5′-cgcggttggtgaggcttctcg-3′ and 5′-gaccgagaagcctcaccaac-3′ were annealed and ligated into the BtgI and RsrII sites of the T7 expression vector pUC18-T7-6S [10]. For the construction of the CB2 and CB1-2 mutants, the hybridized oligonucleotides 5′-tgagccgatatttcataccacaagaatgtgtcgt-3′ and 5′-cgcgacgacacattcttgtggtatgaaatatcggc-3′ were ligated into the Bpu10I and BtgI sites of pUC18-T7-6S and pUC18-T7-6S(CB1), respectively. The CB3 mutant was generated by PCR employing the mutagenic oligonucleotides 5′-ctcggtccgtccgagttgacttaaaactgcgacgac-3′ and 5′-gtcgtcgcagttttaagtcaactcggacggaccgag-3′. DpnI was used for digestion of methylated, parental DNA.

Analysis of mutant 6S RNA binding to $E\sigma^{70}$

We incubated 15 nM 5′-radiolabeled 6S RNA with or without 100 nM $E\sigma^{70}$ holoenzyme for 10 min at 30 °C in

50 mM Tris–acetate (pH 8.0), 10 mM Mg acetate, 0.5 mM DTT, 0.5 mM EDTA and 80 mM K glutamate. Heparin was added (200 ng/μl final concentration) followed by an additional incubation for 10 min at 30 °C. Complexes were separated on a 5% native PAGE.

Molecular docking

Tertiary structure predictions of 6S RNA fragments were obtained by using the automated program, 3dRNA, for RNA tertiary structure prediction [35]. The crystal structure of the *E. coli* σ^{70} holoenzyme was obtained from the Protein Data Bank (4IGC) [27]. Positions 132, 376, 422, 496, 517 and 581 were changed to cysteine residues. Molecular docking of the 6S RNA model to 4IGC polymerase structure was performed with the use of ATTRACT program and a coarse-grained force field for protein–nucleic acid interactions [36,37]. 6S RNA was considered as a set of four independent fragments: central stem (residues 1–41 and 144–184), central bubble (residues 42–58), internal stem (residues 59–130) and short bubble (residues 127–143). Each fragment was extended to include several overlapping nucleotides with its neighboring fragments. A binding mode of DNA in homologous, low-resolution RNA polymerase–promoter complex (PDB ID: 3IYD) was used as a template for the initial placement and modeling (in the case of both bubbles) of RNA fragments prior to docking. RNA fragments were docked independently, using multiple (up to 10,000) starting configurations obtained by random displacements (up to 5 Å) and rotations (to 10°) around the initial placement. Structural flexibility of RNA was modeled by allowing deformations in nine softest normal modes using elastic network energy model. The final 6S RNA structure was assembled using the overlapping sequence regions. In the case of internal stem, docking solutions with possibly minimal distances between substituted amino acids and respective cleavage regions were preferred to lowest-energy-scoring solutions. All atom structural refinement of the docked RNA model was carried out with AmberTools using NAB framework with Amber ff99 force field and generalized Born solvent model [38].

Supplementary data to this article can be found online at http://dx.doi.org/10.1016/j.jmb.2013.07.008

Acknowledgements

We like to thank Dr. C. Meares for generously providing us with the σ^{70} single-cysteine mutants. Many thanks to R. Wurm for her skillful technical help. The work was supported by the Priority Program of the Deutsche Forschungsgemeinschaft SPP1258. P.S. and M.Z. were supported by the Deutsche Forschungsgemeinschaft grant Za 153/19-2.

Received 26 March 2013;
Received in revised form 28 June 2013;
Accepted 4 July 2013
Available online 15 July 2013

Keywords:
non-coding RNA;
FeBABE footprinting;
6S RNA;
RNA polymerase;
structural modeling

Abbreviation used:
EDTA, ethylenediaminetetraacetic acid.

References

[1] Gottesman S, Storz G. Bacterial small RNA regulators: versatile roles and rapidly evolving variations. Cold Spring Harbor Perspect Biol 2011;3:a003789.
[2] Storz G, Altuvia S, Wassarman KM. An abundance of RNA regulators. Annu Rev Biochem 2005;74:199–217.
[3] Storz G. An expanding universe of noncoding RNAs. Science 2002;296:1260–3.
[4] Neußer T, Gildehaus N, Wurm R, Wagner R. Studies on the expression of 6S RNA from *E. coli*: involvement of regulators important for stress and growth adaptation. Biol Chem 2008;389:285–97.
[5] Wassarman KM, Storz G. 6S RNA regulates *E. coli* RNA polymerase activity. Cell 2000;101:613–23.
[6] Geißen R, Steuten B, Polen T, Wagner R. *E. coli* 6S RNA: a universal transcriptional regulator within the centre of growth adaptation. RNA Biol 2010;7:564–8.
[7] Trotochaud AE, Wassarman KM. 6S RNA function enhances long-term cell survival. J Bacteriol 2004;186:4978–85.
[8] Trotochaud AE, Wassarman KM. 6S RNA regulation of *pspF* transcription leads to altered cell survival at high pH. J Bacteriol 2006;188:3936–43.
[9] Hindley J. Fractionation of ^{32}P-labelled ribonucleic acids on polyacrylamide gels and their characterization by fingerprinting. J Mol Biol 1967;30:125–36.
[10] Gildehaus N, Neusser T, Wurm R, Wagner R. Studies on the function of the riboregulator 6S RNA from *E. coli*: RNA polymerase binding, inhibition of *in vitro* transcription and synthesis of RNA-directed *de novo* transcripts. Nucleic Acids Res 2007;35:1885–96.
[11] Trotochaud AE, Wassarman KM. A highly conserved 6S RNA structure is required for regulation of transcription. Nat Struct Biol 2005;12:313–9.
[12] Cavanagh AT, Klocko AD, Liu X, Wassarman KM. Promoter specificity for 6S RNA regulation of transcription is determined by core promoter sequences and competition for region 4.2 of σ^{70}. Mol Microbiol 2008;67:1242–56.
[13] Kim EY, Shin MS, Rhee JH, Choy HE. Factors influencing preferential utilization of RNA polymerase containing sigma-38 in stationary-phase gene expression in *Escherichia coli*. J Microbiol 2004;42:103–10.
[14] Neußer T, Polen T, Geißen R, Wagner R. Depletion of the non-coding regulatory 6S RNA in *E. coli* causes a surprising reduction in the expression of the translation machinery. BMC Genomics 2010;11:165–78.
[15] Barrick JE, Sudarsan N, Weinberg Z, Ruzzo WL, Breaker RR. 6S RNA is a widespread regulator of eubacterial RNA polymerase that resembles an open promoter. RNA 2005;11:774–84.
[16] Shephard L, Dobson N, Unrau PJ. Binding and release of the 6S transcriptional control RNA. RNA 2010;16:885–92.

[17] Wassarman KM, Saecker RM. Synthesis-mediated release of a small RNA inhibitor of RNA polymerase. Science 2006;314:1601–3.
[18] Wurm R, Neußer T, Wagner R. 6S RNA-dependent inhibition of RNA polymerase is released by RNA-dependent synthesis of small *de novo* products. Biol Chem 2010;39:187–96.
[19] Beckmann BM, Hoch PG, Marz M, Willkomm DK, Salas M, Hartmann RK. A pRNA-induced structural rearrangement triggers 6S-1 RNA release from RNA polymerase in *Bacillus subtilis*. EMBO J 2012;31:1727–38.
[20] Cavanagh AT, Sperger JM, Wassarman KM. Regulation of 6S RNA by pRNA synthesis is required for efficient recovery from stationary phase in *E. coli* and *B. subtilis*. Nucleic Acids Res 2011;40:2234–46.
[21] Rediger A, Geissen R, Steuten B, Heilmann B, Wagner R, Axmann IM. 6S RNA—an old issue became blue-green. Microbiology 2012;158:2480–91.
[22] Sharma CM, Hoffmann S, Darfeuille F, Reignier J, Findeiss S, Sittka A, et al. The primary transcriptome of the major human pathogen *Helicobacter pylori*. Nature 2010;464: 250–5.
[23] Campbell EA, Muzzin O, Chlenov M, Sun JL, Olson A, Weinman O, et al. Structure of the bacterial RNA polymerase promoter specificity σ subunit. Mol Cell 2002;9:527–38.
[24] Murakami KS, Masuda S, Campbell EA, Muzzin O, Darst SA. Structural basis of transcription initiation: an RNA polymerase holoenzyme–DNA complex. Science 2002;296: 1285–90.
[25] Vassylyev DG, Sekine S, Laptenko O, Lee J, Vassylyeva MN, Borukhov S, et al. Crystal structure of a bacterial RNA polymerase holoenzyme at 2.6 Å resolution. Nature 2002;417:712–9.
[26] Zhang G, Campbell EA, Minakhin L, Richter C, Severinov K, Darst SA. Crystal structure of *Thermus aquaticus* core RNA polymerase at 3.3 Å resolution. Cell 1999;98:811–24.
[27] Murakami KS. The X-ray crystal structure of *Escherichia coli* RNA polymerase σ^{70} holoenzyme. J Biol Chem 2013;288: 9126–34.
[28] Klocko AD, Wassarman KM. 6S RNA binding to Eσ^{70} requires a positively charged surface of σ^{70} region 4.2. Mol Microbiol 2009;73:152–64.
[29] Meares CF, Datwyler SA, Schmidt BD, Owens J, Ishihama A. Principles and methods of affinity cleavage in studying transcription. Methods Enzymol 2003;371:82–106.
[30] Owens JT, Chmura AJ, Murakami K, Fujita N, Ishihama A, Meares CF. Mapping the promoter DNA sites proximal to conserved regions of sigma 70 in an *Escherichia coli* RNA polymerase-*lacUV5* open promoter complex. Biochemistry 1998;37:7670–5.
[31] Severinova E, Severinov K, Fenyö D, Marr M, Brody EN, Roberts JW, et al. Domain organization of the *Escherichia coli* RNA polymerase σ^{70} subunit. J Mol Biol 1996;263: 637–47.
[32] Rana TM, Meares CF. N-terminal modification of immunoglobulin polypeptide chains tagged with isothiocyanato chelates. Bioconjug Chem 1990;1:357–62.
[33] Malhotra A, Severinova E, Darst SA. Crystal structure of a σ^{70} subunit fragment from *E. coli* RNA polymerase. Cell 1996;87:127–36.
[34] Steuten B, Wagner R. A conformational switch is responsible for the reversal of the 6S RNA-dependent RNA polymerase inhibition in *Escherichia coli*. Biol Chem 2012;393:1513–22.
[35] Zhao Y, Huang Y, Gong Z, Wang Y, Man J, Xiao Y. Automated and fast building of three-dimensional RNA structures. Sci Rep 2012;2:734.
[36] Setny P, Zacharias M. A coarse-grained force field for Protein-RNA docking. Nucleic Acids Res 2011;39:9118–29.
[37] Zacharias M. Protein–protein docking with a reduced protein model accounting for side-chain flexibility. Protein Sci 2003;12:1271–82.
[38] Case DA, Darden TA, Cheatham TE, Simmerling CL, Wang J, Duke RE, et al. AMBER 12. San Francisco, CA: University of California; 2012.
[39] Zhang Y, Feng Y, Chatterjee S, Tuske S, Ho MX, Arnold E, et al. Structural basis of transcription initiation. Science 2012;338:1076–80.
[40] Hudson BP, Quispe J, Lara-Gonzalez S, Kim Y, Berman HM, Arnold E, et al. Three-dimensional EM structure of an intact activator-dependent transcription initiation complex. Proc Natl Acad Sci USA 2009;106:19830–5.
[41] Weeks KM, Crothers DM. Major groove accessibility of RNA. Science 1993;261:1574–7.
[42] Zuker M. Mfold Web server for nucleic acid folding and hybridization prediction. Nucleic Acids Res 2003;31: 3406–15.
[43] Haugen SP, Berkmen MB, Ross W, Gaal T, Ward C, Gourse RL. rRNA promoter regulation by nonoptimal binding of sigma region 1.2: an additional recognition element for RNA polymerase. Cell 2006;125:1069–82.
[44] Murakami KS, Darst SA. Bacterial RNA polymerases: the wholo story. Curr Opin Struct Biol 2003;13:31–9.
[45] Murakami KS, Masuda S, Darst SA. Structural basis of transcription initiation: RNA polymerase holoenzyme at 4.4 Å resolution. Science 2002;296:1280–4.
[46] Owens JT, Miyake R, Murakami K, Chmura AJ, Fujita N, Ishiama A, et al. Mapping the σ^{70} subunit contact sites on *Escherichia coli* RNA polymerase with a σ^{70}-conjugated chemical protease. Proc Natl Acad Sci USA 1998;95: 6021–6.
[47] Riener CK, Kada G, Gruber HJ. Quick measurement of protein sulfhydryls with Ellman's reagent and with 4,4′-dithiodipyridine. Anal Bioanal Chem 2002;373:266–76.

3.3.1 Supplemental material: Steuten *et al.* 2013

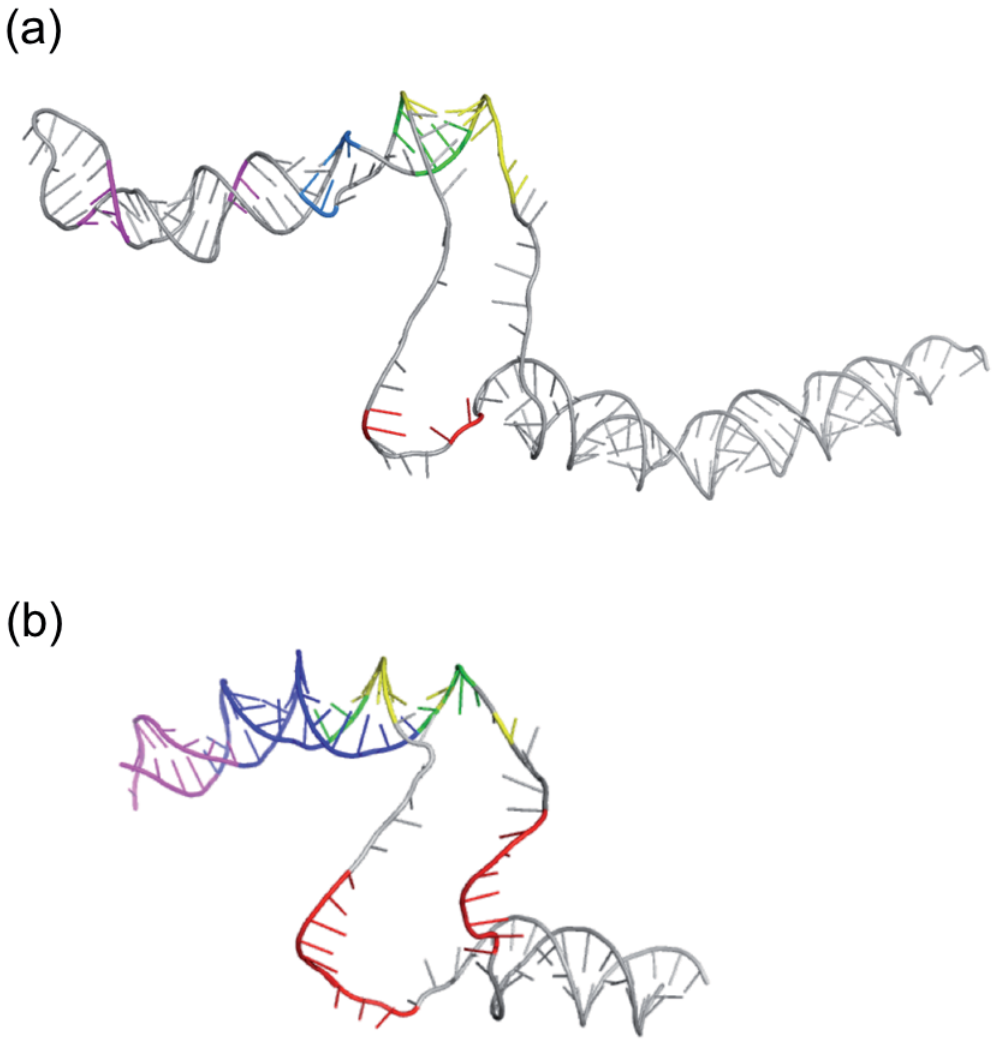

Figure S1: Comparison of the FeBABE cleavage positions of promoter DNA and 6S RNA and their possible arrangements in RNA polymerase complexes. (a) Three-dimensional model of the 6S RNA as presented in Fig. 6a. Colors indicate FeBABE cleavage sites. (b) Three-dimensional structure of a promoter DNA as presented in Fig. 6b. For comparative reasons, information about cleavage sites determined within the RNA polymerase-bound *lac*UV5 promoter DNA initiation complex (Owens *et al.* 1998) have been transferred to the 3IYD DNA model.

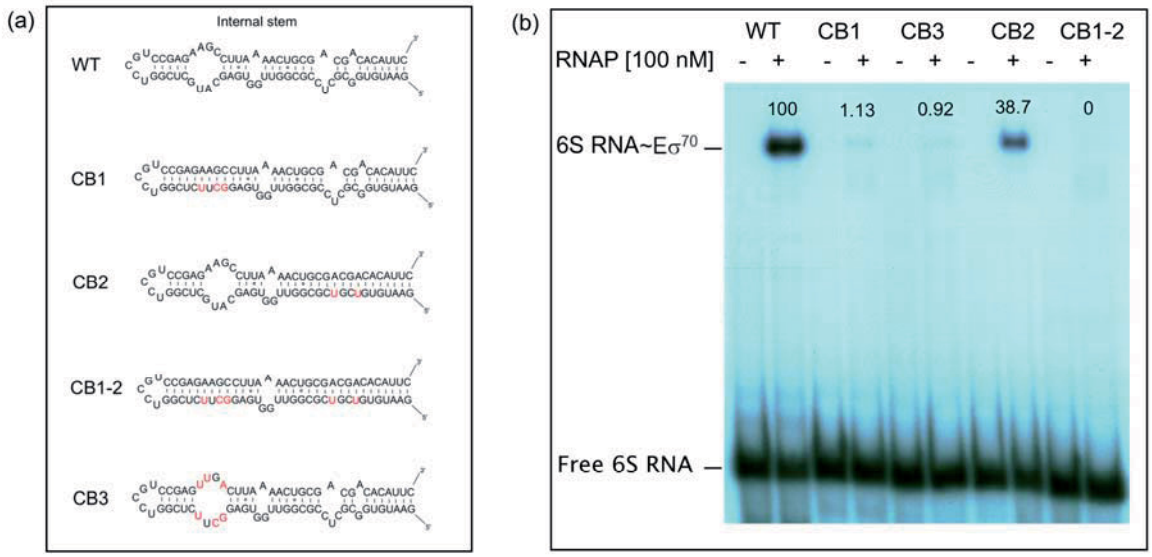

Figure S2: RNA polymerase binding of 6S RNAs with base change mutations in the internal helix. (a) Secondary structure representation of the different 6S RNA constructs are presented, indicating the base change mutations (red) in the internal helix that eliminate internal bulge loops (CB1, CB2 and CB1-2) or complementary changes that restore the bulge loop of CB1 (CB3). (b) RNA polymerase binding analysis of 6S RNAs with bulge loop mutations in the internal stem region. The positions of free RNA and RNA polymerase complexes are indicated at the left margin. The percent complex formed for each RNA is given in each lane relative to wild type, which has been set to 100%. The numbers are mean of four independent experiments (SD_{WT} = ±6.7; SD_{CB1} = ±0.5; SD_{CB2} = ±2.1; SD_{CB3} = ±0.2).

4 Discussion

In the recent years the action of non-coding small RNAs has attracted great interest in research. The ancient dogma of RNA to function solely as protein-coding message had to be revised with the discovery that ncRNAs can regulate all steps of gene expression in all organisms. Several regulatory RNAs, which act by antisense base pairing with mRNAs, protein sequestration or ligand-mediated structural reorganization, had been explored. The considerable mechanism of directly regulating transcription via interaction with the major form of RNA polymerase is comparatively rare. The eubacterial 6S RNA is the prominent representative of the latter group. In this PhD thesis the structural properties of the well-studied *E. coli* 6S RNA as well as predicted cyanobacterial 6S RNAs are analysed in depth. Functional consequences of structural transitions are explored with regard to the growth phase-dependent transcriptional inhibition through 6S RNA. Finally, mapping results allow for the first time the depiction of a tertiary structural model of 6S RNA relative to the known high-resolution *E. coli* RNAP holoenzyme structure. A summarizing discussion of the obtained results will be given in the following section.

4.1 Conclusions from heterologous studies

In chapter 3.1 results of heterologous *in vitro* experiments between four putative 6S RNAs from diverse cyanobacterial species and the *E. coli* σ^{70}-containing holoenzyme of RNA polymerase were presented. All molecules from the distantly related cyanobacteria could be identified as real 6S RNAs that exhibit similar characteristics as previously determined for the *E. coli* (*Eco*) 6S RNA. Among these unique properties are the typic 6S RNA secondary structures, the stable association with RNAP ($E\sigma^{70}$), the inhibition of *in vitro* transcription and the capability to direct the synthesis of pRNAs (Wassarman and Storz 2000; Wassarman and Saecker 2006; Gildehaus *et al.* 2007). Intriguingly, the mapped secondary structure of 6S RNA from *Nostoc sp.* PCC 7120 exhibits the highest degree of similarity with *Eco* 6S RNA (compare 3.2 Fig. 3 (A) and 3.1.1 Fig. S3). Both molecules show the two double-stranded helices, which are interrupted by common bulge loops comparable in size and position. Moreover, the 3' central domain consists of a 4 nt hairpin region that seems to be in equilibrium with a single-stranded state as indicated by the probing results for both 6S RNAs. In contrast, the 6S RNA structures of *Synechocystis sp.*

PCC 6803 and *Synechococcus elongatus* PCC 7942 reveal either an additional hairpin in the closing stem (*Synechocystis*) or altered structural elements in the central domain (*Synechococcus*). The structural similarity between *Eco* and *Nostoc* 6S RNA is also reflected in their functional homology. Both the association with $E\sigma^{70}$ and the inhibition of $E\sigma^{70}$ occur to a similar extent for these two RNAs. In addition the transcription from the *Eco* and the *Nostoc* 6S RNA templates produces pRNAs with a predominant length of about 20 nt whereas the other cyanobacterial pRNAs are up to 30 nt long. These results emphasize the close relationship between structure and function of 6S RNA.

Although there are some differences in the reactivity of each cyanobacterial 6S RNA tested, they do all have one feature in common: they specifically bind to the *Eco* $E\sigma^{70}$. Another example for this heterologous interaction known from the literature is the *Haemophilus influenzae* 6S RNA, which efficiently co-immunoprecipitates with *Eco* RNAP (Wassarman and Storz 2000). This rises the question what is the common structural element or sequence region of these diverging RNAs that determine association with the same protein? From recent studies it is known that σ^{70} region 4.2 is of great importance for the interaction with 6S RNA. Furthermore an "upstream region" of 6S RNA adjacent to the terminal loop was predicted to be a potential binding site for σ^{70} region 4.2 (Cavanagh *et al.* 2008; Klocko and Wassarman 2009). The FeBABE cleavage data and the deduced 6S-RNAP tertiary structure model from 3.3 corroborate that region 4.2 is in close contact with the predicted 6S RNA region. Therefore, the different 6S RNAs from heterologous complexes with *Eco* $E\sigma^{70}$ were used for a multiple sequence alignment and a comparison of their respective secondary structures. This approach focusses on the terminal hairpin and is depicted in Figure 4.1. The alignment was done with the bioinformatics tool LocARNA, which generates a multiple sequence alignment together with a consensus secondary structure (Smith *et al.* 2010). A high degree of conservation in base pairing becomes obvious for the five base pair long helix of the terminal hairpin (residues 89-93 and 99-103 relative to the *E. coli* numbering). While the primary sequences permit a slight variability in this region, both sequence and structure are highly conserved for nucleotides 83-86 (AGCA) and 104-107 (AAGC). These regions constitute a two or three base pairs large double-strand, which is flanked by bulge loops. In the case of *E. coli* there are two base-pair alternatives for

this 6S RNA region (see Fig. 4.1 b), both were experimentally verified indicative of co-existing structures (Barrick *et al.* 2005; Trotochaud and Wassarman 2005). The principle of changing double-stranded and single-stranded conformations around this region is valid for either secondary structure, however. Thus, the importance of these residues for association of 6S RNA with the *E. coli* $E\sigma^{70}$ is highlighted by the heterologous studies. In order to distinguish between a sequence-dependent or structure-dependent interaction of the conserved 6S RNA region and σ^{70} region 4.2 we performed a mutational analysis. According to the three-dimensional model of the 6S-RNAP complex (3.3) the helix-turn-helix motif of σ^{70} region 4.2 faces the major groove of 6S RNA at the conserved region (Fig. 4.2 a). As reported previously bulge loops or termini of helices can interrupt regular A-form helices and widen the deep major groove, increasing the accessibility for protein interactions (Weeks and Crothers 1993). To test whether the bulge loop determines $E\sigma^{70}$ binding capacity of 6S RNA we constructed a mutant 6S RNA with a closed bulge loop at the conserved region (CB1 RNA). Mobility shift assays with $E\sigma^{70}$ revealed that this mutant is highly defective in RNA polymerase binding. CB1 RNA shows a decrease in binding of more than 98% relative to wild type 6S RNA (see 3.3.1, Fig. S2). For the compensatory mutation of the opposite residues of 6S RNA base exchanges were chosen according to best results from secondary and tertiary structure predictions in comparison to wild type 6S RNA. The compensatory CB3 mutant did not restore association to $E\sigma^{70}$ relative to 6S RNA. This observation indicates that the interaction of σ^{70} region 4.2 with this region does not solely depend on the bulge loop structure but also on primary sequence. In a previous study several residues that were changed in the closed bulge mutants were altered as single base substitutions (e.g. C85A or A86G) and displayed decreased binding (Shephard *et al.* 2010). Nevertheless, the CB1 mutant exhibits a stronger binding defect than each of the C85A or A86G mutant indicating that certain residues in this region need to be single-stranded. The failure of CB3 RNA to bind RNA polymerase may be due to the mutation of C107, which showed a strong binding defect as single point mutation C107G. This cytosine residue is present in all heterologous 6S RNAs that bind *E. coli* $E\sigma^{70}$ (Fig. 4.1 a), hence it should be considered as a good candidate for sequence-specific interaction with region 4.2. On the other hand, the single substitution C108G provoked the strongest effect on binding in the study mentioned above. Although this residue C108 is conserved in the γ-proteobacteria (e.g. *E. coli* and *H. influenza*)

(Brown and Ellis 2005), it is absent in the cyanobacterial 6S RNAs, which specifically bind the same RNAP as well. As a consequence the C108 seems to be crucial for association of 6S RNA with RNAP but obviously is dispensable in the case of cyanobacterial 6S RNAs. In summary, the specificity and stability of the 6S RNA-RNAP interaction is modulated by several residues of the conserved region adjacent to the terminal hairpin structure. This region is not a continuous helix because single-stranded bulge loop structures seem to account for the accessibility of σ^{70} region 4.2.

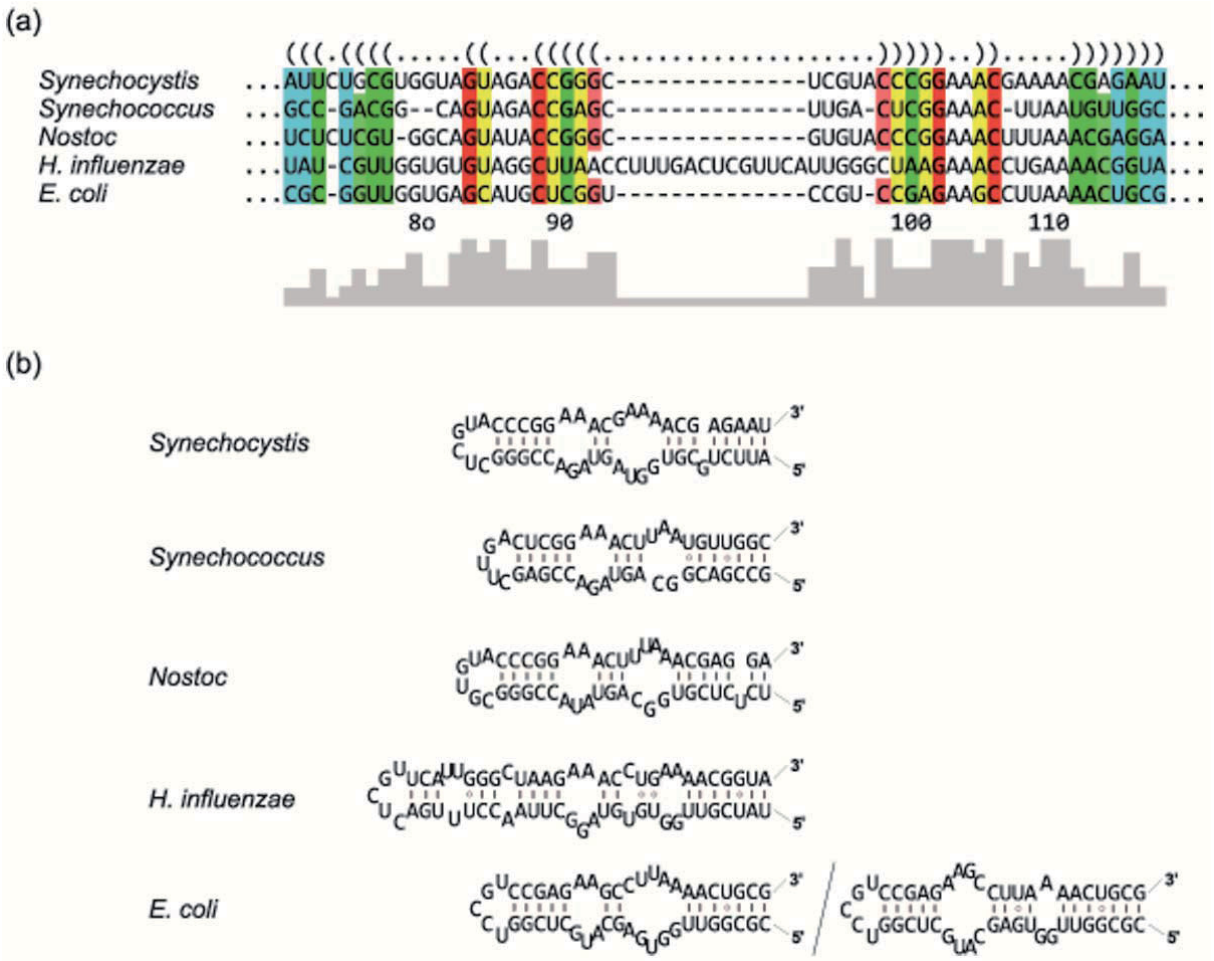

Figure 4.1: Sequence alignment and secondary structures of the terminal stem loop region of different 6S RNAs. (a) A sequence and secondary structure alignment of the denoted 6S RNA's terminal regions was done with LocARNA. The consensus secondary structure is given above as dot-bracket sequence. The colour code of the RNA sequences represents the degree of sequence conservation for base pairing. The numbering refers to *E. coli* 6S RNA and the bars below indicate actual sequence conservation. (b) The aligned sequences are shown as determined secondary structures. There are two alternative foldings of this region for *E. coli* 6S RNA.

4.2 The mechanism of pRNA-mediated structural and functional change of 6S RNA

The characteristic secondary structure of 6S RNA is fundamental for its capability as regulator of RNA polymerase. By virtue of the single-stranded central bubble flanked by double-stranded helices, which together mimic an open promoter DNA, the 5'-portion of the central domain is positioned proximal to the RNA polymerase active centre (see 3.3). This position enables the process of 6S RNA-templated pRNA transcription by naturally DNA-dependent RNA polymerase. Although no structural transitions of the permanently opened central part of 6S RNA were found to be necessary for RNAP binding, 6S RNA undergoes a conformational change upon the synthesis of pRNAs. The results from section 3.2 demonstrate that reannealing of 6S RNA in the presence of a 20mer pRNA leads to an altered secondary structure compared to free 6S RNA. During this rearrangement the 3'-portion of the central domain forms a 9 bp hairpin with the downstream non-template pRNA sequence region that is rendered accessible upon pRNA extension into the closing stem. This newly formed hairpin structure is considered to take part in a series of events that finally triggers the disintegration of the 6S-RNAP complex. The phenomenon of the pRNA-induced structural rearrangement of 6S RNA was simultaneously reported for *B. subtilis* and *E. coli* in two other independent publications (Beckmann *et al.* 2012; Panchapakesan and Unrau 2012). These studies focused on the analysis of the kinetics of the structural alteration and on the release from RNAP with regard to a specific pRNA length or during *status nascendi*. Altogether, their findings and calculation of *E. coli* 6S RNA structure are absolutely consistent with the results from section 3.2. Additional data from 3.2 revealed on the protein level that the decay of the 6S-pRNA-Eσ^{70} complex is accompanied by a preceding release of the σ subunit. The transient 6S-pRNA-core intermediates could also be detected in the absence of the competitor heparin as reported previously (Wurm *et al.* 2010).

The importance of the 6S RNA structural rearrangement for the final collapse of the 6S-RNAP complex is not quite clear. Several considerations argue against a direct involvement in the initial weakening of 6S RNA contacts with RNAP or in the ejection of σ^{70}. The most striking argument is based on mutational analysis in which the formation of the new hairpin structure was prevented. For instance nucleotide substitutions C133A, U134A and U135A of *E. coli* 6S RNA would lower the tendency

of full base pair interactions within the hairpin, but on the other hand did not alter but rather enhanced the release reaction from RNAP (Shephard *et al.* 2010). Even more striking, a complete abolishment of hairpin formation after pRNA transcription still allows the release although more time seems to be required for this reaction (Panchapakesan and Unrau 2012). Hence, it is likely that rather intrinsic properties of the pRNA transcription reaction *per se* trigger the first steps of disrupting contact sites between the σ^{70} subunit and the core RNAP (see 4.3.2). The impeded reannealing of 6S RNA at the 5'-end of the pRNA transcripts in the single-stranded template region and the distinct stability of 6S-pRNA duplex compared to the irregular 6S RNA duplex might contribute to a structural tension between 6S RNA and the RNA polymerase. If the complex decomposition and the release of σ^{70} are achieved by the pRNA transcription reaction itself, the structural rearrangement of 6S RNA probably facilitates this procedure. Understandably, a certain progress of pRNA transcription or in other words a defined length of pRNA transcripts is required to provoke the complex decay. The use of a 20mer pRNA to study the influence on remainder 6S RNA secondary structure in 3.2 is in good accordance with the identification of only 20mer pRNAs within 6S-pRNA hybrids released from RNAP (Wurm *et al.* 2010). However, this is controversial with findings in which the 6S-pRNA-core complex already lacking σ^{70} contains 9 nt long pRNAs and the free 6S-pRNA hybrid contains 13 nt long pRNAs (Panchapakesan and Unrau 2012). This discrepancy can presumably be explained by the different experimental conditions since in the latter study the pRNA transcription reaction is slowed down by limiting NTP concentrations and artificial initiation with dinucleotide primers. As a valid conclusion, short pRNAs (9-13 nt) seem to be a minimal length to induce the release of 6S RNA from RNAP but under normal reaction kinetics longer pRNAs (20 nt) are formed before the final dissociation is achieved.

Whatever the role of the 6S RNA structural alteration during pRNA synthesis plays in the mechanism of dissociation from RNAP, it is absolutely clear that this refolding occurs *in vitro* and *in vivo*. The verification of a pRNA-dependent structural change of 6S RNA *in vivo* using specific DMS-methylation is presented in 3.2, Figure 4.

The individual accumulation of the two 6S RNA forms, either 6S RNA alone or the structurally altered 6S-pRNA hybrid, during a certain growth condition is not unique. While a majority of 6S RNA stably associated to RNAP can be found during the

stationary growth phase, there is a significant fraction of 6S-pRNA hybrids present after a short outgrowth from stationary phase. The presence of free 6S RNA at this condition can be explained by incomplete pRNA transcription and/or *de novo* 6S RNA synthesis. Therefore, the comparison of the *in vivo* methylation patterns is not as clear as results from enzymatic or chemical probing *in vitro*. Nevertheless, specific changes provoked by pRNA-induced refolding can be detected in the 3' central bubble and the downstream region. In agreement with *in vitro* results, the formation of a new double-stranded hairpin can be identified *in vivo* based on the fact that structured helical RNA regions exhibit reduced DMS-reactivity.

The significance of the new hairpin within the structural context of an abundant molecule provokes speculations for additional potential functions behind this structural reorganization. In addition to assisting the release from RNAP the conformational switch might represent a recognition element for the degradation by cellular RNases. This would be consistent with the rapid depletion of 6S-pRNA hybrids during outgrowth from stationary phase (Wurm *et al.* 2010). The resulting RNA turnover is followed by a new accumulation of 6S RNA when cells enter exponential phase again. An enzyme for the degradation of the 6S-pRNA complex has not been identified yet. RNases I, III and P are seemingly not responsible as indicated by Northern Blot analysis of total RNA from respective deletion strains (data not shown).

4.3 Comparison of RNAP interaction with 6S RNA and promoter DNA

The three-dimensional model of the 6S RNA within the RNAP complex presented in chapter 3.3 is the first experimentally verified example displaying a tertiary structure of this regulatory RNA. The model is based on the computational assembly of predicted three-dimensional RNA structures derived from fragments with established secondary structure. The highly structured internal stem and closing stem regions could be predicted whereas the large single-stranded 5' and 3' domains were modelled according to the path of DNA within an open promoter-RNAP complex (Hudson *et al.* 2009). It turned out that the internal stem exhibits the major interaction surface between 6S RNA and $E\sigma^{70}$ as determined by FeBABE footprinting. The tertiary structure of the internal stem was adapted to the RNAP structure so that the

overall distances between the cleavage sites and the respective FeBABE conjugation sites of σ^{70} were minimized. Finally the 6S RNA fragments were fused and the whole molecule was docked to the recently published high-resolution crystal structure of the *E. coli* Eσ^{70} (Murakami 2013). The resolution of this model is rather low and it is inapplicable for determining RNA-protein atomic contacts. Nevertheless the model allows a reliable spatial assignment of neighboring functional regions of 6S RNA and σ^{70} within RNAP. This enables the prediction and the identification of 6S RNA or RNAP residues that are important for binding and pRNA transcription.

4.3.1 The binding mode

The importance of the σ^{70} region 4.2 for interaction with the terminal, irregular stem structure of 6S RNA has already been discussed in chapter 4.1. The FeBABE cleavage data and the modelled 6S-RNAP tertiary structure nicely illustrate the spatial proximity of these two regions (Fig. 4.2 a). Bypassing the limitation of an A-form RNA helix by bulge loop interruption might be a possible explanation for the interplay of the nucleic acid binding motif within σ^{70} domain 4.2 and 6S RNA. In fact, the double-stranded 6S RNA structure consists of a regular A-form helix as shown for a 12 bp RNA duplex crystal structure of *Aquifex aeolicus* 6S RNA (Kondo *et al.* 2013). Moreover, tertiary structure predictions for 6S RNA show that the narrow A-form helical conformation is likely abrogated by internal bulge loops. Nevertheless a proper helix-turn-helix motif that recognizes nucleic acid grooves as proven for the -35 promoter DNA does not seem to be necessary for 6S RNA recognition. Especially, recent alanine scanning mutants of distinct σ^{70} 4.2 residues denote that 4.2 recognition of 6S RNA differs from promoter DNA (Klocko and Wassarman 2009). The 6S RNA binding surface for region 4.2 interactions indeed overlaps, but is also distinct from the DNA binding surface. Notably, positively charged residues in the C-terminal part of the second helix of region 4.2 are crucial for 6S RNA binding in contrast to DNA binding. The importance of extended positive charges implies potential charge-charge interactions between σ^{70} region 4.2 and 6S RNA, which is reported for many RNA-protein contacts (Bahadur *et al.* 2008). Most likely, however, the high affinity and specificity of 6S-RNAP interaction cannot solely be explained by charge-charge interactions. This assumption is supported by the significance of the bulge loop structure and several residues like C107 of 6S RNA (see 4.1). Moreover, involvement of the “basic patch” in 6S RNA binding cannot be confirmed by the 6S

RNA-RNAP complex model for two reasons. First, the model was generated by minimizing the distance between the D581C mutant and the respective 6S RNA cleavage site adjacent to the terminal loop. However, D581C lies in the loop region N-terminal of the second helix of σ^{70} 4.2, thus increasing the distance between the basic residues in the C-terminal portion and 6S RNA. Secondly, it is absolutely conceivable that the σ^{70} subunit undergoes conformational transitions within the holoenzyme upon nucleic acid or transcription factor binding as reviewed in (Decker and Hinton 2009). In the presence of 6S RNA the plasticity of σ^{70} might allow a position or conformation in which both the N-terminal and C-terminal part of the recognition helix of 4.2 can interact with the terminal bulged region of 6S RNA. The flexibility of σ^{70} is not considered in the model because the 6S RNA was docked to the rigid crystal structure of the RNAP holoenzyme alone. Yet, the minor cleavage of the D581C mutant at the far distant residues U77/U78 alludes well to this flexibility. The movement of σ^{70} region 4.2 as a flexible module upon binding of fork-junction DNA was already shown for the *Thermus aquaticus* RNAP holoenzyme (Murakami *et al.* 2002). A similar study with *E. coli* RNAP and a reduced 6S RNA molecule that might allow crystallization would clarify the atomic details of the σ^{70} 4.2-6S RNA interaction.

Coimmunoprecipitation analysis with an Eσ^{70} mutant that lacks σ^{70} region 4.2 revealed detectable amounts of 6S RNA, indicating that the 6S RNA-RNAP interaction is possibly modulated by additional σ^{70} regions others than 4.2 (Cavanagh *et al.* 2008). A comparison with promoter DNA introduces the region 2.4 as candidate for 6S RNA binding due to its participation in -10 promoter element recognition. According to the 6S-RNAP model the junction of the double-stranded internal stem and the single-stranded central domain bends over the α-helical part of region 2.4 like it is the case for the -10 promoter DNA region. Despite this comparable position of RNA and DNA relative to σ^{70} the region 2.4 seems not to participate in 6S RNA interaction, however. A striking hint supporting this assumption is given by 6S RNA mutants in which the single-stranded sequences of the central bubble were interchanged. These mutants were not affected in RNAP binding as far as the single-stranded character and a minimum length of the 5' and 3' central domains are maintained (Trotochaud and Wassarman 2005). In contrast to region 2.4 and similar to region 4.2 the 6S RNA-RNAP complex model establishes σ^{70} region 3.0 as a

potential domain for interaction with 6S RNA. This region consists of an α-helix, which lies in the major groove of DNA contacting a 'TG' motif upstream of the -10 element in extended -10 promoters (Fig. 4.2 b). There is no conservation of a TG (UG) sequence motif in a corresponding region of 6S RNA. Though, region 3.0 again faces an internal stem region that is interrupted by irregular, asymmetric bulge loops as described for region 4.2. Closing of these bulges resulted in a significant decrease of 6S RNA-RNAP complex formation (3.3.1, Fig. S2). Although a sequence-specific component cannot be excluded, this mutational analysis suggests a potential interaction between σ^{70} region 3.0 and the internal stem bulges adjacent to the central bubble (G66/A123 and C69-C71/A120). This interaction would fit to the extended -10 promoter element previously described to render a promoter sensitive towards 6S RNA regulation (Cavanagh *et al.* 2008). A concerted competition of σ^{70} regions 4.2 and 3.0 for 6S RNA or promoter DNA interaction sites could contribute to promoter-specific transcriptional inhibition brought about by 6S RNA.

4.3.2 The transcription mode

The modelled 6S RNA-RNAP complex provides a useful tool for structural ideas about the properties of pRNA transcription as well. Although the position and conformation of the central bubble and the closing stem are speculative since they are modelled to a large degree in analogy to the path of promoter DNA in open RNAP complex, their topology depends on the mapped internal stem and thus is absolutely reasonable. Moreover, the data from chapter 3.3 and the deduced model show that the σ_3-σ_4 linker, referred to as region 3.2, still protrudes deeply into the active site of the RNAP in the presence of bound 6S RNA (Fig. 4.2 c). From RNAP holoenzyme crystal structures this σ^{70} linker domain was hypothesized to play an important role in the promoter escape of DNA-dependent transcription initiation (Murakami *et al.* 2002; Vassylyev *et al.* 2002). Thereby the linker occupies the same space as the nascent RNA transcript of the RNA-DNA hybrid. Only small transcripts of 5 nt length could be generated without steric clash and longer ones of 12 nt length would fill the RNA exit channel fully displacing the linker domain. These transcript lengths correspond to abortive transcription so that the σ^{70} linker is regarded as destabilizer competing with the growing RNA chain. The sequential displacement of the linker probably has consequences for other σ^{70}-core interaction sites resulting in the release of the σ subunit and the transition of the core polymerase into a

processive elongation complex. This scenario is also feasible for the 6S RNA-templated transcription of pRNAs, which, at least the smaller ones, exhibit characteristics of abortive transcripts. Transient 6S-pRNA-core complexes preceded by σ^{70} release were shown to contain 9 nt long pRNAs, obviously sufficiently long for σ detachment in this 6S RNA-dependent reaction (Panchapakesan and Unrau 2012). Given the subsequent synthesis of longer pRNAs (up to 20 nt in *E. coli*) indicates that a short-lived elongation complex is formed on the 6S RNA template. As mentioned in chapter 4.2 the reannealing of the upstream DNA is crucial for the separation of the RNA-DNA hybrid and for threading the growing RNA chain into the exit channel (Vassylyev *et al.* 2007). Considering that this step of reannealing is abolished in 6S RNA-dependent transcription due to initiation in the permanently single-stranded central bubble, the 6S RNA can be compared with single-stranded DNA templates. Transcription from these leads to approximately 20 nt long annealed transcripts whereupon the conserved β' lid domain serves as an obstacle for the upstream edge of the RNA-DNA hybrid. The resultant tension of the transcription complex causes a backsliding which positions the overextended hybrid in the downstream DNA cavity making further transcription impossible (Naryshkina *et al.* 2006). This might be a conceivable mechanism for the transcription of pRNAs, especially considering the congruent transcript lengths. Moreover transcription termination at a maximal pRNA length would be explained. The fact that even longer pRNAs (30 nt) can be generated by *E. coli* RNAP and cyanobacterial 6S RNA (3.1; 4.1) may be attributed to special template properties of these RNAs.

Another functional domain contributing to the abortive character of pRNA transcription might be the σ^{70} region 1.2. This region was shown to interact with the non-template strand in open promoter complexes affecting the half-life of the open complex and the unwinding of downstream DNA (Haugen *et al.* 2008; Bochkareva and Zenkin 2013). Although the absence of any FeBABE-mediated cleavage by the C132 (σ^{70} 1.2) variant argues against the proximity of 6S RNA, more N-terminal residues of region 1.2 were demonstrated to directly interact with the non-template strand downstream of the -10 promoter element (Zhang *et al.* 2012). Such an interaction would also make sense for 6S RNA as the 6S RNA-RNAP model displays a spatial neighborhood between region 1.2 and the 3' central domain (Fig. 4.2 d). Consistent with a potential function in pRNA transcription mutations of residues in the

3’ central domain affected 6S RNA release from RNAP which in turn depends on correct pRNA transcription (Shephard *et al.* 2010). Additional analysis would be required to elucidate a possible involvement of region 1.2 in pRNA transcription.

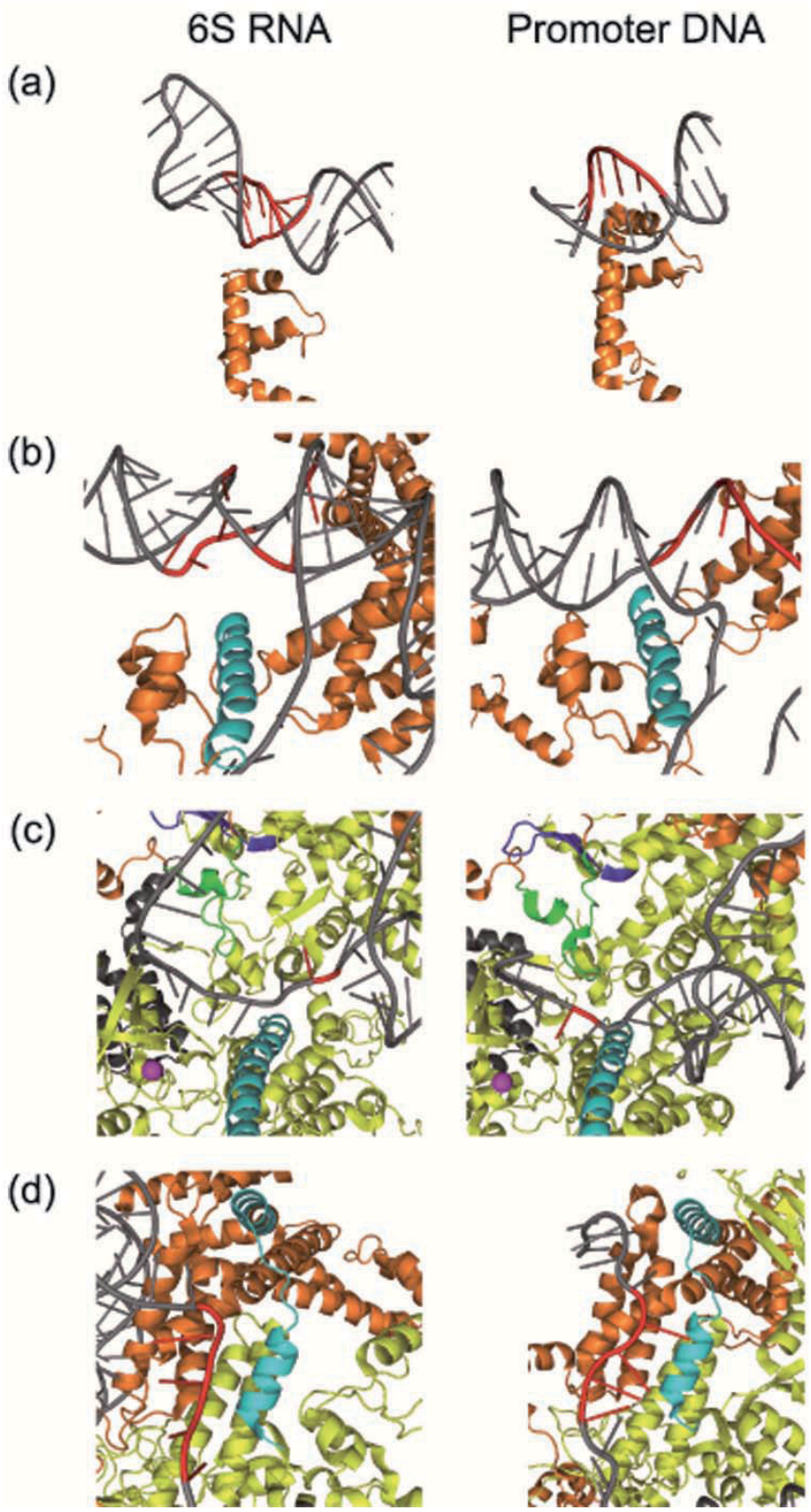

Figure 4.2: Comparison of the RNA polymerase holoenzyme interaction with 6S RNA and promoter DNA, respectively. (a) On the left: *E. coli* σ^{70} region 4.2 together with the 6S RNA terminal hairpin (red: bulge loop C85-G88/A104-C107); on the right: *T. aquaticus* σ^{A} region

4.2 together with the -35 promoter element (red) (pdb ID: 1KU7). (b) Left: the *E. coli* σ^{70} region 3.0 (cyan) together with the 6S RNA bulge loops G66/A123, C69-C71/A120 (red); right: the *E. coli* σ^{70} region 3.0 (cyan) together with the -10 and extended -10 promoter element (red) (pdb ID: 3IYD). (c) On the left: *E. coli* RNAP active site together with the 3' central domain of 6S RNA (red, U44 (pRNA TSS); cyan, β' bridge helix; magenta sphere, Mg^{2+}; green, σ_3-σ_4 linker; blue, β' lid; yellow, β' subunit; orange, σ^{70} subunit; black, ω subunit); On the right: *T. thermophilus* RNAP active site together with a promoter DNA fragment (red, TSS; cyan, β' bridge helix; magenta sphere, Mg^{2+}; green, σ_3-σ_4 linker; blue, β' lid; yellow, β' subunit; orange, σ^{70} subunit; black, ω subunit) (pdb ID: 4G7H). (d) On the left: *E. coli* σ^{70} region 1.2 together with the 3' central domain of 6S RNA (red, G136-C139; cyan, σ^{70} 1.2; yellow, β' subunit; orange, σ^{70} subunit); on the right: *T. thermophilus* σ^{A} region 1.2 together with a promoter DNA fragment (red, discriminator region (GGGA); cyan, σ^{A} 1.2; yellow, β' subunit; orange, σ^{70} subunit) (pdb ID: 4G7H).

5 References

Aviv, M., Giladi, H., Oppenheim, A. B. and Glaser, G. (1996) Analysis of the shut-off of ribosomal RNA promoters in *Escherichia coli* upon entering the stationary phase of growth. *FEMS Microbiol Lett* **140**(1): 71-76.

Bahadur, R. P., Zacharias, M. and Janin, J. (2008) Dissecting protein-RNA recognition sites. *Nucleic Acids Res* **36**(8): 2705-2716.

Baracchini, E. and Bremer, H. (1988) Stringent and growth control of rRNA synthesis in *Escherichia coli* are both mediated by ppGpp. *J Biol Chem* **263**: 2597-2602.

Barrick, J. E., Sudarsan, N., Weinberg, Z., Ruzzo, W. L. and Breaker, R. R. (2005) 6S RNA is a widespread regulator of eubacterial RNA polymerase that resembles an open promoter. *RNA* **11**(5): 774-784.

Beckmann, B. M., Burenina, O. Y., Hoch, P. G., Kubareva, E. A., Sharma, C. M. and Hartmann, R. K. (2011) *In vivo* and *in vitro* analysis of 6S RNA-templated short transcripts in *Bacillus subtilis*. *RNA Biol* **8**(5).

Beckmann, B. M., Hoch, P. G., Marz, M., Willkomm, D. K., Salas, M. and Hartmann, R. K. (2012) A pRNA-induced structural rearrangement triggers 6S-1 RNA release from RNA polymerase in *Bacillus subtilis*. *The EMBO journal* **31**(7): 1727-1738.

Bochkareva, A. and Zenkin, N. (2013) The σ^{70} region 1.2 regulates promoter escape by unwinding DNA downstream of the transcription start site. *Nucleic Acids Res* **41**(8): 4565-4572.

Bohn, C., Rigoulay, C., Chabelskaya, S., Sharma, C. M., Marchais, A., Skorski, P., Borezee-Durant, E., Barbet, R., Jacquet, E., Jacq, A., Gautheret, D., Felden, B., Vogel, J. and Bouloc, P. (2010) Experimental discovery of small RNAs in *Staphylococcus aureus* reveals a riboregulator of central metabolism. *Nucleic Acids Res* **38**(19): 6620-6636.

Brown, J. W. and Ellis, J. C. (2005) Comparative analysis of RNA secondary structures: 6S RNA. Weinheim, Wiley-VCH Verlag GmbH & Co.

Brownlee, G. G. (1971) Sequence of 6S RNA of *E. coli*. *Nat New Biol* **229**(5): 147-149.

Cabrera-Ostertag, I. J., Cavanagh, A. T. and Wassarman, K. M. (2013) Initiating nucleotide identity determines efficiency of RNA synthesis from 6S RNA templates in *Bacillus subtilis* but not *Escherichia coli*. *Nucleic Acids Res* **41**(15):7501-7511.

Carpousis, A. J. and Gralla, J. D. (1980) Cycling of ribonucleic acid polymerase to produce oligonucleotides during initiation *in vitro* at the *lac* UV5 promoter. *Biochemistry* **19**(14): 3245-3253.

Cavanagh, A. T., Chandrangsu, P. and Wassarman, K. M. (2010) 6S RNA regulation of *relA* alters ppGpp levels in early stationary phase. *Microbiology* **156**(Pt 12):3791-800.

Cavanagh, A. T., Klocko, A. D., Liu, X. and Wassarman, K. M. (2008) Promoter specificity for 6S RNA regulation of transcription is determined by core promoter sequences and competition for region 4.2 of σ^{70}. *Mol Microbiol* **67**(6): 1242-1256.

Cavanagh, A. T., Sperger, J. M. and Wassarman, K. M. (2011) Regulation of 6S RNA by pRNA synthesis is required for efficient recovery from stationary phase in *E. coli* and *B. subtilis*. *Nucleic Acids Res* **40**(5):2234-46.

Cavanagh, A. T. and Wassarman, K. M. (2013) 6S-1 RNA function leads to a delay in sporulation in *Bacillus subtilis*. *J Bacteriol* **195**(9): 2079-2086.

Chae, H., Han, K., Kim, K. S., Park, H., Lee, J. and Lee, Y. (2011) Rho-dependent termination of *ssrS* (6S RNA) transcription in *Escherichia coli*: implication for 3' processing of 6S RNA and expression of downstream *ygfA* (putative 5-formyl-tetrahydrofolate cyclo-ligase). *J Biol Chem* **286**(1): 114-122.

Cramer, P., Bushnell, D. A. and Kornberg, R. D. (2001) Structural basis of transcription: RNA polymerase II at 2.8 angstrom resolution. *Science* **292**(5523): 1863-1876.

Decker, K. B. and Hinton, D. M. (2009) The secret to 6S: regulating RNA polymerase by ribo-sequestration. *Mol Microbiol* **73**(2): 137-140.

Espinoza, C. A., Allen, T. A., Hieb, A. R., Kugel, J. F. and Goodrich, J. A. (2004) B2 RNA binds directly to RNA polymerase II to repress transcript synthesis. *Nat Struct Mol Biol* **11**(9): 822-829.

Faucher, S. P., Friedlander, G., Livny, J., Margalit, H. and Shuman, H. A. (2010) *Legionella pneumophila* 6S RNA optimizes intracellular multiplication. *Proc Natl Acad Sci U S A* **107**(16): 7533-7538.

Gildehaus, N., Neusser, T., Wurm, R. and Wagner, R. (2007) Studies on the function of the riboregulator 6S RNA from *E. coli*: RNA polymerase binding, inhibition of *in vitro* transcription and synthesis of RNA-directed *de novo* transcripts. *Nucleic Acids Res* **35**(6): 1885-1896.

Gupta, R. S. and Mathews, D. W. (2010) Signature proteins for the major clades of Cyanobacteria. *BMC Evol Biol* **10**: 24.

Haugen, S. P., Ross, W., Manrique, M. and Gourse, R. L. (2008) Fine structure of the promoter-sigma region 1.2 interaction. *Proc Natl Acad Sci U S A* **105**: 3292-3297.

Hernandez, J. V. and Bremer, H. (1990) Guanosine tetraphosphate (ppGpp) dependence of the growth rate control of *rrnB* P1 promoter activity in *Escherichia coli*. *J Biol Chem* **265**: 11605-11614.

Hindley, J. (1967) Fractionation of ^{32}P-labelled ribonucleic acids on polyacrylamide gels and their characterization by fingerprinting. *J Mol Biol* **30**(1): 125-136.

Hsu, L. M., Zagorski, J., Wang, Z. and Fournier, M. J. (1985) *Escherichia coli* 6S RNA gene is part of a dual-function transcription unit. *J Bacteriol* **161**(3): 1162-1170.

Hudson, B. P., Quispe, J., Lara-Gonzalez, S., Kim, Y., Berman, H. M., Arnold, E., Ebright, R. H. and Lawson, C. L. (2009) Three-dimensional EM structure of an intact activator-dependent transcription initiation complex. *Proc Natl Acad Sci U S A* **106**(47): 19830-19835.

Jeanguenin, L., Lara-Nunez, A., Pribat, A., Mageroy, M. H., Gregory, J. F., 3rd, Rice, K. C., de Crecy-Lagard, V. and Hanson, A. D. (2010) Moonlighting glutamate formiminotransferases can functionally replace 5-formyltetrahydrofolate cycloligase. *J Biol Chem* **285**(53): 41557-41566.

Jishage, M. and Ishihama, A. (1995) Regulation of RNA polymerase sigma subunit synthesis in *Escherichia coli*: Intracellular levels of σ^{70} and σ^{38}. *J Bacteriol* **177**: 6832-6835.

Kim, K. S. and Lee, Y. (2004) Regulation of 6S RNA biogenesis by switching utilization of both sigma factors and endoribonucleases. *Nucleic Acids Res* **32**(20): 6057-6068.

Klocko, A. D. and Wassarman, K. M. (2009) 6S RNA binding to Eσ^{70} requires a positively charged surface of σ^{70} region 4.2. *Mol Microbiol* **73**(2): 152-164.

Kondo, J., Dock-Bregeon, A. C., Willkomm, D. K., Hartmann, R. K. and Westhof, E. (2013) Structure of an A-form RNA duplex obtained by degradation of 6S RNA in a crystallization droplet. *Acta crystallographica*. Section F, Structural biology and crystallization communications **69**(Pt 6): 634-639.

Kusano, S., Ding, Q., Fujita, N. and Ishihama, A. (1996) Promoter selectivity of *Escherichia coli* RNA polymerase Eσ^{70} and Eσ^{38} holoenzymes. *J Biol Chem* **271**: 1989-2004.

Lee, C. A., Fournier, M. J. and Beckwith, J. (1985) *Escherichia coli* 6S RNA is not essential for growth or protein secretion. *J Bacteriol* **161**(3): 1156-1161.

Lee, J. Y., Park, H., Bak, G., Kim, K. S. and Lee, Y. (2013) Regulation of transcription from two *ssrS* promoters in 6S RNA biogenesis. *Molecules and cells* **36**(3):227-234.

Lee, S. Y., Bailey, S. C. and Apirion, D. (1978) Small stable RNAs from *Escherichia coli*: evidence for the existence of new molecules and for a new ribonucleoprotein particle containing 6S RNA. *J Bacteriol* **133**(2): 1015-1023.

Murakami, K. S. (2013) X-ray crystal structure of *Escherichia coli* RNA polymerase σ^{70} holoenzyme. *J Biol Chem* **288**(13): 9126-9134.

Murakami, K. S., Masuda, S., Campbell, E. A., Muzzin, O. and Darst, S. A. (2002) Structural basis of transcription initiation: an RNA polymerase holoenzyme-DNA complex. *Science* **296**: 12185-11290.

Murakami, K. S., Masuda, S. and Darst, S. A. (2002) Structural basis of transcription initiation: RNA polymerase holoenzyme at 4.4 Å resolution. *Science* **296**: 1280-1284.

Murray, H. D., Schneider, D. A. and Gourse, R. L. (2003) Control of rRNA expression by small molecules is dynamic and nonredundant. *Molecular Cell* **12**: 125-134.

Naryshkina, T., Kuznedelov, K. and Severinov, K. (2006) The Role of the Largest RNA Polymerase Subunit Lid Element in Preventing the Formation of Extended RNA-DNA Hybrid. *J Mol Biol* **361**: 634-643.

Neußer, T., Gildehaus, N., Wurm, R. and Wagner, R. (2008) Studies on the expression of 6S RNA from *E. coli*: involvement of regulators important for stress and growth adaptation. *Biol Chem* **389**(3): 285-297.

Neußer, T., Polen, T., Geißen, R. and Wagner, R. (2010) Depletion of the non-coding regulatory 6S RNA in *E. coli* causes a surprising reduction in the expression of the translation machinery. *BMC Genomics* **11**: 165-178.

Nudler, E. and Mironov, A. S. (2004) The riboswitch control of bacterial metabolism. *Trends Biochem Sci* **29**(1): 11-17.

Panchapakesan, S. S. and Unrau, P. J. (2012) *E. coli* 6S RNA release from RNA polymerase requires σ^{70} ejection by scrunching and is orchestrated by a conserved RNA hairpin. *RNA* **18**(12): 2251-2259.

Ponicsan, S. L., Houel, S., Old, W. M., Ahn, N. G., Goodrich, J. A. and Kugel, J. F. (2013) The Non-Coding B2 RNA Binds to the DNA Cleft and Active-Site Region of RNA Polymerase II. *J Mol Biol* **425**(19):3625-3638.

Raghavan, R., Groisman, E. A. and Ochman, H. (2011) Genome-wide detection of novel regulatory RNAs in *E. coli*. *Genome research* **21**(9): 1487-1497.

Richter, D. (1980) Uncharged tRNA inhibits guanosine 3',5'-bis (diphosphate) 3'-pyrophosphohydrolase [ppGppase], the *spoT* gene product, from *Escherichia coli*. *Mol Gen Genet* **178**(2): 325-327.

Sharma, C. M., Hoffmann, S., Darfeuille, F., Reignier, J., Findeiss, S., Sittka, A., Chabas, S., Reiche, K., Hackermuller, J., Reinhardt, R., Stadler, P. F. and Vogel, J. (2010) The primary transcriptome of the major human pathogen *Helicobacter pylori*. *Nature* **464**(7286): 250-255.

Shephard, L., Dobson, N. and Unrau, P. J. (2010) Binding and release of the 6S transcriptional control RNA. *RNA* **16**(5): 885-892.

Smith, C., Heyne, S., Richter, A. S., Will, S. and Backofen, R. (2010) Freiburg RNA Tools: a web server integrating INTARNA, EXPARNA and LOCARNA. *Nucleic Acids Res* **38**(Web Server issue): W373-377.

Storz, G., Vogel, J. and Wassarman, K. M. (2011) Regulation by small RNAs in bacteria: expanding frontiers. *Molecular Cell* **43**(6): 880-891.

Trotochaud, A. E. and Wassarman, K. M. (2004) 6S RNA function enhances long-term cell survival. *J Bacteriol* **186**(15): 4978-4985.

Trotochaud, A. E. and Wassarman, K. M. (2005) A highly conserved 6S RNA structure is required for regulation of transcription. *Nature Structural Biol* **12**: 313-319.

Trotochaud, A. E. and Wassarman, K. M. (2006) 6S RNA Regulation of *pspF* Transcription Leads to Altered Cell Survival at High pH. *J Bacteriol* **188**(11): 3936-3943.

Vassylyev, D. G., Sekine, S. I., Laptenko, O., Lee, J., Vassylyeva, M. N., Borukhov, S. and Yokoyama, S. (2002) Crystal structure of a bacterial RNA polymerase holoenzyme at 2.6 Å resolution. *Nature* **417**: 712-719.

Vassylyev, D. G., Vassylyeva, M. N., Perederina, A., Tahirov, T. H. and Artsimovitch, I. (2007) Structural basis for transcription elongation by bacterial RNA polymerase. *Nature* **448**(7150): 157-162.

Wagner, S. D., Yakovchuk, P., Gilman, B., Ponicsan, S. L., Drullinger, L. F., Kugel, J. F. and Goodrich, J. A. (2013) RNA polymerase II acts as an RNA-dependent RNA polymerase to extend and destabilize a non-coding RNA. *The EMBO journal* **32**(6): 781-790.

Wassarman, K. M. and Saecker, R. M. (2006) Synthesis-mediated release of a small RNA inhibitor of RNA polymerase. *Science* **314**(5805): 1601-1603.

Wassarman, K. M. and Storz, G. (2000) 6S RNA regulates *E. coli* RNA polymerase activity. *Cell* **101**: 613-623.

Watanabe, T., Sugiura, M. and Sugita, M. (1997) A novel small stable RNA, 6Sa RNA, from the cyanobacterium *Synechococcus sp*. strain PCC6301." *FEBS Lett* **416**(3): 302-306.

Waters, L. S. and Storz, G. (2009) Regulatory RNAs in bacteria. *Cell* **136**(4): 615-628.

Weeks, K. M. and Crothers, D. M. (1993) Major groove accessibility of RNA. *Science* **261**(5128): 1574-1577.

Werner, F. and Grohmann, D. (2011) Evolution of multisubunit RNA polymerases in the three domains of life. *Nature Reviews Microbiology* **9**(2): 85-98.

Wurm, R., Neußer, T. and Wagner, R. (2010) 6S RNA-dependent inhibition of RNA polymerase is released by RNA-dependent synthesis of small *de novo* products. *Biol Chem* **39**: 187-196.

Yakovchuk, P., Goodrich, J. A. and Kugel, J. F. (2009) B2 RNA and Alu RNA repress transcription by disrupting contacts between RNA polymerase II and promoter DNA within assembled complexes. *Proc Natl Acad Sci U S A* **106**(14): 5569-5574.

Zaychikov, E., Martin, E., Denissova, L., Kozöov, M., Markovtsov, V., Kashlev, M., Heumann, H., Nikiforov, V., Goldfarb, A. and Mustaev, A. (1996) Mapping of catalytic residues in the RNA polymerase active center. *Science* **237**: 107-109.

Zhang, G., Campbell, E. A., Minakhin, L., Richter, C., Severinov, K. and Darst, S. A. (1999) Crystal structure of *Thermus aquaticus* core RNA polymerase at 3.3 Å resolution. *Cell* **98**: 811-824.

Zhang, Y., Feng, Y., Chatterjee, S., Tuske, S., Ho, M. X., Arnold, E. and Ebright, R. H. (2012). Structural basis of transcription initiation. *Science* **338**(6110): 1076-1080.

6 Appendix

6.1 Review: 6S RNA: recent answers – future questions

Benedikt Steuten, Sabine Schneider and Rolf Wagner
Molecular Biology of Bacteria, Heinrich-Heine-University Düsseldorf, Universitätsstr. 1, D-40225 Düsseldorf, Germany

Summary
6S RNA is a non-coding RNA, found in almost all phylogenetic branches of bacteria. Through its conserved secondary structure, resembling open DNA promoters, it binds to RNA polymerase and interferes with transcription at many promoters. That way, it functions as transcriptional regulator facilitating adaptation to stationary phase conditions. Strikingly, 6S RNA acts as template for the synthesis of small RNAs (pRNA), which trigger the disintegration of the inhibitory RNA polymerase-6S RNA complex releasing 6S RNA-dependent repression. The regulatory implications of 6S RNAs vary among different bacterial species depending on the lifestyle and specific growth conditions that they have to face. The influence of 6S RNA can be seen on many different processes including stationary growth, sporulation, light adaptation or intracellular growth of pathogenic bacteria. Recent structural and functional studies have yielded details of the interaction between *E. coli* 6S RNA and RNA polymerase. Genome-wide transcriptome analyses provided insight into the functional diversity of 6S RNAs. Moreover, the mechanism and physiological consequences of pRNA synthesis have been explored in several systems. A major function of 6S RNA as a guardian regulating the economic use of cellular resources under limiting conditions and stress emerges as a common perception from numerous recent studies.

Introduction
Although 6S RNA was discovered in *Escherichia coli* very early and sequenced as one of the first sRNA its function remained elusive for three decades (Hindley, 1967; Brownlee, 1971). Soon it became known that 6S RNA exists in the cell as part of a large ribonucleoprotein complex (Lee *et al*., 1978) but it was demonstrated only in the year 2000 that the binding partner was the holoenzyme of RNA polymerase (RNAP) (Wassarman and Storz, 2000). A series of subsequent studies have uncovered that in *E. coli* 6S RNA is a highly abundant RNA species, which accumulates tenfold during the bacterial growth cycle (Wassarman and Storz, 2000). Moreover, it was shown that 6S RNA is widespread among different bacteria and exhibits a highly conserved secondary structure consisting of a central bulge flanked by two irregular stem structures. This structure, resembling open promoter DNA, has enabled the prediction and subsequent identification of this regulatory RNA in more than 100 bacterial species so far (Barrick *et al*., 2005). The secondary structure has also led to the initial proposal that 6S RNA functions by mimicking DNA promoters explaining the specific binding of 6S RNA to RNAP (Trotochaud and Wassarman, 2005).

In *E. coli* it was shown that 6S RNA, due to its high concentration and

affinity for the σ^{70}-RNAP holoenzyme ($E\sigma^{70}$), inhibits transcription of many but not all genes during stationary phase (Cavanagh *et al*., 2008). Hence, the term riboregulator had been coined for this unique RNA indicating that 6S RNA, directly and indirectly, affects the response of the cell in a global way. Notably, during late stationary growth 6S RNA sequesters almost all $E\sigma^{70}$, thereby facilitating the efficiency of σ factor change between the *E. coli* housekeeping factor σ^{70} and the stationary phase-specific σ^{38}. 6S RNA does not only bind to RNAP but additionally has the remarkable property to act as a template for the synthesis of small *de novo* transcription products, termed pRNAs (Wassarman and Saecker, 2006; Gildehaus *et al*., 2007). The synthesis of pRNAs has important consequences because it is essential for the release of RNAP-bound 6S RNA, which abandons 6S RNA-dependent repression.

The search for a physiological function of 6S RNA was originally impeded by the lack of a detectable phenotype for either 6S RNA deletion or overexpressing *E. coli* strains when grown under rich laboratory conditions (Hsu *et al*., 1985; Lee *et al*., 1985). However, a 6S RNA-dependent phenotype can readily be observed when cells are grown under limiting conditions or when long-time stress is applied. For example, conditions of late stationary growth provoke a competitive disadvantage of a 6S RNA-deficient strain compared to the wild type. Moreover, these mutant cells exhibit decreased viability after long-term stationary phase (Trotochaud and Wassarman, 2004). Another growth phenotype, related to the loss of 6S RNA, was discovered under conditions of high pH at which cells without 6S RNA are able to survive better than wild-type cells. The direct 6S RNA-dependent regulation of the gene *pspF*, encoding a transcriptional activator in bacterial stress response, was identified as responsible target. Transcription of *pspF* is normally down-regulated by 6S RNA suppressing the phage shock protein response. These results already led to the proposition that 6S RNA generally contributes to efficient allocation of nutrients under limiting conditions and stress (Trotochaud and Wassarman, 2006).

The function of 6S RNA is linked to growth phase-dependent expression

In *E. coli* the 6S RNA gene, *ssrS*, is transcribed as part of a highly conserved bi-cistronic operon together with the gene *ygfA* encoding the enzyme 5-formyltetrahydrofolate cycloligase (Hsu *et al*., 1985; Jeanguenin *et al*., 2010). The operon is controlled by two tandem promoters, P1 (σ^{70}-dependent) and P2 (σ^{38}- and σ^{70}-dependent), which are responding differentially during growth phase (Kim and Lee, 2004). Transcription is further subject to regulation by the nucleoid-associated proteins H-NS, LRP, StpA and FIS (Neußer *et al*., 2008). Moreover, both *ssrS* promoters are differentially autoregulated by 6S RNA (Lee *et al*., 2013). In addition to the regulated expression of the *ssrS* gene contributing to growth phase-dependent accumulation of 6S RNA there is also a differential processing of the primary transcripts modulating the cellular levels of 6S RNA but that of the co-transcribed *ygfA* gene as well (Kim and Lee, 2004). Several Rho-dependent transcription termination sites downstream of the mature 6S RNA sequence have been described, which potentially participate in the regulation of the downstream *ygfA* gene expression (Chae *et al*., 2011). The genetic coupling and co-regulation of *ygfA* and *ssrS* has led to the early assumption of a functional coupling between 6S RNA and YgfA. It is noteworthy in this respect that YgfA is involved in reduction of the cellular folate pool, which is central for the synthesis of

Table 1: Examples for experimentally verified functional diversity of 6S RNA in different bacteria

Function	Occurrence	Remarks	Reference
Escape from stationary phase	*Escherichia coli*		(Wassarman and Saecker,2006; Wurm *et al*., 2007)
	Bacillus subtilis	6S-1 RNA only	(Beckmann *et al*., 2011; Cavanagh *et al*., 2011)
Long-time starvation	*Escherichia coli*		(Trotochaud and Wassarman, 2004)
Survival at high pH	*Escherichia coli*		(Trotochaud and Wassarman, 2006)
Tolerance against oxidative stress (ROS)	*Burgholderia cenocepacia*		(Peeters *et al*., 2010)
Optimal intracellular growth	*Legionella pneumophila* *Salmonella Typhimurium* *Bradyrhizobium japonicum*	Human pathogen Intracellular pathogen Soybean symbiont (root nodules)	(Faucher *et al*., 2010) (Ortega *et al*., 2012) (Madhugiri *et al*., 2012)
Adaptation to dark-light cycle	Cyanobacteria		(Rediger *et al*., 2012)
Delay in sporulation	*Bacillus subtilis*	6S-1 RNA only	(Cavanagh and Wassarman, 2013)

purines and intermediates of the one-carbon metabolism (Jeanguenin *et al*., 2010). Moreover, YgfA has a functional role in the formation of biofilms and multidrug-tolerant persister cells (Ren *et al*., 2004; Hansen *et al*., 2008). Hence, YgfA and 6S RNA share similar functional properties relevant for the adaptation to metabolic limitations during stationary phase.

Although 6S RNAs from numerous different bacteria exhibit a similar expression profile as observed in *E. coli*, with maximal concentrations during stationary phase, it is important to note that stationary phase accumulation is not unique and many bacteria do have quite different expression characteristics consistent with a great functional diversity of 6S RNA (Table 1). An alternative regulation apparently occurs in cells with different or more complex lifestyle. Notable examples are found among the phylum of phototropic cyanobacteria. In *Synechococcus* PCC 6301, for example, 6S RNA expression is maximal during exponential growth (Watanabe et al., 1997) while in *Prochlorococcus* MED4, two different 6S RNA transcripts show differential accumulation, probably coupled to light and S- and G2-like phases (Axmann *et al*., 2007). A complex situation also exists in *Bacillus subtilis* expressing two different 6S RNAs, 6S-1 RNA and 6S-2 RNA, which seem to have diverged functionally and show different temporal expression patterns during growth phases. 6S-1 RNA has a similar expression profile as *E. coli* 6S RNA whereas 6S-2 RNA levels are more or less constant during the growth cycle (Barrick *et al*., 2005; Beckmann *et al*., 2011; Cavanagh *et al*., 2011). Accordingly, 6S-1 RNA, but not 6S-2 RNA, was recently shown to be involved in timing the onset of sporulation (Cavanagh and Wassarman, 2013). Similar to 6S-2 RNA no growth phase-dependent accumulation has been reported for the human pathogen *Helicobacter pylori* (Sharma *et al*., 2010). In case of *Burkholderia* the amount of 6S RNA changes upon stress induced by reactive oxygen species (ROS) (Peeters *et al*., 2010). Further examples for 6S RNAs with alternative expression patterns, indicating functional diversity, comprise the 6S RNA from the soybean symbiont *Bradyrhizobium japonicum*. In this bacteria

6S RNA does not accumulate during stationary phase (Voss *et al*., 2009) but increased levels are found when the cells are in root nodules in contrast to free-living bacteria (Madhugiri *et al*., 2012). A functional pattern, strikingly different from that of *E. coli*, is also found in *Legionella pneumophila*. Contrary to the general prevalent activity of 6S RNA as an inhibitor, 6S RNA from this pathogen activates the expression of many genes involved in the stress response as well as genes encoding type IVB secretion system effectors. The 6S RNA of the parasite was furthermore shown to be important for intracellular growth in host cells and strains defective in 6S RNA show reduced intracellular growth in human macrophages or the protozoan host *Acanthamoeba castellanii*, whereas growth in rich medium is not affected (Faucher *et al*., 2010). More examples are known where 6S RNA function is related to intracellular growth of parasites as for instance in the virulent *S. Typhimurium* strain SL1344, where 6S RNA expression is repressed in non-proliferating intracellular bacteria (Ortega *et al*., 2012). The latter findings support a functional coupling of 6S RNA activity to nutritional limitations and different forms of stress including complex reactions such as the intracellular environment of a host and putative host defense in case of intracellular pathogenic bacteria.

Which genes does 6S RNA actually regulate?

Most of our current understanding by which mechanism 6S RNA-sensitive genes are selected for regulation is based on studies with the model organism *E. coli*. We know that 6S RNA binds almost exclusively to $E\sigma^{70}$ but not or only weakly to core RNAP or other RNAP holoenzymes with alternative sigma factors. This binding specificity reflects the observed preferential inhibition of σ^{70}-dependent promoters, yet a number of exceptions exist and the mechanism for the selection of 6S RNA-dependent promoters is not completely understood (Gildehaus *et al*., 2007; Cavanagh *et al*., 2008). Moreover, a general indirect activation of σ^{38}-dependent promoters due to the inactivation of most of the $E\sigma^{70}$ holoenzymes during stationary phase might be expected but is also not observed (Cavanagh *et al*., 2008; Neußer *et al*., 2010). Again, not all σ^{38}-dependent promoters are affected by 6S RNA. Most of the negatively regulated promoters identified at late stationary growth have been characterized by two features that determine sensitivity towards 6S RNA regulation. It was shown that 6S RNA inhibits σ^{70} promoters with a weak -35 element (i.e. three or fewer matches to consensus), while those with a perfect consensus are not sensitive. The -10 element seems to be of less importance for 6S RNA interference. In contrast, the presence of an extended -10 element employing a ‘TG’ motif two base pairs upstream of the -10 element favors 6S RNA inhibition. Based on these two promoter features hundreds of mapped *E. coli* promoters were predicted to be down-regulated by 6S RNA and a microarray analysis of a late stationary transcriptome reinforced the 6S RNA-dependent transcriptional inhibition for 68% of the predicted genes (Cavanagh *et al*., 2008).

To monitor effects of 6S RNA during exponential and early stationary phase, when cellular concentrations of 6S RNA are already remarkably high, an independent genome-wide microarray analysis was performed with wild-type and 6S RNA deficient cells grown to mid-exponential and early stationary phase. In this study a 6S RNA-dependent differential expression of about 500 genes (inhibition as well as activation) was documented. Again, the regulation observed was not strictly confined to σ^{70} promoters but

included many genes under the control of alternative sigma factors. For many of the differentially expressed genes the promoter characteristics outlined above could not be applied entirely (Neußer *et al*., 2010). It should be noted, however, that the expression of many regulators was affected in the absence of 6S RNA and therefore direct or indirect effects may account for the differential expression of many genes. Some inconsistencies between the above microarray analyses may also be explained by the different growth conditions employed (early stationary versus late stationary growth). In conclusion, the rules to predict 6S RNA-sensitive promoters are applicable in many cases but obviously do not cover all features. Future studies based on the now available more detailed structural information of 6S RNA-RNAP interaction may be helpful to remove remaining ambiguities.

Structural details of specific interaction between 6S RNA and RNAP

Clearly, the structural requirements for specific binding of RNAP reside in the highly conserved 6S RNA secondary structure consisting of a central bubble flanked by two irregularly paired stem regions. Various 6S RNA mutations that support the collapse of the central bubble or reduce its size in either 3' or 5' direction abolish RNAP binding and transcriptional inhibition, which underlines the importance of the central bubble (Trotochaud and Wassarman, 2005). On the other hand, there is no obvious sequence similarity with consensus core promoter sequences within 6S RNA. Intriguingly, besides σ^{70} no or only modest interaction of 6S RNA occurs with other forms of RNAP ($E\sigma^{38}$, $E\sigma^{32}$ or core RNAP) even though they belong to the same σ-factor family indicating that potential interactions with these enzymes are probably nonspecific or of less physiological importance. No association could be observed between 6S RNA and σ factors alone.

The molecular details of the interaction between 6S RNA and $E\sigma^{70}$ have been limited until recently. Several nucleotides of the 3' side of the central bubble and the flanking stem regions have been shown to be in close contact with RNAP subunits β, β' and σ^{70} (Wassarman and Storz, 2000; Trotochaud and Wassarman, 2005; Gildehaus *et al*., 2007). Moreover residues around position U44, representing the transcription start site for pRNA synthesis in the 5' side of the *E. coli* 6S RNA central bubble, were mapped close to the active center of RNAP (Wassarman and Saecker, 2006). The association of 6S RNA and RNAP depends to a large degree on σ^{70} region 4.2, also known to be responsible for the recognition of the -35 promoter DNA element. A mutational analysis of this region showed that a stretch of positively charged amino acid residues are important for 6S RNA binding. The binding surface overlaps but is also distinct from the -35 DNA promoter region (Cavanagh *et al*., 2008; Klocko and Wassarman, 2009). Restricted by the size of the molecule and/or the lack of suitable crystals previous approaches to determine the complete three-dimensional structure or any high-resolution structure of 6S RNA have been unsuccessful so far. A recent X-ray crystallographic attempt has only yielded limited information on the 12 bp closing stem structure from *Aquifex aeolicus* 6S RNA. This study ascertains a regular A-form RNA helix for this double-stranded 6S RNA region (Kondo *et al*., 2013).

Recently, our view of the three-dimensional structure of the complete 6S RNA has been improved significantly by a mapping study of the regulatory RNA in complex with σ^{70}-containing RNAP holoenzyme (Steuten *et al*., 2013). In this study 6S RNA positions were identified in

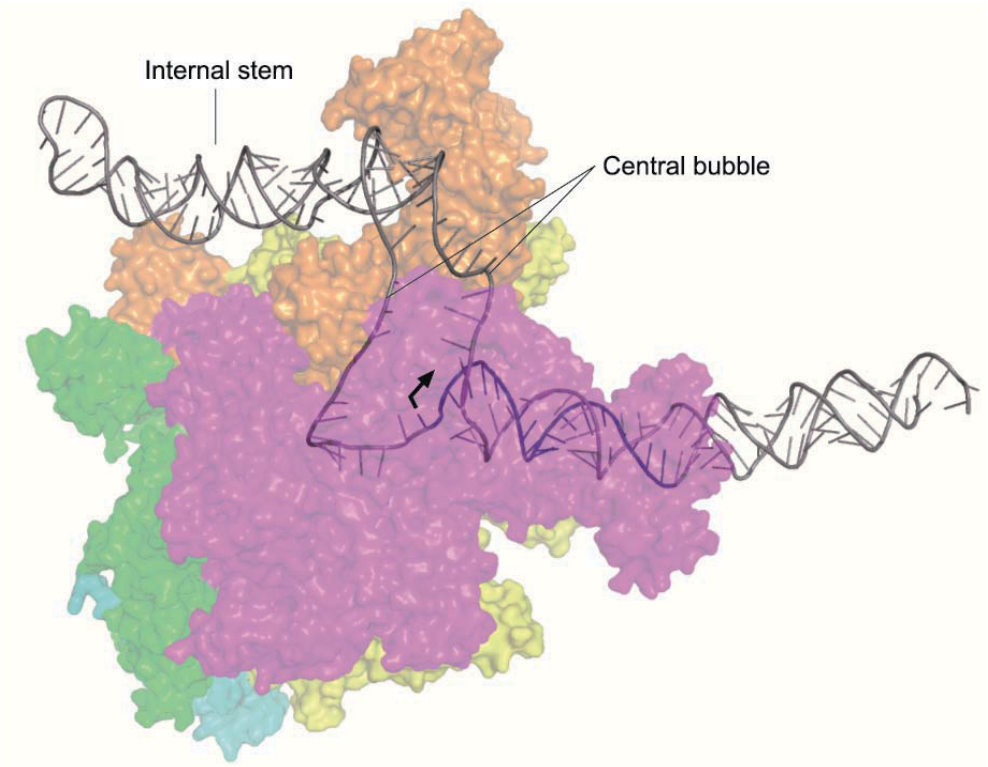

Figure 1: A three-dimensional model of the *E. coli* 6S RNA-RNAP complex.
The 6S RNA molecule is shown as cartoon in grey. The double-stranded internal stem and the single-stranded central bubble are labelled. The pRNA transcription start site is marked by an arrow and the pRNA template region is highlighted in blue. The $E\sigma^{70}$ (pdb ID: 4igc) is displayed in transparent surface representation. Subunits are coloured as follows: σ^{70}, orange; β', yellow; β, magenta; α_I, green; α_{II}, cyan.

close proximity with RNAP holoenzyme and a three-dimensional model of 6S RNA in complex with RNAP was constructed (Murakami, 2013). The deduced model displays details of the spatial neighborhood of the 6S RNA-RNAP interaction surface and allows the identification of defined nucleotides of the 6S RNA internal stem region in proximity to known functional amino acids of the $E\sigma^{70}$ holoenzyme (Fig. 1). Parallel experiments with mutant 6S RNAs underline the importance of the conserved internal stem bulge regions in RNAP binding. Results with these mutants revealed that RNAP recognition does not only depend on the 6S RNA secondary structure but apparently also has a sequence-dependent component consistent with a recent proposal (Shephard *et al*., 2010; Steuten *et al*., 2013).

The physiological effect(s) of pRNA synthesis

The finding that 6S RNA can function as a template for the *de novo* transcription of pRNAs is of particular interest. This reaction has not only been observed for 6S RNA from *E. coli* but also for quite a number of different bacteria either by direct biochemical characterization or deep sequencing approaches. Well-characterized examples comprise 6S-1 RNA from *B. subtilis* (Beckmann *et al*., 2011; Cavanagh *et al*., 2011; Cabrera-Ostertag *et al*., 2013) or a selection of 6S RNAs from different cyanobacteria (*Synechocystis*, *Synechococcus*, *Prochlorococcus* and *Nostoc*) indicating that synthesis of pRNAs with very similar properties as noted for *E. coli* occurs in cyanobacteria as well (Rediger *et al*., 2012). pRNAs derived from 6S RNAs of different bacteria show a certain degree of sequence conservation but are not identical and may exhibit variable length.

Furthermore, the presence of two different pRNAs, initiated from opposite sites of the central bubble of one and the same 6S RNA, has been documented in *H. pylori* (Sharma *et al*., 2010). Although the universal existence of pRNAs has not been proven by systematic analyses it was suggested that they also occur in *L. pneumophila* (Faucher and Shuman, 2011; Weissenmayer *et al*., 2011) and probably many other strains expressing 6S RNA as well. It is reasonable to assume therefore that it is a general property of 6S RNA to act as template for pRNA synthesis.

For *E. coli* 6S RNA and 6S-1 RNA from *B. subtilis* it was demonstrated *in vitro* and *in vivo* that pRNA synthesis is obviously linked to the cellular NTP status and requires elevated NTP substrate concentrations compared to normal DNA-dependent transcription. 6S RNA-templated transcription generally initiates within the central bubble and for *E. coli* position U44 was identified as the start site resulting in pRNAs of 10 nt to 20 nt in length. Based on perfect complementarity the nascent pRNAs form hybrids with the 6S RNA template. In particular the longer RNA duplex structures between pRNAs and the 6S RNA template strand are exceptionally stable causing a rearrangement of the 6S RNA secondary structure, which facilitates the dissociation of the σ subunit from the inhibitory 6S RNA-RNAP complex. Several studies have elucidated the details of the structural rearrangement of *E. coli* and *B. subtilis* 6S RNAs during pRNA synthesis involving the formation of a new hairpin structure (Beckmann *et al*., 2012; Panchapakesan and Unrau, 2012; Steuten and Wagner, 2012). Following the dissociation of σ, the complete complex decays resulting in the release of core RNAP and the 6S RNA-pRNA hybrid (Wassarman and Saecker, 2006; Shephard *et al*., 2010; Wurm *et al*., 2010; Beckmann *et al*., 2011; Cavanagh *et al*., 2011). The 6S RNA-pRNA hybrid is then rapidly degraded by unknown cellular nucleases (Wassarman and Saecker, 2006; Gildehaus *et al*., 2007; Wurm *et al*., 2010).

Remarkably, during stationary phase, when 6S RNA levels are highest, pRNAs are hardly detectable in *E. coli*, probably because of the existent low NTP concentrations. However, under conditions of outgrowth from stationary phase, which is accompanied by an increase in NTP pools, a rapid burst of pRNA synthesis with concomitant decay of the inhibitory RNAP complex is observed. This reaction is fast and *in vivo* pRNA synthesis occurs immediately (in a range of seconds) after nutritional upshift. pRNAs of increasing length accumulate in a time-dependent manner (10-13 nt at first, subsequently replaced by 16-20 nt), of which the longer ones remain stably bound to the 6S RNA template. The synthesis of pRNAs ceases after approximately 10 minutes and free pRNAs vanish from the cell due to their short half-life of less than 30 seconds (Wurm *et al*., 2010). Moreover, 6S RNA, which is metabolically stable under normal growth conditions, becomes degraded upon pRNA transcription probably resulting from the loss of RNAP protection and reorganization of the 6S RNA secondary structure due to hybrid formation with pRNA (Wassarman and Saecker, 2006; Wurm *et al*., 2010). The release of σ^{70} and free RNAP core, following pRNA synthesis, provides sufficient enzyme to resume mRNA transcription and enables new exponential growth of the cells. In short, 6S RNA encodes its own regulatory RNA (pRNA), which triggers the reversal of 6S RNA-dependent inhibition (Kugel and Goodrich, 2007). It is clear that efficient reversal of this inhibition is important for rapid adaptation to environmental changes for the cell. Expression of a mutant *E. coli* 6S

RNA, which was modified in the 5' side of the central bubble, showing neither pRNA transcription nor release from $E\sigma^{70}$, resulted in significant delay of outgrowth. In addition, overexpression of this mutant in stationary grown cells leads to decreased viability, further underlining the importance of de-repression of 6S RNA inhibition by pRNA-mediated release (Cavanagh *et al*., 2011). Whether promoting the dissociation of the inhibitory complex between RNAP and 6S RNA is the only function for pRNAs is not yet known. For example, in *H. pylori* pRNA synthesis is observed during mid-log growth and not restricted to outgrowth probably indicating an alternative physiological role (Sharma *et al*., 2010).

Role of 6S RNA as "resource sentinel" during stress

An informative result from the genome-wide transcriptome analysis of 6S RNA-deficient *E. coli* cells was the finding that 6S RNA affects the expression of many genes involved in central metabolism. Most remarkably, a concerted inhibition of the expression of genes constituting the translation machinery (genes for ribosomal proteins, ribosomal RNA, translation factors, enzymes responsible for ribosome modification and assembly) was observed at the onset of stationary phase. It is important to know that ribosome biosynthesis plays a central role in growth adaptation (Wagner, 2009). Concomitant with the observed down-regulation of components for ribosome biogenesis a corresponding increase of the global regulator for growth rate control and stringent response, ppGpp, was demonstrated in absence of 6S RNA (Neußer *et al*., 2010). Whereas the basal ppGpp level is directly linked to the cell growth rate (Baracchini and Bremer, 1988; Potrykus *et al*., 2011) 6S RNA deletion strains show an enhanced ppGpp level without noticeable change in growth rate. In *E. coli* the ppGpp concentration is adjusted by two different enzymes, the ribosome-associated RelA, responsible for the rapid synthesis to high concentrations (stringent response), and the bi-functional SpoT regulating the basal ppGpp concentration by a balanced synthesis and hydrolysis activity (Potrykus and Cashel, 2008; Wagner, 2010). The 6S RNA-dependent change in the ppGpp level could be demonstrated in both *relA*$^+$ and *relA*$^-$ strains ruling out that RelA-dependent ppGpp synthesis is responsible for the enhanced ppGpp pool (Geißen *et al*., 2010; Neußer *et al*., 2010). Hence, this effect must rather be the result of altered SpoT activity. Curiously, an independent study demonstrated that transcription of *relA* is inhibited by 6S RNA during early stationary phase, thus also leading to elevated ppGpp levels in a 6S RNA deletion strain (Cavanagh *et al*., 2010). While both results are difficult to interpret they do not contradict each other. More experiments are necessary to unravel this ambiguity and to elucidate the direct link between 6S RNA and ppGpp. An appropriate question in this respect is to find out, if 6S RNA acts as a potential direct effector of SpoT, as shown for several other regulatory molecules, such as acyl carrier protein (ACP), CgtA or even tRNA (Richter, 1980; Battesti and Bouveret, 2006; Raskin *et al*., 2007).

The link between 6S RNA and ppGpp does also involve the transcription factor DksA, a synergistic co-regulator of ppGpp. Initial experiments indicated that both 6S RNA and pRNA levels are reduced in a *dksA* deletion strain (Heilmann, Olgeisser and Wagner, unpublished). Thus, analyzing the interconnection between 6S RNA and the ppGpp/DksA network of growth rate regulation is a promising challenge.

Consistent with a role of 6S RNA in general metabolism many 6S RNA-dependent genes in *E. coli* are

differentially expressed also during exponential growth (Neußer *et al*., 2010; Geißen *et al*., 2010). Next to transporters and stress regulators several important enzymes of the purine metabolism are affected. Remarkably, many genes involved in purine metabolism are co-transcribed or directly flank bacterial 6S RNA genes. Examples comprise *ygfA* in *E. coli*, *purK*, often found upstream of 6S RNA genes in cyanobacteria, or *purD* downstream of the *H. pylori* 6S RNA gene. The NTP pool, which directly depends on purine metabolism, is also an important determinant for ribosome synthesis. Interestingly, it can be shown that 6S RNA affects the transcription of rRNAs, the key molecules for ribosome synthesis, by influencing the cellular ATP/GTP ratio (Geißen *et al*., 2010). Note that an enhanced NTP pool is also required for pRNA synthesis, thus in turn affecting 6S RNA activity. In conclusion, further studies to unravel the complex relation between 6S RNA and the cellular nucleotide level are desirable.

Further support for the general function of 6S RNA in regulating the economic use of scarce resources under growth limitations or stress is based on a recent study analyzing the phenotype of 6S-1 RNA deletion in *B. subtilis*. It was found that cells lacking 6S-1 RNA initiate the formation of endospores at earlier times than wild-type cells indicating that 6S-1 RNA is important for regulation of developmental processes upon starvation or nutrient limitation. Moreover, a faster reduction of the nutrient content of the environment for the 6S-1 RNA deletion strain compared to either wild type or 6S-2 RNA deletion strains suggests a role of 6S-1 RNA in balancing the economic use of limited resources (Cavanagh and Wassarman, 2013).

Functional homologs of 6S RNA in eukaryotes

Interestingly, functional homologues of bacterial 6S RNA can actually be found in eukaryotic systems. Mouse B2 RNA and human Alu RNA bind with high specificity to RNA polymerase II thereby repressing transcription at promoters related to heat shock. In contrast to 6S RNA the eukaryotic RNA regulators co-occupy RNA polymerase II and DNA, thus preventing proper DNA-RNAP interactions during closed complex formation. The altered conformation of such a ternary complex remains transcriptionally inactive on the DNA (Espinoza *et al*., 2004; Yakovchuk *et al*., 2009). Moreover, B2 RNA was mapped at the DNA cleft and the active site region of RNAP II (Ponicsan *et al*., 2013). In contrast to bacterial 6S RNA, B2 RNA does not give rise to pRNAs but can serve as a template for a 18 nt extension on its 3’ end by RNAP II. This reaction destabilizes the RNA-RNAP interaction. Removal of B2 RNA from RNAP II is catalysed by an additional factor present in nuclear extracts, however (Wagner *et al*., 2013).

Conclusion and future prospects

Variable expression levels and the existence of 6S RNA in phylogenetic distant bacteria reflect the considerable functional diversity observed for this regulatory RNA. In fact, regulation by this versatile RNA is not restricted to a small number of defined genes but has evolved to affect a broad spectrum of genes depending on the lifestyle and physiology of diverse bacteria. As a common element, regulation by 6S RNA is embedded into networks governing the adaptation to environmental changes. These adaptation processes comprise escape from stationary phase, the economic use of nutrients and improved fitness under diverse stresses, but also delay in sporulation, regulation of virulence factors

or optimal intracellular growth. Often genes regulating central metabolism, such as the translational machinery, synthesis and salvage of NTPs, or one-carbon metabolism are affected. In order to understand the role of 6S RNA in all of these diverse processes it does not suffice to improve specificity criteria for 6S RNA-sensitive promoters rather it is necessary to disentangle direct from indirect effects and to identify more of the potential network players involved. The general importance of pRNAs also demands future attention. Although abandoning 6S RNA-dependent regulation can be attributed as a clear function we may have seen only one aspect of its potential tasks. Many challenging questions are waiting for answers.

Acknowledgement

We like to thank people from the laboratory for helpful discussions. Work from this laboratory was funded by the Deutsche Forschungsgemeinschaft SPP 1258.

References

Axmann, I. M., J. Holtzendorff, B. Voss, P. Kensche and W. R. Hess (2007). Two distinct types of 6S RNA in *Prochlorococcus*. *Gene* **406**: 69-78.

Baracchini, E. and H. Bremer (1988). Stringent and growth control of rRNA synthesis in *Escherichia coli* are both mediated by ppGpp. *J Biol Chem* **263**: 2597-2602.

Barrick, J. E., N. Sudarsan, Z. Weinberg, W. L. Ruzzo and R. R. Breaker (2005). 6S RNA is a widespread regulator of eubacterial RNA polymerase that resembles an open promoter. *RNA* **11**: 774-784.

Battesti, A. and E. Bouveret (2006). Acyl carrier protein/SpoT interaction, the switch linking SpoT-dependent stress response to fatty acid metabolism. *Mol Microbiol* **62**: 1048-1063.

Beckmann, B. M., O. Y. Burenina, P. G. Hoch, E. A. Kubareva, C. M. Sharma and R. K. Hartmann (2011). *In vivo* and *in vitro* analysis of 6S RNA-templated short transcripts in *Bacillus subtilis*. *RNA Biol* **8**: 839-849.

Beckmann, B. M., P. G. Hoch, M. Marz, D. K. Willkomm, M. Salas and R. K. Hartmann (2012). A pRNA-induced structural rearrangement triggers 6S-1 RNA release from RNA polymerase in *Bacillus subtilis*. *EMBO J* **31**: 1727-1738.

Brownlee, G. G. (1971). Sequence of 6S RNA of *E. coli*. *Nat New Biol* **229**: 147-149.

Cabrera-Ostertag, I. J., A. T. Cavanagh and K. M. Wassarman (2013). Initiating nucleotide identity determines efficiency of RNA synthesis from 6S RNA templates in *Bacillus subtilis* but not *Escherichia coli*. *Nucleic Acids Res*.

Cavanagh, A. T., P. Chandrangsu and K. M. Wassarman (2010). 6S RNA regulation of *relA* alters ppGpp levels in early stationary phase. *Microbiology* **156**: 3791-3800.

Cavanagh, A. T., A. D. Klocko, X. Liu and K. M. Wassarman (2008). Promoter specificity for 6S RNA regulation of transcription is determined by core promoter sequences and competition for region 4.2 of σ^{70}. *Mol Microbiol* **67**: 1242-1256.

Cavanagh, A. T., J. M. Sperger and K. M. Wassarman (2011). Regulation of 6S RNA by pRNA synthesis is required for efficient recovery from stationary phase in *E. coli* and *B. subtilis*. *Nucleic Acids Res* **40**: 2234-2246.

Cavanagh, A. T. and K. M. Wassarman (2013). 6S-1 RNA function leads to a delay in sporulation in *Bacillus subtilis*. *J Bacteriol* **195**: 2079-2086.

Chae, H., K. Han, K. S. Kim, H. Park, J. Lee and Y. Lee (2011). Rho-dependent termination of *ssrS* (6S RNA) transcription in *Escherichia coli*: implication for 3' processing of 6S RNA and expression of downstream *ygfA* (putative 5-formyl-tetrahydrofolate cyclo-ligase). *J Biol Chem* **286**: 114-122.

Espinoza, C. A., T. A. Allen, A. R. Hieb, J. F. Kugel and J. A. Goodrich (2004). B2 RNA binds directly to RNA polymerase II to repress transcript synthesis. *Nat Struct Mol Biol* **11**: 822-829.

Faucher, S. P., G. Friedlander, J. Livny, H. Margalit and H. A. Shuman (2010). *Legionella pneumophila* 6S RNA optimizes intracellular multiplication. *Proc Natl Acad Sci U S A* **107**: 7533-7538.

Faucher, S. P. and H. A. Shuman (2011). Small Regulatory RNA and *Legionella pneumophila*. *Front Microbiol* **2**: 98.

Geißen, R., B. Steuten, T. Polen and R. Wagner (2010). *E. coli* 6S RNA: a universal transcriptional regulator within the centre of growth adaptation. *RNA Biology* **7**: 564-568.

Gildehaus, N., T. Neusser, R. Wurm and R. Wagner (2007). Studies on the function of the riboregulator 6S RNA from *E. coli*: RNA polymerase binding, inhibition of *in vitro* transcription and synthesis of RNA-directed *de novo* transcripts. *Nucleic Acids Res* **35**: 1885-1896.

Hansen, S., K. Lewis and M. Vulic (2008). The Role of Global Regulators and Nucleotide Metabolism in Antibiotic Tolerance in *Escherichia coli*. *Antimicrob Agents Chemother* **52**: 2718-2726.

Hindley, J. (1967). Fractionation of 32P-labelled ribonucleic acids on polyacrylamide gels and their characterization by fingerprinting. *J Mol Biol* **30**: 125-136.

Hsu, L. M., J. Zagorski, Z. Wang and M. J. Fournier (1985). *Escherichia coli* 6S RNA gene is part of a dual-function transcription unit. *J Bacteriol* **161**: 1162-1170.

Jeanguenin, L., A. Lara-Nunez, A. Pribat, M. H. Mageroy, J. F. Gregory, 3rd, K. C. Rice, V. de Crecy-Lagard and A. D. Hanson (2010). Moonlighting glutamate formiminotransferases can functionally replace 5-formyltetrahydrofolate cycloligase. *J Biol Chem* **285**: 41557-41566.

Kim, K. S. and Y. Lee (2004). Regulation of 6S RNA biogenesis by switching utilization of both sigma factors and endoribonucleases. *Nucleic Acids Res* **32**: 6057-6068.

Klocko, A. D. and K. M. Wassarman (2009). 6S RNA binding to $E\sigma^{70}$ requires a positively charged surface of σ^{70} region 4.2. *Mol Microbiol* **73**: 152-164.

Kondo, J., A. C. Dock-Bregeon, D. K. Willkomm, R. K. Hartmann and E. Westhof (2013). Structure of an A-form RNA duplex obtained by degradation of 6S RNA in a crystallization droplet. *Acta Crystallogr Sect F Struct Biol Cryst Commun* **69**: 634-639.

Kugel, J. F. and J. A. Goodrich (2007). An RNA transcriptional regulator templates its own regulatory RNA. *Nat Chem Biol* **3**: 89-90.

Lee, C. A., M. J. Fournier and J. Beckwith (1985). *Escherichia coli* 6S RNA is not essential for growth or protein secretion. *J Bacteriol* **161**: 1156-1161.

Lee, J. Y., H. Park, G. Bak, K. S. Kim and Y. Lee (2013). Regulation of transcription from two *ssrS* promoters in 6S RNA biogenesis. *Mol Cells*.

Lee, S. Y., S. C. Bailey and D. Apirion (1978). Small stable RNAs from *Escherichia coli*: evidence for the existence of new molecules and for a new ribonucleoprotein particle containing 6S RNA. *J Bacteriol* **133**: 1015-1023.

Madhugiri, R., G. Pessi, B. Voss, J. Hahn, C. M. Sharma, R. Reinhardt, J. Vogel, W. R. Hess, H. M. Fischer and E. Evguenieva-Hackenberg (2012). Small RNAs of the *Bradyrhizobium/Rhodopseudomonas* lineage and their analysis. *RNA Biol* **9**: 47-58.

Murakami, K. S. (2013). The X-ray Crystal Structure of *Escherichia Coli* RNA Polymerase σ^{70} Holoenzyme. *J Biol Chem* **288**: 9126-9134.

Neußer, T., N. Gildehaus, R. Wurm and R. Wagner (2008). Studies on the expression of 6S RNA from *E. coli*: involvement of regulators important for stress and growth adaptation. *Biol Chem* **389**: 285-297.

Neußer, T., T. Polen, R. Geißen and R. Wagner (2010). Depletion of the non-coding regulatory 6S RNA in *E. coli* causes a surprising reduction in the expression of the translation machinery. *BMC Genomics* **11**: 165-178.

Ortega, A. D., J. Gonzalo-Asensio and F. Garcia-del Portillo (2012). Dynamics of Salmonella small RNA expression in non-growing bacteria located inside eukaryotic cells. *RNA Biol* **9**: 469-488.

Panchapakesan, S. S. and P. J. Unrau (2012). *E. coli* 6S RNA release from RNA polymerase requires σ^{70} ejection by scrunching and is orchestrated by a conserved RNA hairpin. *RNA* **18**: 2251-2259.

Peeters, E., A. Sass, E. Mahenthiralingam, H. Nelis and T. Coenye (2010). Transcriptional response of *Burkholderia cenocepacia* J2315 sessile cells to treatments with high doses of hydrogen peroxide and sodium hypochlorite. *BMC Genomics* **11**: 90.

Ponicsan, S. L., S. Houel, W. M. Old, N. G. Ahn, J. A. Goodrich and J. F. Kugel (2013). The Non-Coding B2 RNA Binds to the DNA Cleft and Active-Site Region of RNA Polymerase II. *J Mol Biol*.

Potrykus, K. and M. Cashel (2008). (p)ppGpp: Still Magical? *Annu Rev Microbiol* **62**: 35-51.

Potrykus, K., H. Murphy, N. Philippe and M. Cashel (2011). ppGpp is the major source of growth rate control in *E. coli*. *Environ Microbiol* **13**: 563-575.

Raskin, D. M., N. Judson and J. J. Mekalanos (2007). Regulation of the stringent response is the essential function of the conserved bacterial G protein CgtA in *Vibrio cholerae*. *Proc Natl Acad Sci U S A* **104**: 4636-4641.

Rediger, A., R. Geissen, B. Steuten, B. Heilmann, R. Wagner and I. M. Axmann (2012). 6S RNA - an old issue became blue-green. *Microbiology* **158**: 2480-2491.

Ren, D., L. A. Bedzyk, S. M. Thomas, R. W. Ye and T. K. Wood (2004). Gene expression in *Escherichia coli* biofilms. *Appl Microbiol Biotechnol* **64**: 515-524.

Richter, D. (1980). Uncharged tRNA inhibits guanosine 3',5'-bis (diphosphate) 3'-pyrophosphohydrolase [ppGppase], the spoT gene product, from *Escherichia coli*. *Mol Gen Genet* **178**: 325-327.

Sharma, C. M., S. Hoffmann, F. Darfeuille, J. Reignier, S. Findeiss, A. Sittka, S. Chabas, K. Reiche, J. Hackermuller, R. Reinhardt, P. F. Stadler and J. Vogel (2010). The primary

transcriptome of the major human pathogen *Helicobacter pylori*. *Nature* **464**: 250-255.

Shephard, L., N. Dobson and P. J. Unrau (2010). Binding and release of the 6S transcriptional control RNA. *RNA* **16**: 885-892.

Steuten, B., P. Setny, M. Zacharias and R. Wagner (2013). Mapping the Spatial Neighborhood of the Regulatory 6S RNA Bound to *Escherichia coli* RNA Polymerase Holoenzyme. *J Mol Biol* **425**: 3649-3661.

Steuten, B. and R. Wagner (2012). A conformational switch is responsible for the reversal of the 6S RNA-dependent RNA polymerase inhibition in *Escherichia coli*. *Biol Chem* **393**: 1513-1522.

Trotochaud, A. E. and K. M. Wassarman (2004). 6S RNA function enhances long-term cell survival. *J Bacteriol* **186**: 4978-4985.

Trotochaud, A. E. and K. M. Wassarman (2005). A highly conserved 6S RNA structure is required for regulation of transcription. *Nature Structural Biol.* **12**: 313-319.

Trotochaud, A. E. and K. M. Wassarman (2006). 6S RNA Regulation of *pspF* Transcription Leads to Altered Cell Survival at High pH. *J Bacteriol* **188**: 3936-3943.

Voss, B., M. Holscher, B. Baumgarth, A. Kalbfleisch, C. Kaya, W. R. Hess, A. Becker and E. Evguenieva-Hackenberg (2009). Expression of small RNAs in Rhizobiales and protection of a small RNA and its degradation products by Hfq in *Sinorhizobium meliloti*. *Biochem Biophys Res Commun* **390**: 331-336.

Wagner, R. (2009). Translational components in prokaryotes: genetics and regulation of ribosomes. *Encyclopedia of Life Sciences, Nature Publishing Group, Macmillan Publishers Ltd., London. [ELS]*.

Wagner, R. (2010). *ppGpp Signalling.* in Bacterial Signaling, Kraemer, R. and Jung, K. (Eds.), Wiley VCH, Weinheim.

Wagner, S. D., P. Yakovchuk, B. Gilman, S. L. Ponicsan, L. F. Drullinger, J. F. Kugel and J. A. Goodrich (2013). RNA polymerase II acts as an RNA-dependent RNA polymerase to extend and destabilize a non-coding RNA. *EMBO J* **32**: 781-790.

Wassarman, K. M. and R. M. Saecker (2006). Synthesis-mediated release of a small RNA inhibitor of RNA polymerase. *Science* **314**: 1601-1603.

Wassarman, K. M. and G. Storz (2000). 6S RNA regulates *E. coli* RNA polymerase activity. *Cell* **101**: 613-623.

Watanabe, T., M. Sugiura and M. Sugita (1997). A novel small stable RNA, 6Sa RNA, from the cyanobacterium *Synechococcus* sp. strain PCC6301. *FEBS Lett* **416**: 302-306.

Weissenmayer, B. A., J. G. Prendergast, A. J. Lohan and B. J. Loftus (2011). Sequencing illustrates the transcriptional response of *Legionella pneumophila* during infection and identifies seventy novel small non-coding RNAs. *PLoS One* **6**: e17570.

Wurm, R., T. Neußer and R. Wagner (2010). 6S RNA-dependent inhibition of RNA polymerase is released by RNA-dependent synthesis of small *de novo* products. *Biol Chem* **39**: 187-196.

Yakovchuk, P., J. A. Goodrich and J. F. Kugel (2009). B2 RNA and Alu RNA repress transcription by disrupting contacts between RNA polymerase II and promoter DNA within assembled complexes. *Proc Natl Acad Sci U S A* **106**: 5569-5574.

6.2 Point-of-View article (Geißen *et al*. 2010)

POINT-OF-VIEW

RNA Biology 7:5, 1-5; September/October 2010; © 2010 Landes Bioscience

E. coli 6S RNA

A universal transcriptional regulator within the centre of growth adaptation

René Geißen,[1] Benedikt Steuten,[1] Tino Polen[2] and Rolf Wagner[1,*]

[1]Institut für Physikalische Biologie; Heinrich-Heine-Universität Düsseldorf; Düsseldorf, Germany; [2]Institut für Biotechnologie 1; Forschungszentrum Jülich GmbH; Jülich, Germany

Bacterial 6S RNA has been shown to bind with high affinity to σ^{70}-containing RNA polymerase, suppressing σ^{70}-dependent transcription during stationary phase, when 6S RNA concentrations are highest. We recently reported a genome-wide transcriptional comparison of wild-type and 6S RNA deficient *E. coli* strains. Contrary to the expected σ^{70}- and stationary phase-specific regulatory effect of 6S RNA it turned out that mRNA levels derived from many alternative sigma factors, including σ^{38} or σ^{32}, were affected during exponential and stationary growth. Among the most noticeably downregulated genes at stationary growth are ribosomal proteins and factors involved in translation. In addition, a striking number of mRNA levels coding for enzymes involved in the purine metabolism, for transporters and stress regulators are altered both during log- and stationary phase. During the study we discovered a link between 6S RNA and the general stress alarmone ppGpp, which has a higher basal level in cells deficient in 6S RNA. This finding points to a functional interrelation of 6S RNA and the global network of stress and growth adaptation.

Key words: regulatory RNA, growth regulation, transcription, RNA polymerase, NTP pool

Submitted: 06/08/10

Revised: 07/08/10

Accepted: 07/09/10

Previously published online: www.landesbioscience.com/journals/rnabiology/article/12969

*Correspondence to: Rolf Wagner; Email: r.wagner@rz.uni-duesseldorf.de

Bacterial 6S RNA—A Transcriptional Regulator

6S RNA from *E. coli* had been discovered as stable RNA already 40 years from now. Clear information on its possible function in the cell was lacking until recently, however.[1] Only after it had been shown that 6S RNA exists in the cell as stable complex, associated with RNA polymerase (RNAP), the molecule as such and the physiological consequences of the above finding became a major point of interest.[2] The fact, that the cellular concentration of 6S RNA increases about ten-fold from exponential to stationary growth, together with the finding that stable complexes between 6S RNA were observed with the holoenzyme Eσ^{70}, but not with Eσ^{38}, core RNA polymerase or the isolated σ factors, has lead to the conclusion that 6S RNA supports the required change of transcriptional specificity from exponential to stationary growth. According to this, the role of 6S RNA in the cell had been regarded as functionally related to the anti-sigma factor Rsd, which is considered to specifically inactivate σ^{70} during stationary phase.[3,4] This view is generally accepted today and many studies performed in vivo and in vitro have been presented, supporting the role of 6S RNA as Eσ^{70}-specific repressor during the growth change from logarithmic to stationary phase.[2,5-7]

There have been some early indications, however, which were not entirely consistent with such a straightforward function of this abundant RNA molecule. For instance, there is no easily detectable phenotype in the growth behavior of *wt* and 6S RNA deficient cells, although during stationary phase almost all Eσ^{70} RNAP holoenzymes are supposed to be sequestered in a transcriptionally inactive complex with 6S RNA. Only under long time starvation or stress conditions the deletion of the 6S RNA gene (*ssrS*) has noticeable consequences for the cells.[6,7] Moreover, in vitro studies did not support the obvious

conclusion that only Eσ^{70}-specific promoters should be inhibited while Eσ^{38}-dependent promoters should not.[8] The more restrictive postulate, supported by a microarray study, that among the typical Eσ^{70}-specific promoters only those with an extended-10 recognition element and a weak-35 consensus are sensitive to 6S RNA-dependent regulation, reduced some of the conflicts but did not answer exactly the actual specificity of 6S RNA transcriptional regulation.[9] This dissatisfying situation had inspired us to conduct an unbiased whole genome transcriptional analysis comparing *wt* and *ssrS* deficient strains during log and stationary phase of growth. The outcome of this investigation was surprising.[10] Some interesting implications had been extracted from the data, which already point to unanticipated additional functional links of 6S RNA. Here we extent and deepen some of the consequences from our recent study, which were not discussed extensively so far, and which support a more central metabolic importance for the wide-spread riboregulator 6S RNA.

Does the Specificity of 6S RNA Regulation Correlate with Promoter Strength?

The fact that almost as many genes showed altered expression levels at exponential- and stationary phase of growth has been unexpected, given the assumed function of 6S RNA to facilitate the transcriptional efficiency during shift from exponential to stationary growth. Moreover, the view that 6S RNA exclusively affects Eσ^{70} holoenzymes with a marked specificity for promoters characterized by a weak-35 recognition element and extended-10 promoters must be expanded. There are several possible reasons, which may account for the observed differences. The latter conclusion was largely based on a microarray study, where expression patterns of selected promoters were studied after long-time starvation.[9] The results of the Neusser et al. study were obtained during log and early stationary phase, representing completely different physiological states.[10]

While we are obviously lacking a complete explanation some of our recent in vitro studies support a very straightforward conclusion, namely a direct correlation between 6S promoter specificity and promoter strength. This simple conclusion is supported by a transcriptional analysis in vitro under competitive multi-promoter conditions, which revealed that the efficiency of 6S RNA-dependent inhibition correlates with the strength of the respective promoter (Geißen R, et al. unpublished).

6S RNA Deficiency Results in Altered Expression Levels of Functionally Related Gene Families

One problem with microarray analysis is that within a large pile of data there is often much more hidden behind the surface than is self-evident and researchers with a different focus may disclose correlations from the data not readily discernible for others with a different view. For instance, scientists specialized in cell metabolism and enzymology may recognize completely other clues compared to those with a main interest in gene regulation. Hence, there is always some bias in interpreting microarray data. To reduce this bias we looked for groups of functionally related genes, which were affected. Among the differentially expressed genes affected in the same way we noted several groups with common properties. In our study we termed these genes as "meaningful" and representative groups consist of genes, which were either previously predicted to be related to the *ssrS* transcription unit, or which are members of a family with common or related functions, e.g., regulatory- or stress-related functions. The most striking group, which was downregulated at stationary phase of growth in the *ssrS* deficient strain comprise genes encoding components of the translation machinery, such as ribosomal proteins, translation factors or enzymes responsible for ribosome modification and assembly.

In addition to the genes for many stress-related proteins, transporters and transcriptional regulators, we noticed a differential expression for several remarkable enzymes involved in the biosynthesis and salvage of purines. Notable examples are *guaD*, *add* and *folD,* encoding guanine deaminase, adenine deaminase or a bifunctional 5,10-methylene-tetrahydrofolate dehydrogenase/5,10-methylene-tetrahydrofolate cyclohydrolase, respectively. This observation is of special interest, because the gene *ygfA*, which is co-transcribed with the 6S RNA genes of many enterobacterial and γ-proteobacterial *ssrS* transcription units, encodes a predicted methenyltetrahydrofolate synthetase, functionally related to *folD*. Hence, together with the differentially regulated genes in purine metabolism, *ygfA*, co-transcribed with 6S RNA, may represent a link between the *ssrS* operon and the synthesis and degradation of purines.

There is another interesting line of evidence underlining the assumption that 6S RNA is functionally linked with the purine metabolism. Comparative genome studies show that most of the cyanobacterial 6S RNA genes are flanked by an upstream *purK* reading frame, which encodes an important enzyme for the de novo purine synthesis (I. Axmann, personal communication). Accordingly, the recently published transcriptome analysis of the major human pathogen *Helicobacter pylori* reveals that a *purD* gene is located downstream of the gene for *H. pylori* 6S RNA.[30]

The NTP Pool Composition Affects the Synthesis of rRNAs, the Rate-limiting Components of the Translation Machinery

It is known that changes in the NTP pool will ultimately also affect the synthesis of ribosomes. A coordinate repression of ribosomal constituents was one of the major findings from our transcriptome analysis. Ribosome biogenesis depends directly on the rate of rRNA synthesis because rRNA transcription determines the rate of ribosome formation.[11,12] Among the many regulatory components involved in rRNA transcription the concentration of the starting nucleotides has specific consequences for rRNA transcription under condition of nutritional stress when ppGpp signaling is induced because transcription of rRNA promoters are particularly sensitive to NTP concentrations at elevated ppGpp concentrations.[13-15]

6S RNA Affects Transcription from rRNA Promoters Dependent on the Nature of their Starting Nucleotide

All but one of the seven major *E. coli* rRNA P1 promoters require ATP as initiating NTP. The exception is the *rrnD* P1 promoter, which initiates with a GTP. Hence, the NTP requirements for synthesis are different for the individual rRNA promoters (Kolmsee et al. unpublished). This is different in *B. subtilis*, where GTP is the predominant substrate for rRNA transcription.[16,17] If the absence of 6S RNA affects the cellular NTP pool one might expect a change in the differential use of rRNA promoters, depending on the nature of their starting NTP. We have analyzed, therefore, if 6S RNA has an influence on the activity of rRNA P1 promoters, which either start with ATP or GTP, respectively. The analysis was performed with *rrnB* P1 (starting with A) or *rrnD* P1 (starting with G) promoters, present as *cat* fusion constructs on plasmids, which were transformed in *wt* and the corresponding *ssrS* deficient mutant cells. Clearly, in the *ssrS* deficient strain, the transcripts directed from *rrnD* P1 (starting with G) are significantly reduced, compared to *rrnB* (**Fig. 1**). When the same analysis was performed with a *rrnD* P1 mutation, where the start position was changed from G to A, the difference in the amount of transcripts was lost (*rrnD*^{mut}; **Fig. 1**). The result strongly supports a difference in the GTP versus ATP pools in the *ssrS* minus strain. Whether this assumption is correct will be seen by future direct analyses quantifying the NTP pools in the different strains.

The Inhibition of RNAP Activity by 6S RNA is itself Linked to the NTP Pool

One of the remarkable properties of 6S RNA is its ability to act as a template for the transcription of small de novo RNAs.[8,18] This unique activity is responsible to abrogate the 6S RNA-dependent inhibition of Eσ^{70}, when stationary cells resume growth due to nutritional improvement. The reaction, which requires unusually high NTP concentrations, is almost certainly triggered by a rapid increase in the cellular NTP pools following the nutritional upshift.[18,19] In this way, a nutritional upshift from stationary growth causes a burst of 6S RNA-templated de novo transcripts synthesized by RNAP bound to 6S RNA. The reaction leads to decomposition of the inhibitory 6S RNA-RNAP complex and releases RNAP for efficient transcription, enabling cells to resume exponential growth again.[19]

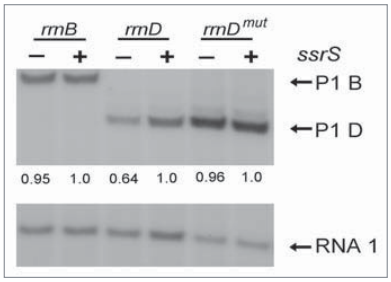

Figure 1. 6S RNA-dependent difference in transcription of rRNA promoters starting with either GTP or ATP as initial nucleotides. Results are shown from a primer extension analysis with total RNA from strains MG1655 or the *ssrS* deficient mutant, indicated by (+) or (-) above the lanes, respectively. The strains were transformed with vectors that contain the different rRNA P1 promoters as fusion constructs with a *cat* gene (Kolmsee et al. unpublished). The different ribosomal RNA P1 promoters *rrnB* (starting with A), *rrnD* (starting with G) and a mutant *rrnD* promoter (*rrnD*^{mut}) with altered initiation site (G to A) are indicated above the lanes. Bands characteristic for the primer extension products derived from *rrnB* P1, *rrnD* P1 or *rrnD*^{mut} P1 are indicated at the margin as P1 B or P1D, respectively. RNA 1 indicates transcripts derived from the plasmid encoded RNA 1 gene, which served as internal control. The ratio of the relative transcription efficiencies of the different *rrn* promoters in *ssrS*$^{-}$ versus wild-type strains, normalized to the internal control RNA 1, are given as numbers below the lanes.

Involvement of 6S RNA in General Stress and Growth Adaptation

It is important for the cell, in order to resume exponential growth, that the protein synthesizing machinery is adapted to the new growth rate. The rRNA promoter activities play a pivotal role at this stage. Accordingly, many of the responsible rRNA regulators are activated during upshift. Next to the adjustment of the ppGpp level to the new growth rate the two transcription factors FIS and H-NS, involved in the regulation of rRNA synthesis, are among the first proteins that are synthesized following nutritional upshift.[20,21] Interestingly, ribosomes are itself known as important sensors for the adaptation to different forms of stress, such as the change of the nutritional status or temperature.[22] The established link between 6S RNA, the ppGpp metabolism and the synthesis of ribosomes, uncovered in the recent transcriptome analysis interconnects this regulatory RNA with the complex regulatory network of growth adaptation.[23] Moreover, the comparatively high concentration of 1,000 6S RNA molecules per cell during exponential growth, which matches already 40% of the total RNAP, may be taken as evidence that the regulatory task of 6S RNA within that network is not only restricted to the stationary phase transition.[2,24]

Possible Link between 6S RNA and the Fatty Acid Metabolism

Lead by the effect of 6S RNA on the basal ppGpp concentration a careful re-evaluation of the microarray date revealed another interesting aspect of a more general involvement of 6S RNA in cell metabolism. A group of differentially expressed genes indicate a possible link between 6S RNA and fatty acid degradation and/or carbon metabolism.[25] Among the genes are *fadR*, which showed slightly increased mRNA levels (1.5-fold) in the 6S deficient strain. The gene *fadR* codes for FadR, which coordinately regulates fatty acid biosynthesis and degradation at the level of transcription.[26] Further genes with altered expression levels that indicate a link to the fatty acid or lipid metabolism are *fadD*, which showed decreased mRNA levels in the 6S deficient strain and which

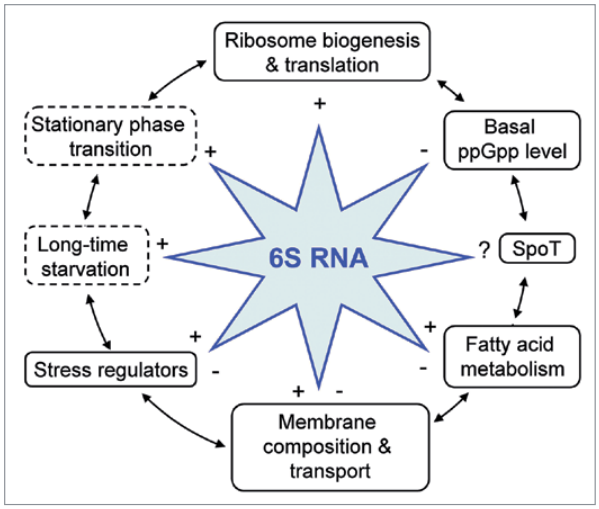

Figure 2. Cartoon depicting the proposed central integration of 6S RNA into the complex networks of stress and growth adaptation. Depicted are links between the 6S RNA and different processes related to stress and growth adaptation according to our recent data.[10] The symbols + or - denote a positive or negative influence on the respective process. The question mark indicates that no direct correlation has been established yet. The links to the processes in the dashed boxes are based on established literature data.[6,7]

is repressed by FadR. FadD encodes acyl-CoA synthetase, which is responsible for transport and activation of exogenous fatty acids prior to their subsequent degradation or incorporation into phospholipids or *plsX*, which encodes a fatty acid/phospholipid synthesis protein. Another example is *yfcY* (*fadI*), a member of the *fadIJK* operon, which has parallel functions as the *fadABD* operon and is required for aerobic fatty acid utilization.[27]

The interrelation of 6S RNA with fatty acid and lipid biosynthesis and turnover is of special interest because regulation of lipid turnover and reorganization will prolong the survival of growth arrested *E. coli* cells. The FadR regulon is therefore interconnected with the general stress response of *E. coli*. As essential components of membranes the composition, reorganization and turnover of lipids is responsible, among other important functions, for housing transport systems necessary for the acquisition of nutrients.[28] Fatty acid metabolism, on the other hand, is directly related with the universal stress response of the cell. FadR, for instance is required for growth-phase regulation of *uspA* (coding for the universal stress protein UspA) important for stasis and survival.[29] Other genes, like *plsX*, identified as differentially expressed, are directly regulated by ppGpp. Moreover, expression of the ribosomal gene *rpmF* (L32) is linked to the *fabHDG* operon transcription. The circle closes here because the acyl carrier protein (ACP), an essential cofactor for fatty acid biosynthesis, is known to affect the activity of SpoT, which leads to the accumulation of ppGpp and thus linking fatty acid starvation to the SpoT-dependent network.[15,25] Based on our data an extended view of the central regulatory role of the 6S RNA molecule in *E. coli* could be drawn, which involves the complex networks of stress and growth adaption (**Fig. 2**).

Although all the different links named above point to a central role of 6S RNA in stress-related metabolism we may have missed many cues due to a lack of severe phenotype. We think it is a worthwhile idea, therefore, to conduct a metabolome analysis of *wt* and *ssrS* deficient strains, which might unravel much more interconnections as we have seen by now.

Acknowledgements

We like to thank all the people from the lab for valuable discussions. This study was supported by the grant WA455/12-2 of the priority program SPP1258 from the Deutsche Forschungsgemeinschaft to R.W.

References

1. Brownlee GG. Sequence of 6S RNA of *E. coli*. Nat New Biol 1971; 229:147-9.
2. Wassarman KM, Storz G. 6S RNA regulates *E. coli* RNA polymerase activity. Cell 2000; 101:613-23.
3. Jishage M, Ishihama A. Transcriptional organization and role of the *Escherichia coli rsd* gene, encoding the regulator of RNA polymerase Sigm D. J Bacteriol 1999; 181:3768-76.
4. Mitchell JE, Oshima T, Piper SE, Webster CL, Westblade LF, Karimova G, et al. The *Escherichia coli* regulator of sigma 70 protein, Rsd, can upregulate some stress-dependent promoters by sequestering sigma 70. J Bacteriol 2007; 189:3489-95.
5. Trotochaud AE, Wassarman KM. A highly conserved 6S RNA structure is required for regulation of transcription. Nature Structural Biol 2005; 12:313-9.
6. Trotochaud AE, Wassarman KM. 6S RNA function enhances long-term cell survival. J Bacteriol 2004; 186:4978-85.
7. Trotochaud AE, Wassarman KM. 6S RNA Regulation of *pspF* Transcription Leads to Altered Cell Survival at High pH. J Bacteriol 2006; 188:3936-43.
8. Gildehaus N, Neusser T, Wurm R, Wagner R. Studies on the function of the riboregulator 6S RNA from *E. coli*: RNA polymerase binding, inhibition of in vitro transcription and synthesis of RNA-directed de novo transcripts. Nucleic Acids Res 2007; 35:1885-96.
9. Cavanagh AT, Klocko AD, Liu X, Wassarman KM. Promoter specificity for 6S RNA regulation of transcription is determined by core promoter sequences and competition for region 4.2 of sigma 70. Mol Microbiol 2008; 67:1242-56.
10. Neußer T, Polen T, Geißen R, Wagner R. Depletion of the non-coding regulatory 6S RNA in *E. coli* causes a surprising reduction in the expression of the translation machinery. BMC Genomics 2010; 11:165-78.
11. Yates JL, Nomura M. Feedback regulation of ribosomal protein synthesis in *E. coli*: localization of the mRNA target sites for repressor action of ribosomal protein L1. Cell 1981; 24:243-9.
12. Wagner R. Translational components in prokaryotes: genetics and regulation of ribosomes, in Enzyclopedia of Life Sciences (ELS). John Willey & Sons: Chichester 2009.
13. Gaal T, Bartlett MS, Ross W, Turnbough C, Gourse RL. Transcription regulation by initiating NTP concentration: rRNA synthesis in bacteria. Science 1997; 278:2092-7.
14. Paul BJ, Ross W, Gaal T, Gourse RL. rRNA transcription in *Escherichia coli*. Annu Rev Genet 2004; 38:749-70.
15. Wagner R. *ppGpp Signalling*. Bacterial Signalling, Krämer R, Jung K, Weinheim, Eds. Wiley-VCH Verlag 2010; 395-414.
16. Krasny L, Tiserova H, Jonak J, Rejman D, Sanderova H. The identity of the transcription +1 position is crucial for changes in gene expression in response to amino acid starvation in *Bacillus subtilis*. Mol Microbiol 2008; 69:42-54.
17. Krasny L, Gourse RL. An alternative strategy for bacterial ribosome synthesis: *Bacillus subtilis* rRNA transcription regulation. EMBO J 2004; 23:4473-83.
18. Wassarman KM, Saecker RM. Synthesis-mediated release of a small RNA inhibitor of RNA polymerase. Science 2006; 314:1601-3.
19. Wurm R, Neußer T, Wagner R. 6S RNA-dependent inhibition of RNA polymerase is released by RNA-dependent synthesis of small de novo products. Biol Chem 2010; 39:187-96.

20. Laurent-Winter C, Lejeune P, Danchin A. The *Escherichia coli* DNA-binding protein H-NS is one of the first proteins to be synthesized after a nutritional upshift. Res Microbiol 1995; 146:5-16.
21. Ball CA, Osuna R, Ferguson KC, Johnson RC. Dramatic changes in Fis levels upon nutrient upshift in *Escherichia coli*. J Bacteriol 1992; 174:8043-56.
22. VanBogelen RA, Neidhardt FC. Ribosomes as sensors of heat and cold shock in *Escherichia coli*. Proc Natl Acad Sci USA 1990; 87:5589-93.
23. Marr AG. Growth rate of *Escherichia coli*. Microbiol Rev 1991; 55:316-33.
24. Piper SE, Mitchell JE, Lee DJ, Busby SJ. A global view of *Escherichia coli* Rsd protein and its interactions. Mol Biosyst 2009; 5:1943-7.
25. Battesti A, Bouveret E. Acyl carrier protein/SpoT interaction, the switch linking SpoT-dependent stress response to fatty acid metabolism. Mol Microbiol 2006; 62:1048-63.
26. DiRusso CC, Metzger AK, Heimert TL. Regulation of transcription of genes required for fatty acid transport and unsaturated fatty acid biosynthesis in *Escherichia coli* by FadR. Mol Microbiol 1993; 7:311-22.
27. Campbell JW, Morgan-Kiss RM, Cronan JE Jr. A new *Escherichia coli* metabolic competency: growth on fatty acids by a novel anaerobic beta-oxidation pathway. Mol Microbiol 2003; 47:793-805.
28. DiRusso CC, Nystrom T. The fats of *Escherichia coli* during infancy and old age: regulation by global regulators, alarmones and lipid intermediates. Mol Microbiol 1998; 27:1-8.
29. Farewell A, Kvint K, Nystrom T. uspB, a new sigmaS-regulated gene in *Escherichia coli* which is required for stationary-phase resistance to ethanol. J Bacteriol 1998; 180:6140-7.
30. Sharma CM, Hoffmann S, Darfeuille F, Reignier J, Findeiss S, Sittka A, et al. The primary transcriptome of the major human pathogen *Helicobacter pylori*. Nature 2010; 464:250-5.

Zusammenfassung

Die Transkription von Genen ist ein grundlegender Prozess in allen biologischen Systemen. In prokaryotischen Zellen wird die gesamte Transkription durch lediglich eine RNA Polymerase (RNAP) katalysiert, welche daher einer komplexen Regulation unterliegt. Die Aktivität der RNAP wird durch verschiedenste, zelluläre Komponenten, wie Proteine, niedermolekulare Verbindungen und Nukleinsäuren, kontrolliert. Obwohl Ribonukleinsäure (RNA) das eigentliche Produkt der Transkription ist, stellt die bakterielle 6S RNA ein Paradebeispiel für die Regulation der Transkription durch eine kleine, nicht-kodierende RNA (ncRNA) dar. In dieser Dissertation wurden funktionelle und strukturelle Details der 6S RNA-RNAP Interaktion genauer untersucht.

Neben der 6S RNA aus *E. coli* wurden die Sekundärstrukturen verschiedener 6S RNAs aus phylogenetisch entfernten Cyanobakterien analysiert. Aufgrund der strukturellen Ähnlichkeit wurden diese 6S RNAs für heterologe *in vitro* Studien mit der RNAP aus *E. coli* verwendet. Trotz des Fehlens größerer Sequenz-Konservierung weisen die 6S RNAs aus *E. coli* und den cyanobakteriellen Spezies sehr ähnliche Eigenschaften auf. Dazu gehören die spezifische Bindung an die RNAP sowie das pRNA-vermittelte Ablösen von der RNAP. Die einheitliche Struktur der 6S RNA erlaubt eine präzise Lokalisierung im aktiven Zentrum der RNAP, wodurch in einer ungewöhnlichen, RNA-abhängigen Transkription kurze *product* RNAs (pRNAs) synthetisiert werden können. Eine strukturelle Analyse der resultierenden 6S-pRNA Hybride hat gezeigt, dass die 6S RNA einer Konformationsänderung unterliegt, welche das Ablösen von der RNAP fördert und dadurch den intrazellulären Abbau der 6S RNA einleitet. Die Bedeutung der strukturellen Veränderung der 6S RNA nach pRNA Transkription *in vivo* konnte durch eine chemische footprint Analyse untermauert werden.

In dieser Arbeit wurden darüber hinaus Regionen der 6S RNA-RNAP Interaktion genauer charakterisiert. Dazu wurde die räumliche Nachbarschaft zwischen funktionellen Domänen der RNAP σ^{70} Untereinheit und der 6S RNA durch Anwendung der chemischen Nuklease FeBABE bestimmt. Die räumliche Zuordnung der 6S RNA Spaltungspositionen sowie die Zuhilfenahme von Tertiärstrukturvorhersagen für 6S RNA Fragmente erlaubten die Modellierung einer drei-dimensionalen 6S RNA Struktur relativ zu der hoch-aufgelösten Kristallstruktur der RNAP aus *E. coli*. Dieses Modell gibt die größtenteils helikale Topologie der 6S RNA wider und beschreibt einen plausiblen Pfad der RNA entlang der RNAP. Eine Erweiterung der Analysen mittels 6S RNA Mutanten hebt die Bedeutung von asymmetrischen *bulge loops* innerhalb der 6S RNA *internal stem* Struktur als potentielle Interaktionsstellen für die RNAP hervor.

Erklärung

Hiermit erkläre ich, dass ich die vorliegende Dissertation eigenständig und ohne unerlaubte Hilfsmittel angefertigt habe. Die Dissertation wurde in dieser oder ähnlicher Form noch bei keiner anderen Institution eingereicht. Ich habe bisher keine erfolglosen Promotionsversuche unternommen.

Düsseldorf, 01.10.2013

Benedikt Steuten